REGIONAL LOCALIZATION OF BINDING AND PARSING IN THE BRAINS OF STROKE PATIENTS USING PERCEPTUAL TESTS

A thesis presented to the graduate faculty of
New England College of Optometry in partial fulfillment of
the requirements for the degree of Master of Science

Jameel Kanji O.D.

May, 2015

REGIONAL LOCALIZATION OF BINDING AND PARSING IN THE BRAINS OF STROKE PATIENTS USING PERCEPTUAL TESTS

Jameel Kanji, O.D.

This manuscript has been read and accepted by the Thesis Examination Committee in satisfaction of the thesis requirement for the degree of Master of Science.

3-2-2015
Date

Frank Thorn, O.D., Ph.D.
Graduate Faculty Advisor

Nancy J. Coletta, O.D., Ph.D.
Thesis Committee Member

Sidney Diamond, M.D.
Thesis Committee Member

Pawan Sinha, Ph.D.
Thesis Committee Member

5-11-15
Date

Nancy J. Coletta, O.D., Ph.D.
Director of Graduate Studies

New England College of Optometry

ABSTRACT

REGIONAL LOCALIZATION OF BINDING AND PARSING IN THE BRAINS OF STROKE PATIENTS USING PERCEPTUAL TESTS
Jameel Kanji O.D.
New England College of Optometry, 2015

Ostrovsky et al. (2006, 2009) showed that children recovering after bilateral congenital cataract removal have great difficulty with visual parsing/segmentation and binding tasks, even though their visual acuity is adequate and they use fine details when performing other tasks. Segmentation and binding, allow us to recognize and interpret objects in the environment, and are opposite sides of the same continuum. Segmentation allows us to recognize that two or more abutting surfaces are separate objects, while binding, allows us to recognize that abutting surfaces are in fact part of the same object. These vision-based perceptual abilities are thought to be more important than vision acuity in everyday life. Over the course of many months, presumably through interaction with the environment using motion information, these individuals learn to perform static parsing and binding.

There are select cases in which traumatic brain injury patients develop a reduced ability to properly use these two visual organizational principles leading to perceptual confusions. We have studied a group of 57 neurological patients who have had strokes in various brain regions, putting them at risk for developing mild versions of such deficits, in order to uncover the neural structures that underlie these rarely tested yet important visual perceptions. We have combined brain localization of stroke lesions using MRI and CT scans with a subjective perceptual test adapted from Ostrovsky et al., to investigate the patients' ability to recognize shapes and real objects, to perform segmentation and binding, and to recognize faces.

The results of the study reveal the complex nature of the visual functions being studied, as there are likely different types of segmentation and binding based on different stimulus features. Unique cortical pathways may govern these visual perceptions, involving the occipital lobe, and temporal/parietal areas; this depends on the stimuli involved. Brain atrophy/small infarcts caused by aging, and basal ganglia lesions do not cause deficits of interest. The results also suggest a link between Segmentation and Binding. Unlike the Ostrovsky et al. study, independent motion of the shapes or objects, did not help brain lesion patients for the segmentation task we used, which questions how possible recovery from these deficits is, and what the mechanism of recovery may be.

Table of Contents

List of Figures & Tables

Figures

Tables

ACKNOWLEDGMENTS

There are countless individuals who made this a reality, and I am grateful for their contributions.

Thank you to Drs. James Comerford, Nancy Coletta, faculty from the New England College of Optometry, for your advice and assistance. A special thank you to Dr. Li Deng for your insight and assistance with regards to statistical analysis.

Thank you to Drs. Richard Held, Yuri Ostrovsky, and Pawan Sinha, from the Sinha Lab for Vision Research at MIT for your valuable input. A special thank you to Dr. Sidney Diamond for all of your contributions to the thesis and your expertise in the neurological analysis of this study.

Thank you to Drs. Lu Fan and Chen Jie of the Wenzhou Medical University for your support. A special thank you to Wu Ende and Chen Xin for your efforts in Wenzhou China, spending countless hours gathering, sorting and entering the data, as well as helping with statistics.

Dr. Frank Thorn (faculty at New England College of Optometry), thank you for your incredible support, encouragement and guidance, and for the opportunity to undertake this project. Without you, this would not have been possible.

Lastly, I would like to thank my family, for their continued love and support.

INTRODUCTION AND BACKGROUND

Eyesight is an exceptionally vivid yet dependable sense. It allows us to navigate and interact with the world around us, as well as appreciate sunsets, vast mountain ranges, and a stranger's glance. Many of us think that crisp 20/20 visual acuity implies perfect vision. But what about the case where your visual acuity is 20/20, yet you cannot understand or properly interact with the world around you? In 'The Man Who Mistook His Wife for a Hat,' neurologist and author Oliver Sacks describes the case of a brilliant musician and music teacher Mr. P, who despite having good vision and perceptual abilities his whole life, develops an overwhelming inability to correctly recognize objects and faces. Mr. P commonly mistakes doorknobs for children's heads and cannot recognize his students' faces until he hears their voices. Mr. P even mistook his wife's head for his hat (Sacks, 1985)! Mr. P clearly has a profound visual perception deficit. This creates mishaps, embarrassments, and an inability to function on a day-to-day basis much more than if he had reduced visual acuity. Such extreme life altering deficits are not commonly seen; however, there are many cases in which patients develop a reduced ability to recognize faces, shapes or objects that they have seen throughout their lives.

It is important to understand the root of these perceptual problems and in the future how to help patients overcome these deficits. We have studied a group of neurological patients who have had strokes that may put them at risk for developing mild versions of such deficits. In so doing we seek to better understand the way in which the brain analyzes visual information from a scene into a coherent and meaningful picture.

The present project is inspired by the work of Pawan Sinha's group in the Department of Brain and Cognitive Sciences at MIT and their initiative 'Project Prakash.' 'Prakash' means 'light,' and the goal of the project is to aid those with correctable congenital blindness in India

while learning about the development of vision by the brain. Pawan Sinha and his colleagues used an extensive protocol to test the perceptual abilities of children who were recovering from surgical removal of dense bilateral cataracts after the presumed age of the critical period of neural plasticity had ended. Apart from the ability to distinguish bright light from darkness, these children had been blind before the surgery. Following the surgery, these children still suffered from poor visual acuity (<20/200); however, the visual acuity loss seemed to be a minor handicap compared to the inability of some to interpret what they saw due to a severe loss of binding and segmentation (Mandavilli, 2006; Ostrovsky, Andalman, & Sinha, 2006; Ostrovsky, Meyers, Ganesh, Mathur, & Sinha, 2009)

Segmentation and binding are opposite sides of the same coin. Segmentation allows us to recognize that two or more abutting surfaces are separate objects, not connected parts of the same object. Binding, on the other hand, allows us to recognize that abutting surfaces are in fact part of the same object, not different neighboring objects. The inability to properly use these two visual organizational principles can lead to related perceptual confusions. If two objects that are transparent or are just outlines overlap, we normally see two overlapping objects. Children recovering after congenital cataract removal see the overlapping area as a separate object belonging to neither of the actual overlapping objects. When the objects break apart like this it is known as 'over-segmentation' (figure 1b). With multiple overlapping objects, the boundaries of the objects can break each other into many meaningless parts (figure 1c). Once the objects are broken into separate meaningless regions and fragments based on low-level attributes such as hue, luminance and intervening borders, it is difficult to construct reality based object representations and can therefore destroy visual binding and a meaningful understanding of the world around us (Ostrovsky et al., 2009).

A B C

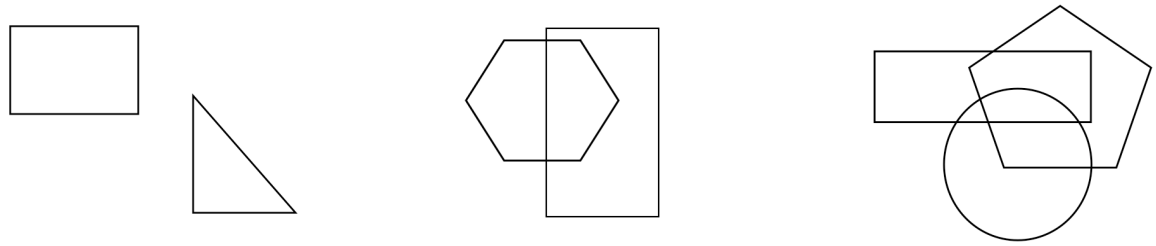

Figures 1A, B & C: Examples of over-segmentation and disruption of binding in post-surgical cataract subjects with simple images.

(A) Two separate objects (a rectangle and a triangle) are easily identified. (B) Two overlapping objects (a hexagon and a rectangle); post-surgical cataract patients see three objects, with the overlapping area seen as a separate object. They are unable to bind the overlapping and non-overlapping parts of two objects into a hexagon and a rectangle. (C) Shows three overlapping objects; post-surgical cataract patients carefully count each overlapping closed space as a separate object. Therefore, they count 7 objects. This represents a strong and unusual inability, over-segmentation, to bind the images into three overlapping but separate objects. Yet the clarity of their vision is adequate for them to count each little area.

Ostrovsky et al. (2009) showed that motion is a powerful cue allowing these patients to bind all the parts in an object into one. This is consistent with the Gestalt principle of common direction (Koffka, 1935) but is often ignored in modern perception research. We hypothesize that motion will serve as an important cue for object segmentation in the neurological patients of this study. Thus, if a previously unrecognizable figure is moved as a whole on a stable background, it will be immediately recognized as a unified object by the patients. These patients would see the cube in figure 2A as three abutting surfaces or objects when it is stable. When it moves, it immediately binds into one object; when it stops moving, it immediately breaks apart or segments into three objects again. The cow in figure 2B is the most famous example of a lack of binding from the Sinha lab. When the cow is stable, the patients count many separate black and white objects against a green background. When the cow is moved as a unified object, the patients immediately see it as a single object with its parts bound together; when it stops moving,

it immediately segments into many pieces. Therefore, post-surgical cataract patients reveal profound deficits in the ability to perform static parsing and binding.

A)

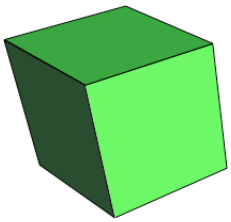

B)

Figures 2A & B: Examples of over-segmentation and disruption of binding in post-surgical cataract subjects with complex images.

(A) A single 3-D object. Post-surgical cataract patients usually see the 3 sides as 3 separate objects by relying on hue and luminance as cues. This represents an inability to perform binding. In figure 2B the post-surgical cataract children carefully count 3 black areas and 5 or 6 white areas as separate objects, and sometimes two more black areas are counted for the cow's shadow. Therefore, they see 8 to 11 black or white objects rather than a cow. If the 3 sides of the cube (figure 2A) are moved together while the rest of the page remains static, the children suddenly see it as a unified object although they will not recognize its three dimensionality. Similarly if the cow is moved against the grass background (common motion), the child suddenly realizes it is a unified object and may even recognize it as an animal.

The ability to automatically perform parsing and binding is one of the slowest aspects of vision to learn in the recovering bilateral cataract patients, and usually takes more than a year. It is not known if the recovery is ever complete.

These and other deficits also appear in some neurological patients (L. Robertson, Treisman, Friedman-Hill, & Grabowecky, 1997; L. C. Robertson & others, 2003). Based on these curious findings, we have used an abbreviated Project Prakash protocol on patients who have just had strokes (many of whom have a visual complaint). We have had access to large numbers of patients in the neurology department of the Wenzhou Medical University. We analyzed a group of these patients in order to better identify the nature of the stroke lesions that

cause a loss in the visual perceptual abilities (binding and parsing) found in the recovering congenital cataract children; and in so doing, work to uncover the neural structures that underlie these rarely tested yet important abilities.

Visual Perception and Cortical Pathways

The identification of a brain area as important to a specific function normally requires evidence of individual neuron receptive fields consistent with the function, fMRI BOLD (Functional Magnetic Resonance Imaging Blood Oxygenation Level Dependent) studies to show an area's active involvement in the function, the ability of a lesion in the area to disrupt the function, and if possible the ability of central stimulation in the area to trigger the function.

The receptive fields of neurons in the visual system have been carefully described by Hubel and Weisel primarily, during the 1960s and 70s. Most ganglion cells (known as parvocells) in higher primates are either excited or inhibited by a small central point within the visual field, with an opposing surround so that the ganglion cells are unresponsive to changes in ambient illumination. Instead they respond to small light or dark spots that are color-coded. A lesser number of ganglion cells (known as magnocells) are responsive to large moving objects and are unresponsive to color. These response patterns are repeated in the lateral geniculate nucleus and layer 4 of the striate cortex and provide the starting point for the brain's response to visual stimuli. In layer 4 of the striate cortex (primary visual cortex or V1) the color coded concentric receptive field information of the parvocellular system is divided into color specific neurons and pattern specific neurons in layers 2 and 3. The pattern specific neurons are sensitive to light or dark lines of a specific thickness and orientation and sometimes direction of movement. The color specific neurons have very weak spatial information. The magnocellular

system activates neurons in striate cortex layer 4 that are sensitive to large moving lines without color specificity. These extensions of the parvocellular and magnocellular system in V1 layers 2, 3 and 4 then send their visual information to many other cortical areas (Constantine-Paton, 2008).

Adjacent to V1 is the secondary visual area (V2) followed by V3, V3a, V4, V4a all within the occipital lobe and V5, V5a at the border of the dorsal temporal lobe. The multitude of information modes in the striate cortex has been divided and allocated to these different cortical areas with binocular fusion and stereopsis prominent in V2, line orientation in V3 and V3a, color in V4 and V4a, motion direction in V5 and V5a (see Zeki, 1993, for a comprehensive review). Here is where basic visual information ceases and cortical areas are transformed into areas of exotic specificity. Anterior to this is the biological motion area and in the lateral ventral occipital lobe and adjacent inferotemporal cortex there are areas primarily responsive to facial recognition, facial expression, hands, body, manipulatable objects, scenes like houses, and letter shapes. It is known that small stroke lesions in these areas can disrupt these specific functions. In fact, some people are poor at these tasks throughout life suggesting that these areas do not all develop equally well in different people (Furl, N., et al, 2011).

Once information is processed in V1 and V2 in the posterior occipital lobe, it continues into two multi-stage paths extending from V1/V2. Recognition of objects and visual shapes occurs through the ventral cortical pathway, which runs from V1 and V2 to V3, V4 and then to sub-regions of the lateral ventral occipital lobe and the adjacent inferotemporal (IT) cortex (Mishkin, Ungerleider, & Macko, 1983). In this hierarchical pathway, the early stages of the visual pathway lead to subsequently more complex forms of visual processing (Pasupathy & Connor, 1999, 2002).

Representation of the spatial location of objects and the people themselves in the environment occurs through the dorsal cortical pathway (occipito-parietal projection system), which travels from V1 and V2 to V5/MT (medial temporal area) and then projects to other areas including MST (medial superior temporal area), and VIP and LIP (ventral and lateral intraparietal areas) (Rizzolatti & Matelli, 2003). Such cortical pathways culminate in specifically useful functional localizations. For example, the inferior parietal lobe analyzes spatial object information for the purposes of grasping objects in the environment (before projecting to the pre-motor cortex to initiate the motor response) (Jeannerod, Arbib Ma Fau - Rizzolatti, Rizzolatti G Fau - Sakata, & Sakata, 1995). The idea that specific higher order functions may be localized to particularly defined areas of cortical real estate is best exemplified by cortical lesion studies throughout the years.

Cortical Disruption and Sensory-Motor Deficits

In the past two centuries the idea of a relationship between localized brain lesions and resulting sensory-motor deficits has surfaced through isolated patient cases. Dr. Paul Broca in 1861 first described such a case, in which a lesion to the left frontal lobe in a region now known as 'Broca's area' disrupted the ability to produce language. This is called 'Broca's aphasia**.'** These patients have great difficulty speaking or writing their thoughts; however, they are able to understand language and do not have motor impairments to their hands, tongue or other areas that may preclude them from expressing themselves. Nearly a decade later, Dr. Carl Wernicke described another case of disrupted language; however, this patient with a lesion in the posterior part of the superior temporal lobe had trouble understanding spoken and written language. This patient was able to speak, but the language was incomprehensible. These early studies, as well as work of J.Hughlings Jackson, Fritsch and Hitzig, Dejerine and others in the 19th century were

crucial in rationalizing the concept of specific functional localization in the brain. Critchley, Bender, Hacaen, Luria, Bay, and others in the latter half of the 20th century have described neurological lesions that tend to localize brain areas involved with different higher order functions(Dubuc). Relating localized brain lesions to sensory-motor deficits has recently become an active area of study since the advent of the CT (Computerized Tomography) scan, MRI (Magnetic Resonance Imaging) and fMRI (Functional Magnetic Resonance Imaging). Technological improvements have even paved the way for imaging studies of higher order processes such as emotion, personality, decision making, and much more.

We have combined brain localization of stroke lesions using MRI and CT scans with a protocol to investigate the patients' ability to recognize shapes and real objects, to perform segmentation and binding normally, and to recognize faces as opposed to objects. The protocol is from a longer protocol used by Pawan Sinha's group to test the vision of children after bilateral congenital cataract removal.

METHODS

Participants

Frank Thorn, Professor of Vision Science at the New England College of Optometry, working with Chen Jie, the Director of the Wenzhou Medical University's (WMU) Low Vision Clinic, started a project to replicate Project Prakash in Wenzhou China. They then proposed testing the Project Prakash protocol on stroke patients seeking to localize the brain regions associated with the specific perceptual losses shown in children recovering from congenital cataract blindness. Two graduate students from the WMU, Wu Ende and Chen Xin, and me from NECO, then worked together to refine the protocol and began testing patients. Dr. Liu, Director of the WMU Second Affiliated Hospital Department of Neurology Clinic, worked closely with the group to identify appropriate patients based on the patient histories. Pawan Sinha and Yuri Ostrovsky provided guidance with the Project Prakash protocol. Dr. Sidney Diamond, who had worked with some of the Wenzhou children recovering from removed cataracts, provided invaluable assistance in understanding the MRI and CT brain images of patients and understanding the cause and expected prognosis of such brain lesions. Wu Ende will use this work as the basis for his PhD thesis. I am using it as the basis for my MS thesis.

Subjects

This study was conducted at the Wenzhou Medical University Second Affiliated Hospital in Wenzhou, China through an ongoing partnership between our institutions. We had access to patients in the Neurology and Neurosurgery wards as well as the Cataract Surgery ward of the Wenzhou Medical University Eye Hospital. In addition, we had the opportunity to work with the head of the neurology department Dr. Liu and her staff. A particular set of criteria was used to

select our sample for the study. Participants in the study were drawn from a prescreened patient pool within the departments of Neurology and Neurosurgery.

Pre-Screening and Participant Selection for Neurological Subjects of Interest

A total of 59 subjects from the Neurology and Neurosurgery departments participated in the study. For the purposes of this study, these patients were grouped together as 'neurological patients.' Pre-screening for these participants involved the examination of computerized patient records of patients currently admitted in the ward. The initial criteria for inclusion in the study were: 1) a recent history of acute onset brain trauma, due to stroke or another neurological event within the past 2-3 weeks, with special interest in a hemorrhage or lesion in the occipital lobe or occipital-temporal or occipital-parietal pathways; 2) Patients with binocular vision, and no history of amblyopia, strabismus, ocular surgery, diplopia, or current/previous eye disease outside of resolved surface inflammatory/infectious disease; 3) feedback from Dr. Li about whether or not the patient of interest has the stamina, strength and willingness to participate in the study, especially if the patient is elderly (70s and 80s); and 4) should have a visual complaint involving object recognition or identification, face recognition, etc. It was essential that participants fulfilled the first criterion, as testing the patient during the critical time of their condition would provide the best chance of identifying any visual perceptual deficit. The second criterion was used to ensure that the visual acuity of the patient was not previously compromised and might potentially lead to poor testing results. The third criterion was used in the patient screening to indicate that subjects had the ability to complete the testing with good reliability. The fourth criterion proved to be difficult to screen for, as the case histories focused more on location of headache, nausea, vomiting, double vision and body weakness; while, neurological

examination focused on limb and facial sensation and pain, as well as certain reflexes (e.g. Babinski reflex) and typical medical findings such as blood pressure and pulse. Patient records revealed only a few cases in which the visual symptoms were of interest. In such cases, if the patient met the first three criteria, they were included in the study.

Due to the difficulty of meeting the fourth criterion, we retained the first three criteria and subsequently sought out a greater diversity of lesion locations (with the inclusion of basal ganglia, frontal lobe and other lesion locations) so as not to miss out on any potentially interesting findings. Looking through the patient records before examination allowed us to ensure that an MRI or CT scan was conducted for each patient, for our reference. The MRI and CT scans were not examined on-site by our group during the screening; however, the interpretation of the scans by the neurologists in the department was read in order to evaluate whether the lesion outlined would be of interest for inclusion in the study.

Testing Introduction and Patient History

Once patients were selected via pre-screening for inclusion in the study, the examiners met with the patients in their hospital rooms. At this time, no information was known about the patient; the examiners knew simply the patient's ID and bed number. A brief introduction was given to the patient and their family members about the purpose of testing (e.g. "We would like to test your vision and ability to understand the objects in the world, as these things can be effected by a stroke") after which, permission was asked of the patient and family member for testing. A brief patient history was taken before testing commenced. This was done to ensure that the patient was correctly matched with their patient file in the computer database, as well as to determine the presence of any visual perceptual symptoms. The patient history included: name,

age, occupation/job, symptom history (does the patient complain of decreased memory or trouble seeing objects after the stroke?), and any relevant medical history.

Control Groups

The neurological patients' family member or spouse was tested for the purpose of establishing a control group. In this study, the group was referred to as 'relatives.' Spouses were preferred as there was a high likelihood that they would be closely matched with the neurological patients in age, ethnicity, social standing, language, etc. Only 13 subjects were included in the 'relatives' control group, as the majority of family members declined the testing. It is our understanding that the family members of the patients did not believe there was a benefit in comparing the results of a 'healthy' individual to that of the in-hospital patient.

In order to enrich the size of the control group, we sought out patients that were going through a similar in-hospital experience as our neurological patients. This led us to the cataract surgery department at the Wenzhou Medical University hospital, where patients from neighbouring towns and villages who were identified as having operable visually significant cataracts were brought to the hospital for surgery. Patients either had surgery for one eye or both eyes, which changed the length of their hospital stay and the timing for participation in the study. For one eye, the hospital stay was three nights and four days: first day was check-in and preparation; second day was the cataract surgery; third day was observation and participation in the study; fourth day was checkout. For both eyes, the hospital stay was four nights and five days: first day check-in and preparation; second day cataract surgery of first eye; third day cataract surgery of second eye; fourth day observation and participation in the study; and fifth day was checkout. Note that in China a hospital stay of at least three nights after cataract surgery

is standard procedure. Releasing the patient on the same day is considered scandalous. During the evening of the last night in the hospital, the examiners went to the cataract surgery department and introduced the study to patients, while identifying individuals who were: 1) binocular with no history of amblyopia, strabismus, diplopia or current/previous eye disease outside of current cataracts or resolving surface inflammation from cataract surgery; and 2) were determined to have the stamina, strength and willingness to participate in the study, especially if the patient was elderly (70s and 80s), as per a patient-examiner discussion. Upon permission by the patient, testing was initiated. As one eye had already undergone cataract surgery, these patients had an eye patch over their treated eye, effectively making them monocular. The pre-screening for neurological patients required binocular visual status, so eye patches were removed for the purposes of the testing, and replaced at its conclusion. For the purposes of this study and due to the inclusion of two control groups, the cataract patients will be referred to as 'cataracts,' with 21 subjects making up this group.

Testing Conditions

In the case of the neurological patients, testing was done in the hospital rooms where the patients were kept. In the Neurology and Neurosurgery wards there were typically either 2 or 4 patients in a room. Before testing commenced, curtains were pulled around the patient to isolate them from their neighbours. In the cataract surgery ward, there were typically 4-8 patients in each room. Cataract patients were either tested in their rooms if they were unable to walk well, or in an isolated examination room across the hall if they were able to walk there.

Patients who were tested in their rooms were asked to sit up right in their beds to provide for a good view of the laptop computer screen for testing. If the patient was unable to sit-up in

the bed, the head of the bed was manually elevated. The laptop computer sat on a small table, which was placed on the patient's bed over his/her legs, with a set viewing distance of 1 meter from the patient's eyes at eye level.

For those in the 'relatives' group, testing was conducted in a separate study room away from their in-hospital family member, much like the testing for some cataract patients. The relatives were asked to sit on a chair at a desk, with the laptop positioned 1 meter away at eye level.

Testing instructions for all subjects were provided orally in Mandarin or a local Wenzhou dialect. At least one member of the 3-person examiner group spoke Mandarin. For those subjects who did not understand Mandarin, the instructions were relayed through a family member or a member of the neurological staff who could speak Mandarin and could translate it to the necessary dialect. Some test questions involved verbal responses, while others required patients to point at the screen using their finger or a pointing stick. A few patients were non-verbal and depended only on their limb mobility as a means of communication. Those patients that had limited limb mobility would only respond verbally.

Subjective Ophthalmic and Perceptual Tests

With the purpose of the study in mind, we developed appropriate low-level and higher-level vision and perceptual tests and subsequently tested patients with traumatic brain injury damage (strokes, infarctions, hemorrhages). The higher-order tests are designed to uncover neural mechanisms underlying perception, such as those involved in binding, parsing and face perception The higher order tests use colored figures and patterns, as well as unique intermixed shapes that the patient must discover. It is important that subjects being tested on the higher

order tests have adequate visual acuity to detect essential elements of a pattern. Furthermore, in many of the higher order tests, specific colors contribute to the robustness of the visual effect being tested. Thus, it is important to test each patient's visual acuity and color vision prior to the administration of the higher order tests. The low-level vision tests are designed to measure factors that may interfere with the ability to parse and bind objects. This will ensure that there is a clearer distinction between a patient with a perceptual or cognitive deficit and one with a low-level visual problem. The ophthalmic and higher-order tests are organized in an effective procedural flow within a computerized testing system that enables efficient examination of visual functions in patients of different abilities and with different neurological disruptions, with both the lower and higher order tests structured to follow the same format. Since most of the patients were tested in their hospital beds, the entire protocol had to be adapted to that environment. All tests were administered on a 13" MacBook Pro at a distance of 1 meter. The 1-meter testing distance is standard to all of the testing as it provides the most flexible viewing distance in terms of subject inclusion. Most patients can point to and reach the computer screen with their own arms or with a small pointer. While this distance may not be ideal for certain presbyopic patients who have reading glasses at a closer distance, it allows those who do not have their reading glasses with them to participate in the study without much difficulty.

Higher Level Perceptual Tests

The higher-order perceptual tests used in this study were adapted from the protocol developed by Pawan Sinha's group at MIT (Ostrovsky et al., 2009) used for post-operative congenital cataract patients. In the current study, binding and parsing will be studied in the stroke population to understand the neural locus of these higher visual processes. Therefore, select

slides were chosen from the Sinha protocol for greater specificity. For the purposes of this study, this test will be referred to as the Wenzhou Protocol. It is made up of 109 slides that include 76 questions and takes an average of 15-20 minutes to administer to patients through a power point presentation. The slide timer in power point was used to determine how long subjects spent on each slide. Patients were asked to provide accurate responses as quickly as they could, and were not told about a time cut-off for the testing. However, for the purposes of efficiency and to avoid patient fatigue, when an individual slide timer reached 30 seconds, the subject was asked to provide a final response, otherwise the slide was marked as 'incorrect' and the next slide was shown.

The protocol comprises various types of visual perception tests. In order to better understand the results of each type of visual perception test for an individual patient, distinct categories of the Wenzhou Protocol were formed. The categories are:

a) Basic Shape Matching (refer to figure 3) with 11 slides;

b) Static unfilled figures (refer to figure 4), contains 5 slides.

c) Motion of unfilled figures, contains 5 slides that are identical to static unfilled figures, however the overlapping figures have independent motion and move uniquely in circular patterns while overlapping the other shapes.

d) Masking/distractors (refer to figure 5), contains 7 slides

e) Figure ground/depth (refer to figure 6), has 3 slides

f) Specific segmentation (refer to figure 7), contains 5 slides

g) Total static segmentation, is the sum of static unfilled figures, masking/distractors, and specific segmentation, for a total of 17 slides.

h) Total binding (refer to figure 8), contains a total of 6 slides, and was subdivided into two subgroups:

- i) 3-D objects has 3 slides (figure 8a)
- ii) line binding contains 3 slides (figure 8b)

i) Naming a Real Object (refer to figure 9), has 15 slides

j) Visual Memory (refer to figure 10), contains 10 slides

k) Face Perception (refer to figure 11), has 8 slides.

Each category of testing has stimuli of varying degrees of difficulty, which may be created by stimulus changes including: color, size, contrast, motion, distractors shapes or masking. In the majority of slides, the subject is required to observe a figure on the left side of the screen and to match this with a similar appearing shape or stimulus on the right side of the screen. However, other slides require different types of subjective responses, such as stating how many shapes or figures are seen, or naming an everyday object presented on the slide. Before each change in the type of response, an example slide is shown to introduce the subject to the style or type of response they must provide. If requested, subjects may take a rest break during the testing only at the end of a section when a new instruction slide appears. Later, a ninth and final category was formed from the 76 questions of the Wenzhou Protocol. It was observed, that 75 of the 76 questions showed shapes or figures that would easily be distinguished by a normal observer as individual figures, even if they were overlapping with others. More specifically in the ‘object segmentation’ category, all but one of the questions followed this rule. As this odd powerpoint image did not follow this principle, it added a new level of complexity, and was therefore removed from the protocol. For this question, the figure of interest was not a stand-

alone object that was overlapping with others, but was a figure that emerged from the way in which other figures overlapped. We refer to this removed slide as the 'Hidden Object' (refer to Figure 12). The final number of questions for the Wenzhou Protocol was left at 75.

The results we report for a neurological patient are based on his or her performance on each of the six categories of Wenzhou Protocol. Performance in the different categories provides the basis for distinctions between the types of visual perception deficits.

A) B)

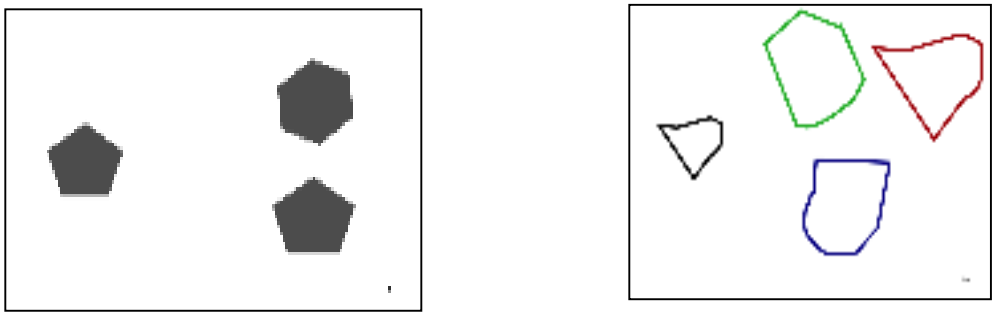

Figures 3A & B: Examples of Shape Matching questions on the Wenzhou Protocol

Shape Matching – 11 questions where subjects view a sample stimulus on the left hand side of the screen and find the resembling figure amongst the set of shapes on the right side of the screen. A) Shows a simple shape-matching slide from the Wenzhou Protocol, while B) shows a matching slide with color and size manipulations that makes it more difficult.

A) B)

Figures 4A & B: Examples of Unfilled Figures questions on the Wenzhou Protocol

Static Unfilled Figures – Requires the subject to parse out an object that may be partially covered or overlapping with another object or shape. The figures presented in these questions are stationary and are outlined, not coloured in. There are 5 such questions in the Wenzhou Protocol. Slide A) asks subjects to match the shape on the left (3-lobed figure) to its counterpart shape on the right side by pointing to its location. This is a segmentation task, as the two figures on the right are overlapping. The three-lobed figure can only be found by 'segmenting' or 'parsing' it from the other shape. Slide B) is also a segmentation task; however subjects are asked to indicate how many individual figures they see. In this case, there are 3 unique overlapping figures.

A) B)

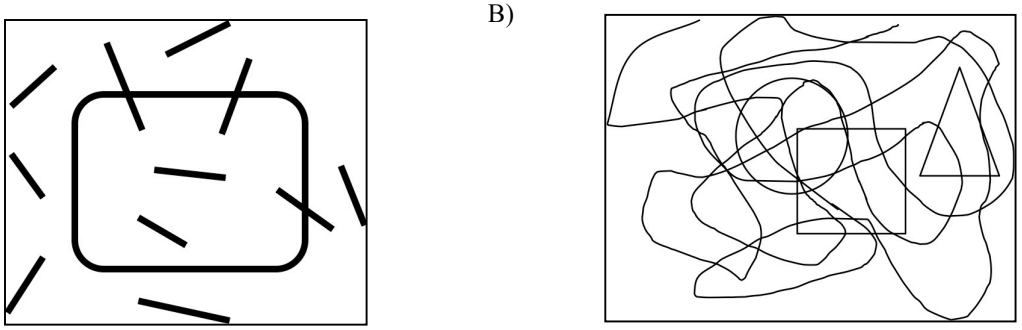

Figures 5A & B: Examples of Masking and Distractor questions on the Wenzhou Protocol

Masking and Distractor Slides– requires the subject to parse out an object or shape in the presence of line distractors or a background of masking scribbled lines. Note that this task is static, with no moving shapes or figures. There are 7 slides in this group included in the Wenzhou Protocol. Slide A) asks the subject to identify what shape (square) is seen in the presence of multiple overlapping distractor lines. Slide B) asks the subject to identify the closed shapes (circle, square and triangle) seen in the presence of a confusing scribble background. The overlap of the circle and square adds an additional level of difficulty for this task.

Figure 6: Example of Figure Group Depth Question on the Wenzhou Protocol

Figure Ground and Depth – contains slides with two colored 2-D figures with one figure overlapping the other. The subject indicates which figure is 'on top' of the other. The Wenzhou Protocol contains 3 slides for depth segmentation. In Figure 6 the orange/red figure is 'on top' of the blue figure. This is a segmentation task, as subjects are required to parse out the two overlapping figures and use this information to indicate which figure is in front of the other.

A) B) C)

Figures 7A, B & C: Examples of Specific Segmentation on the Wenzhou Protocol

Specific Segmentation – contains 5 slides. Examples of three of the slides are shown above in A, B and C. Slide A) is an example of a segmentation task with overlapping translucent grey figures. Subjects were asked to state the number of individual figures seen. There are 3 figures in the slide; however, the overlapping regions that have darker grey shading may appear to be individual figures to those who have a segmentation deficit. Slide B) asks subjects to state the number of wooden blocks seen. Note, that shadows and placement of the blocks makes this parsing task moderately difficult. Slide C) shows a complex matching task that asks the subject to match the shape on the left to its counterpart on the right. This is unlike the shape matching task shown in Figure 3, as it relies on parsing out the overlapping figures on the right side in order to match correctly.

A) B)

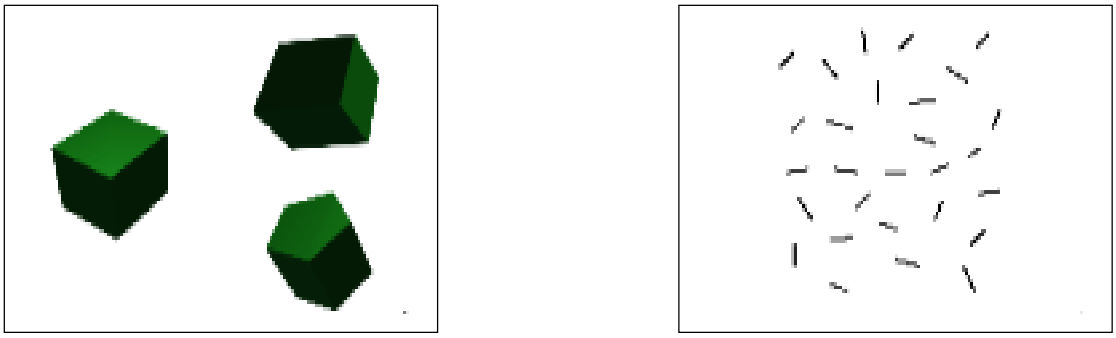

Figures 8A & B: Examples of Binding Only questions on the Wenzhou Protocol

Binding Only – These slides focus on binding with the use of different stimulus forms. There are 6 slides in the Wenzhou Protocol specifically for binding, with 3-D objects and line binding making up these slides. A) is an example of shape matching of 3-D objects with orientation manipulation. The shaded faces of the 3-D objects may appear to be different figures to an individual with a binding deficit. There are 3 slides in the Wenzhou Protocol with 3-D objects. In B) the longest continuous line must be identified amongst the distractor lines. The subject must 'fill-in' the blanks between the lines in order to bind them together in one continuous line. There are 3 such slides in the Wenzhou Protocol.

A)

B)

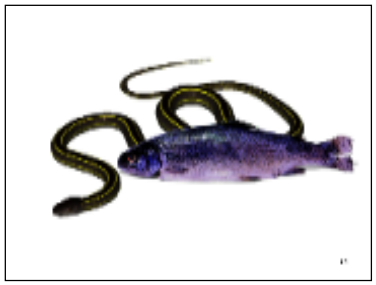

Figures 9A & B: Examples of Naming Real Objects questions on the Wenzhou Protocol

Naming Real Objects – 15 slides of everyday real world images were shown, which require segmentation and binding for recognition. In these slides, the subject is required to name and state the number of everyday objects and/or figures that are seen. This requires the ability to separate or segment out individual figures and bind these figures to identify the objects they comprise. A) shows an example of figure-ground. The figure (the red apple) is masked by the background of green leaves and tree branches. B) A more complex slide with one winding snake and one fish that are overlapping. Due to the nature of the overlapping figures, a person with defective parsing and binding may perceive more than one snake.

A) B) C)

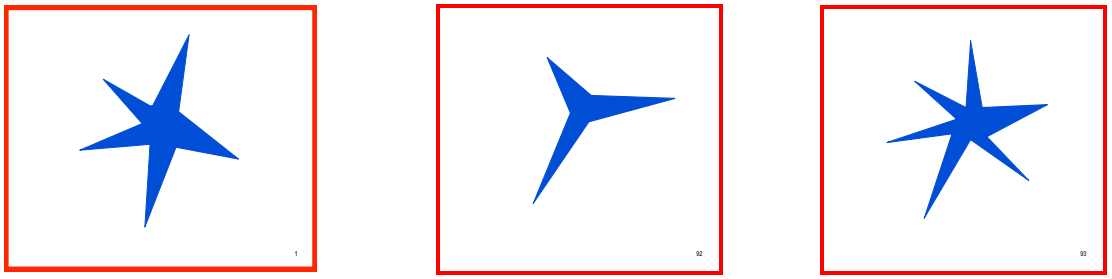

D) E) F)

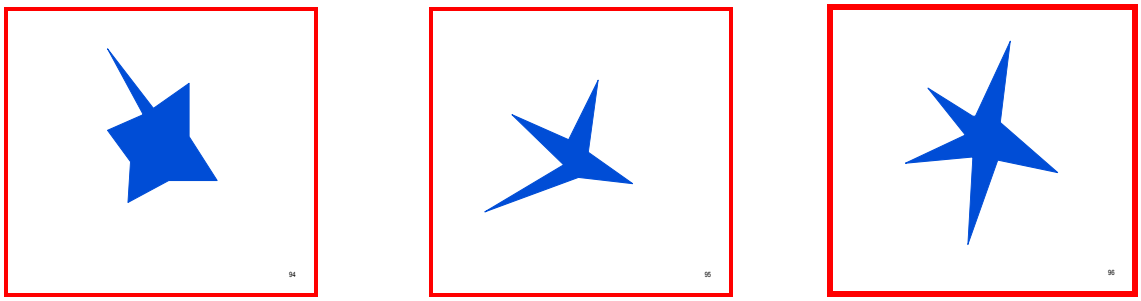

Figures 10A-F: Example of one Visual Memory Question on the Wenzhou Protocol

Visual Memory – In this task, subjects are asked to remember the figure presented on the screen. After 15 seconds, 5 subsequent figures are shown. The subject must indicate whether the figure presented was the same as the one that was memorized. In this example, A is the figure of interest which must be memorized. Then figures B-F are shown one by one, with the subject correctly responding ‘no’ for figures B-E and correctly saying ‘yes’ to F which resembles the figure in A. The Wenzhou Protocol contains two such figure memorizations, with each figure having 5 slides to be matched, for a total of 10 slides in this section.

A) B)

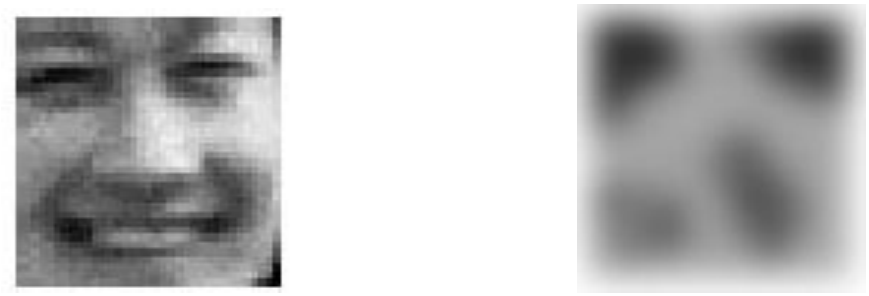

Figures 11A & B: Examples of Face Perception questions on the Wenzhou Protocol

Face Perception – In this task, subjects are shown a picture and must indicate whether each picture depicts a human face, by answering 'yes' or 'no.' The Wenzhou Protocol contains 8 slides for face perception. A) is a human face, while B) is not.

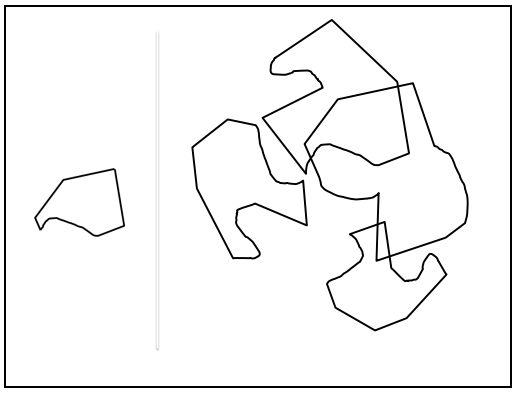

Figure 12: Image of the Hidden Object question that was removed from the Wenzhou Protocol

Hidden Object – This slide was removed from the protocol. Notice that although this appears to be a question similar to those in the object segmentation category, it does not follow the same rules as the simple matching and segmentation tasks where the shapes on the right of the screen are stand alone shapes or have some overlap. In this question, the figure of interest is created by the overlapping outlines of two shapes. This question adds a new level of complexity unseen before in the Wenzhou Protocol and was therefore removed.

Visual Acuity

Visual acuity is one of the most important subjective tests for ophthalmic clinicians, even though it may not be an especially good predictor of visual performance. In this study, subjects' visual acuity was found using a newly developed acuity test and a 'traditional' acuity test. Both

visual acuity tests were created using Power Point after careful calculations for the Apple MacBook Pro 13" at a 1 meter testing distance with standardized screen brightness setting of 12 of 16 bars on the laptop scale (this was the brightness setting for which the color vision test was created).

The new acuity test will be referred to as the 'Isolated Landolt C Test'. As its name suggests, the 'Isolated Landolt C Test' uses a single black 'Landolt C' that is manipulated in size and direction. The Landolt C was chosen due to its simple form, as the clinical patients included in this study may have difficulty with more complex optotypes. In addition, Landolt C tests have been used successfully in China. The size of the optotype in the 'Isolated Landolt C Test' was manipulated in LogMAR steps. This is similar to the Freiburg Vision Test (FRacT test) (Bach, 1995) where the patient identifies the orientation of a single isolated Landolt C that is oriented in one of four primary directions (refer to Figure 13). The subjects were first shown an example slide of a large isolated Landolt C and told to point in the direction (left, right, up or down on the computer screen) of the 'opening' of the 'C.' After this example, subjects began the acuity task with the 1.3 logMAR (20/400 snellen acuity) letter. A staircase procedure was used in which each step was equivalent to one line on a LogMAR chart. With every correct response, the size of the Landolt C decreased by 0.1 log units, and with every incorrect response, the size increased by 0.1 log units. The test ended once two consecutive incorrect responses were given.

A) B)

Figures 13A & B: Images of the Landolt C used in the visual acuity test

A) shows the four possible directions of the Landolt Cs in the acuity tests (up, down, left or right). The subject must identify the location of the Landolt C opening. B) shows a typical slide on the isolated Landolt C acuity test with only one figure presented at a time. In this case, the C opens 'to the right.'

The 'traditional' acuity test also uses Landolt Cs; however, it contained a standard full-line of the optotype, as in configuration of the ETDRS chart. We refer to this acuity test as the 'Crowded Landolt C Acuity Test'. Two versions of the crowded acuity test were administered, with the only difference being the distance between the multiple Cs in a line. One version contained a 5-stroke spacing, which is equivalent to one letter width, the standard space between lines on an ETDRS LogMAR chart; the other contained 1-stroke space between Cs, which approaches the spacing between letters in text. This is illustrated in figure 14. In the interest of testing efficiency, the crowded acuity tests were both started at 0.2 log units above the subject's isolated Landolt C acuity. For example, if the subject's isolated visual acuity was 0.7 logMAR (20/100 Snellen acuity), then the test began at 0.9 logMAR (20/159 Snellen acuity) acuity. With more than 50% correct responses on the screen, the size of the Landolt C decreased by 0.1 log units, and with less than 50% correct responses, the size increased by 0.1 log units. If the subject is unable to provide any reliable answers with the starting acuity, the size of the letters may be increased (in 0.1 logMAR steps) until reliable responding is reached (with at least 50% correct responses) before proceeding with smaller letter sizes.

A) B) C)

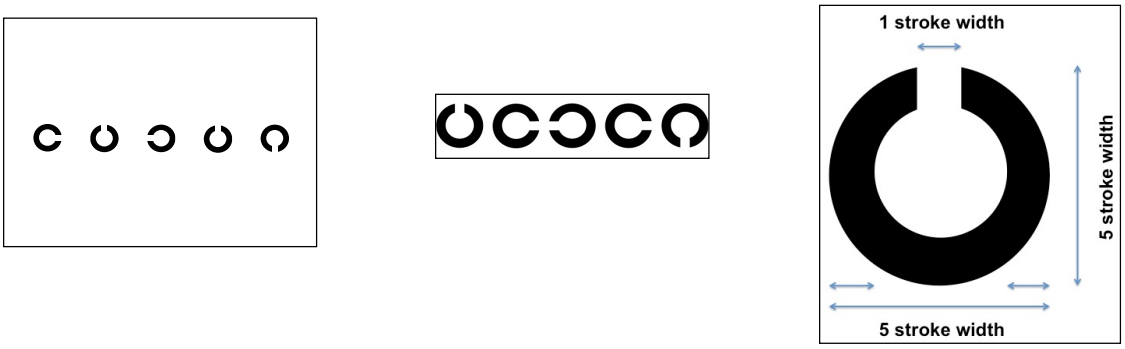

Figures 14A, B & C: Example of two versions of the Landolt C acuity test used, and image of Landolt C stroke width calculation

A) and B) show the two crowded Landolt C acuity tests used. The difference between the two acuity tests is in the spacing between the Cs, which is represented by 'stroke width.' 1 stroke width is the thickness of a line within the letter as well as the size of the opening of the C (as shown in figure C)). Note that the Landolt C is a total of 5 stroke widths in height and length. A) uses 5 stroke spacings between each Landolt C on the line, while B) has 1 stroke space between each Landolt C on the line. The subject must identify the direction where each Landolt C opens (up, down, left or right).

Brain Imaging with Magnetic Resonance Imaging (MRI) or Computerized Tomography (CT)

In the Neurology and Neurosurgery Department of the Wenzhou Medical University Hospital neurologists used one of two brain imaging techniques that were included in the study: MRI or CT scan. The majority of patients in the study had an MRI scan (46 patients) with the minority having a CT scan (11 patients). As not to interfere with the care of the patient, neurologists were free to make the appropriate imaging technique requisition according to their expert medical opinion, followed by their diagnosis and treatment, after which investigators of the current study had access to the patient's records and were able to look at the brain images. The MRI scans contain T-1 weighted images, which outline the anatomy of the tissues, and/or T-2 weighted images, which reveal hemorrhaging and/or edema. The advantages of MRI for the purposes of this study are: high contrast resolution of the soft tissue to detect damage and high sensitivity to tissue edema. While CT scans have the advantages of sensitivity for detection of

calcifications, intracerebral hemorrhages, and visualization of the anatomy of skull. CT scans are used when magnetic resonance imaging (MRI) cannot be done, as in patients with metal prostheses or other implanted metal objects. Furthermore motion artifacts do not degrade CT images as greatly as MRI scans. The main disadvantages of CT for the purposes of this study include: low sensitivity for imaging acute infarction and large vessel occlusion (Gilman, 1998; Silver B, 2014).

Determination of Lesion Location and Size

After data collection was completed, the MRI/CT scans of the neurological patients and their case histories were recovered from the computer database of the Wenzhou Medical University. The medical reports contained information regarding the Wenzhou neurologist's thoughts on the etiology and location of the brain lesion; however, for the purposes of the study, we did not feel that this was specific enough. In an effort to more accurately identify the specific types of lesions, as well as their size (in centimeters), a thorough study of the medical history with associated close review of the head scans was done under the direction of Neurologist Dr. Sidney Diamond at the Massachusetts Institute of Technology (MIT). Dr. Diamond was a senior neurologist for many years and has published several research articles on the vision of neurological patients. Dr. Diamond was given whatever case history was available for each patient (often likely in error), as well as the head imaging. Without knowledge of the final diagnosis of the patient (given by the Wenzhou neurologists) and blind to the results of the subjective ophthalmic and perceptual testing, Dr. Diamond provided his own unbiased interpretation of the etiology, approximation of size (using the scale on the imaging slides) and location of the brain lesions. By undergoing such a detailed independent study of each patient,

we were able to separate the neurological patients into different groups depending on lesion size and location for statistical analysis.

Neurological Subject Categorization Based on Lesion Location

One method of studying the brain lesions was to look at the location based on the neuro-imaging. Vasculature of the brain was used in addition to brain imaging to determine which brain areas were impacted by the lesion. Note that arteries supply oxygen and nutrients to the brain tissue, while veins carry deoxygenated blood to the heart. Occlusion of these vessels or hemorrhaging can cause lack of oxygenation and improper nutrient supply to the brain tissue causing loss of the tissue. Blood is supplied to the brain via the left and right common carotid arteries and the right and left vertebral arteries. There are two divisions of the common carotid artery: external carotid artery supplies the face and scalp; internal carotid artery supplies the anterior three-fifths of the brain, not including parts of the occipital and temporal lobes. The vertebrobasilar arteries supply the posterior two-fifths of the brain, parts of the cerebellum and the brainstem. The internal carotid and vertebrobasilar arteries form the 'circle of Willis,' a circle of communicating arteries, from which other arteries arise and take blood to all parts of the brain (refer to figure 15A). The main arteries that arise include: the anterior cerebral artery (ACA), which branches from the internal carotid and supplies the frontal lobe and parts of the parietal lobe; the middle cerebral artery (MCA) is the largest branch of the internal carotid artery (it is most commonly occluded in stroke), and supplies a part of the frontal lobe, and the lateral aspects of the temporal and parietal lobes; and the posterior cerebral artery (PCA), arises from either the basilar artery or internal carotid artery, supplies the temporal and occipital lobes (refer to figure 15B and C for a map of where these arteries distribute blood). Each of these major

arteries have smaller branches. A subset of branching arteries that arise from the middle cerebral artery, are the lenticulostriate arteries. These are deep penetrating arteries that supply the basal ganglia, internal capsule and the surrounding areas (refer to figure 15D). Occlusions to these arteries cause multiple small infarcts, which are known as lacunar strokes. We refer to lacunar strokes as 'small white matter infarcts' or 'small infarcts' in this study (Blood Vessels of The Brain, n.d.).

Figures 15A, B, C & D: Images depicting blood supply in the brain

15A)

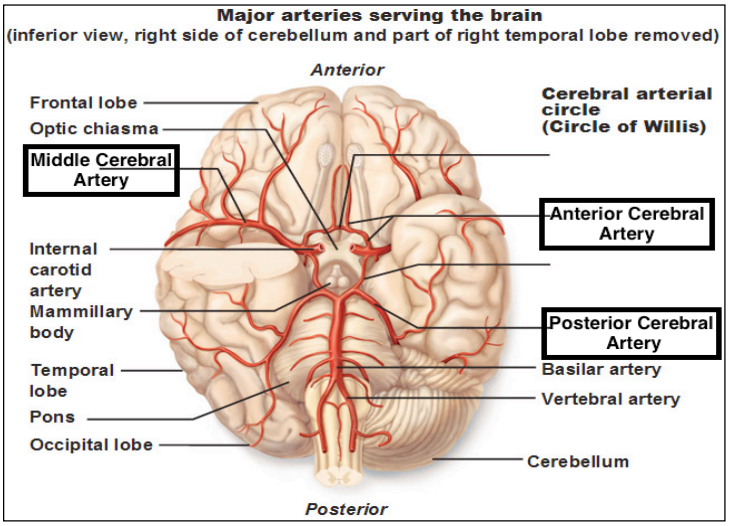

(Antranik, 2011)

The image above shows the circle of Willis, where the vertebrobasilar arteries and internal carotid arteries meet. It also shows the three main arteries that branch off of this circulation: anterior cerebral artery, middle cerebral artery, posterior cerebral artery.

15B)

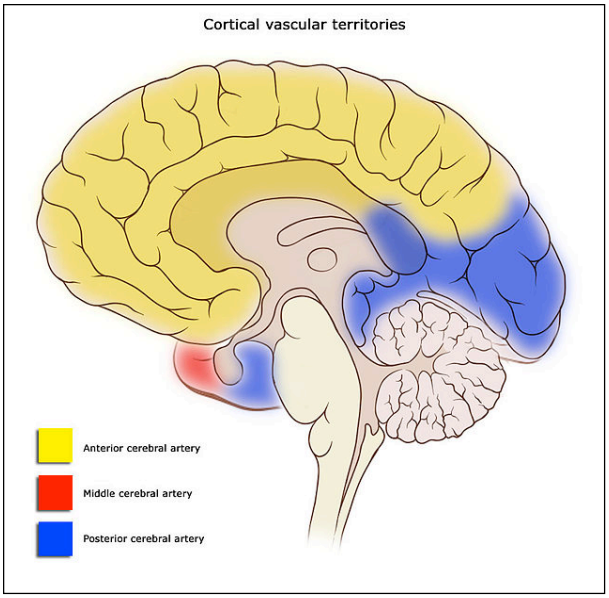

15C)

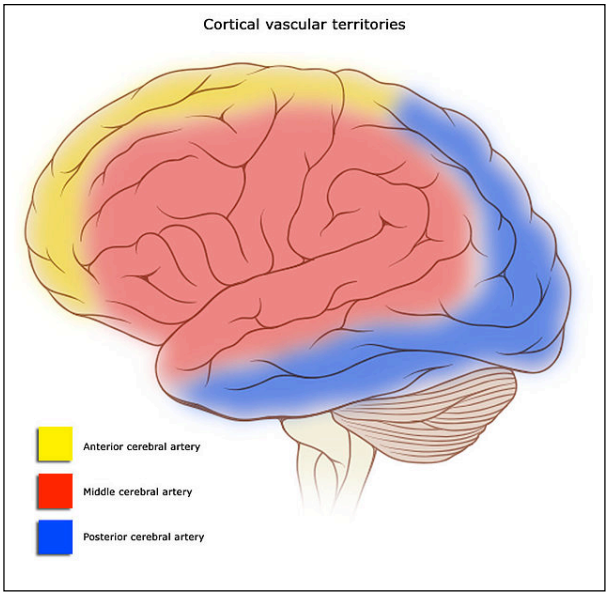

(Lynch P., 2008)

The images above show brain images with medial view (B) lateral view (C) to outline the cortical regions where the anterior, middle and posterior cerebral arteries supply blood. Note that the anterior cerebral artery (ACA) supplies the frontal lobe and parts of the parietal lobe, the middle cerebral artery (MCA) supplies a part of the frontal lobe, and the lateral aspects of the temporal and parietal lobes; and the posterior cerebral artery (PCA) supplies the temporal and occipital lobes.

15D)

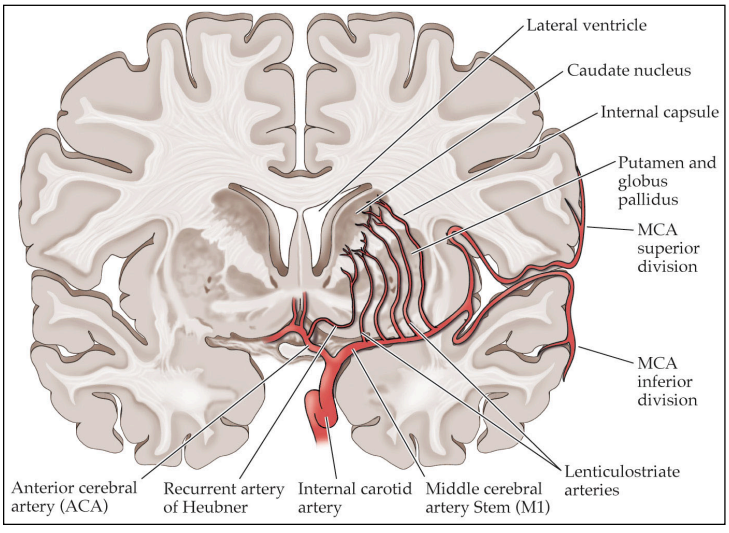

(Sinauer Associates Inc. 2002)

The image above shows the lenticulostriate arteries, which branch off of the middle cerebral artery. These arteries supply the basal ganglia, internal capsule and other adjacent areas. Occlusions of these vessels result in small white infarcts, which are referred to as lacunar infarcts.

Based on the brain imaging and keeping blood supply architecture in mind, lesions were grouped into one of eight distinct groups. Four lesion groups were made based on the four lobes of the brain: a) frontal lobe (2 subjects in this group), b) parietal lobe (4 subjects), c) temporal lobe (3 subjects), and d) occipital lobe (7 subjects) (Appendix A shows examples of lesions included in this study located within these four lobes).

Another group was created to include lesions within the subcortical nuclei including the basal ganglia, thalamus and paraventricular areas, this has been named e) basal ganglia (See Appendix A). There are 11 subjects in this group.

Cases with either small infarcts and/or global brain atrophy without an identifiable stroke lesion, were placed in a unique group named f) atrophied brain. These brain changes are typically observed only in an elderly population. General brain atrophy was assessed by the shrinkage of the cortical gyri. Normally the gyri fill the cranium and press together. The patients judged to have general brain shrinkage (or atrophy) show enlarged spaces between the brain and the cranium and enlarged spaces between neighboring gyri indicating a significant loss of brain volume. MRI brain sections from two of these patients are shown in Appendix A. Most of these patients had both general brain atrophy and multiple small infarcts. The small infarcts were less than 3 mm in any dimension. They usually occurred in white matter, near the first or second ventricle, or in the region of the basal ganglia, due to occlusion of the lenticulostriate arteries. Ten or more infarcts could be easily identified in each of the patients with small infarcts (Appendix A). There are 9 subjects in this group.

Subjects found to have no identifiable lesion on their MRI/CT scan as well as no brain atrophy changes were placed in a group entitled g) neurotypical, as their brains appeared like that

of a normal individual. There are 3 subjects in this group; however, one of them did have a previous history of stroke with no visible brain lesion at this time.

Lastly, an eighth and final group emerged for those patients who had complicated lesions that were not isolated to one lobe or to the basal ganglia, but spanned large areas to include two of groups a)-e) (lesion spans multiple lobes and/or the basal ganglia, or one lobe and the basal ganglia). This group is referred to as h) temporal-parietal+, since all of these lesions included the temporal or parietal lobes or both (Appendix A). Due to the small samples sizes for parietal and temporal lobe only categories, these patients were also included in the temporal-parietal+ group. There are 25 subjects in this group. No further localization was done within this patient category.

It is important to note that if patients showed a lesion larger than 3mm in size, in the presence of brain atrophy findings, they were not placed in the brain atrophy category, but in the category that most accurately explained the location of the lesion, whether it was isolated to one of the brain's lobes, to the basal ganglia, or to multiple areas. In addition, vascular boundaries did not apply strictly to hemorrhagic lesions.

Neurological Subject Categorization Based on Lesion Size

In order to understand the impact of lesion size on testing results, neurological groups that were found to have significant results, were subdivided into two groups for the purposes of within group comparison. One group contained small lesions, less than 4cm for the average lesion dimension. The other group contained large lesions, greater than 4cm for the average lesion dimension. Average lesion dimension was calculated by taking the sum of the length, width and height of a lesion (based on MRI/CT scan measurement scales) and dividing by three. Appendix A shows examples of small and large lesions.

Analysis and Statistics

The primary objective of the study is to gain a better understanding of the neural basis of shape, object and face recognition through binding and segmentation. This was done by first identifying unique brain lesion groups according to size and anatomical location. Each group's results on the Wenzhou Protocol was then individually compared to that of the control group via statistical analysis with a significance level set at $p=0.05$ using JMP statistical software from SAS Institute.

The Wilcoxon Rank Sum Test was the statistical test used. Although the data had equal variance, it was not normally distributed; therefore, a T-test cannot be used. The data is also unpaired between comparative groups; therefore, the unpaired non-parametric version of the T-test was used (Wilcoxon Rank Sum Test). For more information about the variance and normality testing of the data, please see Appendix B.

The major variables of interest were: 'location of brain lesions' (e.g. basal ganglia, occipital lobe), and 'lesion size' (small vs. big) for only two lesion locations (occipital lobe and temporal-parietal+). These two variables were compared for each of the categories of the Wenzhou Protocol. 'Time' was a secondary variable analyzed for each of the categories of the Wenzhou Protocol, within 'lesion location.'

In addition, to study the validity of our results, Pearson correlation coefficients were calculated from the regression program in JMP to determine the impact on Wenzhou Protocol testing by visual acuity.

RESULTS

Control Group Analysis

Two control groups were included in the study: relatives (13 subjects) and cataracts (21 subjects). Table 1a shows demographics of the two groups: number and percentage of subjects in each group, as well as the mean and standard deviation of the age in each group. On average, "cataract" subjects are approximately 19 years older than "relative" subjects in this study.

Table 1a: Number and age of control patients that belong to the cataract and relative groups

Variable	**Cataracts**	**Relatives**
Number of Subjects (N=34)	21 (61.76%)	13 (38.24%)
Age (Mean ± SD)	69.2 ± 8.69	50.3 ± 9.98

To determine whether the two groups can be combined into one large control group, a Wilcoxon Rank Sum test was used to compare their means on the Wenzhou Protocol. Table 1b shows the results of this analysis, including the total number of incorrect questions out of 75, as well as the number of incorrect questions for each of the categories of the test.

Table 1b: Mean errors for relatives and cataract subjects for the total Wenzhou Protocol

Wenzhou Protocol Categories	Number of Questions	Cataracts [Mean(SD)]	Relatives [Mean(SD)]	P-value
Total # of Incorrect on the Protocol	75	4.5 (4.7)	3.3 (3.1)	0.64
Shape Matching	11	0.43 (0.98)	0.31 (0.63)	0.94
Total Segmentation	17	1.3 (1.6)	1.5 (1.8)	0.79
Specific Segmentation	5	0.57 (0.81)	0.54 (0.97)	0.75
Seg. - static unfilled figures	5	0.57 (0.75)	0.23 (0.44)	0.19
Seg. - motion unfilled figures	5	0.095 (0.30)	0.0 (0.0)	0.28
Masking/Distractors	7	0.19 (0.51)	0.69 (0.95)	0.046*
Figure Ground/Depth	3	0.14 (0.36)	0.23 (0.44)	0.54
Total Binding	6	0.62 (0.81)	0.15 (0.56)	0.047*
Binding - 3D shapes	3	0.57 (0.75)	0.077 (0.28)	0.030*
Binding - line binding	3	0.048 (0.22)	0.077 (0.28)	0.76
Name Real Object/Recognition	15	0.48 (0.87)	0.077 (0.28)	0.14
Visual Memory	10	0.71 (0.78)	0.62 (0.51)	0.91
Face Perception	8	0.71 (0.78)	0.46 (0.66)	0.37

*Shows significance of $p<0.05$. Based on the Wilcoxon rank sum test.
Only three categories showed significance: masking/distractors, total binding and binding with 3D shapes.

Table 1c: Average Time taken on Wenzhou protocol by relatives and cataract subjects

Wenzhou Protocol Categories	Cataracts Time (seconds) (Mean ± SD)	Relatives Time (seconds) (Mean ± SD)	P-value
Total Average time for Wenzhou Protocol categories	39.7 ± 15	30.4 ± 8.3	0.018*
Shape Matching	6.0 ± 2.2	4.4 ± 1.2	0.028*
Total Segmentation	7.1 ± 2.9	5.7 ± 1.8	0.1
Specific Segmentation	9.2 ± 3.8	6.3 ± 1.4	0.017*
Seg. - static unfilled figures	5.8 ± 3.0	4.4 ± 1.4	0.16
Seg. - motion unfilled figures	5.0 ± 1.9	4.2 ± 1.2	0.23
Masking/Distractors	6.6 ± 3.2	6.1 ± 3.0	0.51
Figure Ground/Depth	4.3 ± 3.6	3.2 ± 1.4	0.41
Total Binding	5.5 ± 2.6	3.8 ± 1.2	0.012*
Binding - 3D shapes	5.5 ± 3.4	3.4 ± 0.98	0.014*
Binding - line binding	5.5 ± 3.5	4.1 ± 1.6	0.14
Name Real Object/Recognition	5.3 ± 2.6	3.6 ± 1.4	0.049*
Visual Memory	2.7 ± 1.5	2.5 ± 1.1	0.52
Face Perception	3.8 ± 1.8	3.2 ± 1.8	0.07

*Shows significance of $p<0.05$. Based on the Wilcoxon rank sum test.
Six categories showed significance: total average time, shape matching, specific segmentation, total binding, binding with 3D shapes and naming a real object.

The two control groups did not show a significant difference for total errors on the Wenzhou Protocol, with $p=0.64<0.05$. However, cataract patients took longer to complete the Wenzhou Protocol testing ($P=0.018$), which is likely attributed to their older age (Refer to table 1c for Time taken to answer questions on the Wenzhou Protocol).

Only a few categories showed a significant difference between the groups. Masking/distractor slides were significant with $P=0.046$. Cataract patients performed better than relatives for this category. If a difference were to be found between the two groups, one would hypothesize that older cataract subjects would perform worst than the relatives. In addition, "cataract" and "relatives" took the same amount of time on average to answer questions on this section of the Wenzhou Protocol. We suggest this difference in performance on masking/distractor slides is due to chance.

The total binding category also showed a borderline significant difference with $P=0.047$. The cataract subjects performed worst than the relative subjects, and took a significantly longer amount of time on the task ($P=0.012$). To investigate this further, we looked at the two types of binding (line binding and 3D shapes). Only binding with 3D shapes reached statistical significance, with $P=0.03$. Cataract subjects performed approximately 7 times worst than the relatives for this task. Cataract patients also spend significantly longer on this task than relatives ($P=0.014$). The poor performance on total binding by cataract patients is explained by the poor performance on 3D shape binding alone. We do not believe that cataract patients have a true deficit in binding, as line binding is far from significant, with $P=0.76$.

Since the great majority of Wenzhou Protocol category comparisons between cataracts and relatives revealed no significant difference, the two groups were combined together into a

larger control group. This group is referred to as ‘controls,’ and is the main comparison group for analysis of the neurological lesions.

Neurological Patient Analysis

59 neurology patients were tested, 2 were later removed, as there was no report of reason for admission. For statistical analysis the 57 remaining brain lesions have been separated into categories according to location and size of lesions based on the CT or MRI images. The results of this analysis are shown below.

Lesion Location Analysis

With the lesion location groups in mind, statistical analysis was performed for each category of the Wenzhou Protocol between the lesion area of interest and the control patients.

There are 2 patients with lesions isolated to the frontal lobe, 4 with lesions in the parietal lobe, 3 with lesions isolated to the temporal lobe, and 3 labeled as ‘neurotypical’ (because no lesions were found). Despite large lesions in some of these patients, their perceptual performance was similar to that of the control groups and with their small sample size no significant differences from the controls were shown for these groups.

Brain Atrophy/Small Infarct Patients

The brain atrophy/small infarct group contains 9 subjects. Table 2a shows the number of brain atrophy and control subjects, as well as the mean and standard deviation of the age in the group. On average ‘atrophy/small infarct’ patients are only 2 years older than the control patients.

Their results on the Wenzhou Protocol are shown in Table 2b. These patients, except for one or two, performed very well on the Wenzhou Protocol even though their brain functionality appears to be endangered since they have extensive atrophy and many punctate white matter lesions. This is supported by the results in table 2, which show that although aging patients take a little longer on average to answer most of the questions, they do not take significantly longer than controls. These findings suggest that lesion size and location are more important than diffuse/generalized brain atrophy and small white matter infarctions.

Table 2a: Number and age of atrophy/small infarct subjects and control patients included in the study

Variable	Controls	Atrophy/Small Infarct Patients
Number of Subjects	34	9
Age (Mean ± SD)	62.0 ± 13.0	64.1 ± 12.6

Table 2b: Mean errors for brain atrophy/small infarct subjects vs. controls for the total Wenzhou Protocol

Wenzhou Protocol Results	Number of Questions	CONTROLS (Mean ± SD)	Atrophy/Small Infarct (Mean ± SD)	P-value
Total # of Incorrect on the protocol	75	4.1 ± 4.2	3.7 ± 4.7	0.50
Shape Matching	11	0.38 ± 0.85	0.33 ± 0.85	0.97
Total Segmentation	17	1.4 ± 1.7	1.2 ± 1.6	0.83
Specific Segmentation	5	0.56 ± 0.86	0.33 ± 0.50	0.68
Seg. - static unfilled figures	5	0.44 ± 0.66	0.33 ± 1.0	0.26
Seg. - motion unfilled figures	5	0.059 ± 0.24	0.0 ± 0.0	0.49
Masking/Distractors	7	0.38 ± 0.74	0.55 ± 1.3	0.91
Figure Ground/Depth	3	0.18 ± 0.39	0.22 ± 0.44	0.77
Total Binding	6	0.44 ± 0.75	0.11 ± 0.33	0.24
Binding - 3D shapes	3	0.38 ± 0.65	0.0 ± 0.0	0.072
Binding - line binding	3	0.059 ± 0.24	0.11 ± 0.33	0.61
Name Real Object/Recognition	15	0.32 ± 0.73	0.0 ± 0.0	0.15
Visual Memory	10	0.68 ± 0.68	1.3 ± 2.7	0.76
Face Perception	8	0.62 ± 0.74	0.44 ± 0.73	0.50

*Shows significance of $p<0.05$ based on the Wilcoxon rank sum test.
None of the comparisons are statistically significant.

Table 2c: Average Time taken on Wenzhou protocol by brain atrophy/small infarct subjects

Wenzhou Protocol Categories	**Controls Time (seconds) (Mean ± SD)**	**Atrophy/Small Infarct Time (seconds) (Mean ± SD)**	**P-value**
Total Average time for Wenzhou Protocol categories	36.1 ± 13.3	40.5 ± 18.7	0.71
Shape Matching	5.4 ± 2.0	5.8 ± 3.4	0.79
Total Segmentation	6.5 ± 2.6	7.2 ± 3.6	0.96
Specific Segmentation	8.4 ± 3.7	8.4 ± 3.7	0.75
Seg. - static unfilled figures	5.3 ± 2.6	6.9 ± 4.7	0.86
Seg. - motion unfilled figures	4.7 ± 1.7	5.6 ± 3.1	0.85
Masking/Distractors	6.4 ± 3.1	6.5 ± 3.4	0.93
Figure Ground/Depth	3.8 ± 2.9	5.0 ± 3.9	0.39
Total Binding	4.8 ± 2.3	5.8 ± 2.8	0.23
Binding - 3D shapes	4.7 ± 2.9	5.6 ± 2.4	0.11
Binding - line binding	5.0 ± 3.0	6.0 ± 3.6	0.29
Name Real Object/Recognition	4.6 ± 2.4	3.8 ± 1.2	0.69
Visual Memory	2.6 ± 1.3	3.4 ± 2.6	0.75
Face Perception	3.6 ± 1.8	3.9 ± 1.9	0.72

*Shows significance of $p<0.05$.
None of the comparisons are statistically significant.

Basal Ganglia Patients

There were 11 subjects in the basal ganglia group. Refer to table 3a for the mean and standard deviation age of the group, Note, that basal ganglia patients have a similar average age as controls, only 3 years younger. The performance of the basal ganglia patients on the Wenzhou Protocol is shown in Table 3b.

Table 3a: Number and age of basal ganglia patient included in the study

Variable	**Basal Ganglia Patients**
Number of Subjects	11
Age (Mean ± SD)	59.3 ± 9.8

Table 3b: Mean errors for basal ganglia subjects vs. controls for the total Wenzhou Protocol

Wenzhou Protocol Results	Number of Questions	CONTROLS (Mean ± SD)	BASAL GANGLIA (Mean ± SD)	P-value
Total # of Incorrect on the protocol	75	4.1 ± 4.2	4.3 ± 5.0	0.81
Shape Matching	11	0.38 ± 0.85	0.63 ± 1.0	0.39
Total Segmentation	17	1.4 ± 1.7	1.3 ± 1.85	0.81
Specific Segmentation	5	0.56 ± 0.86	0.73 ± 1.3	0.90
Seg. - static unfilled figures	5	0.44 ± 0.66	0.091 ± 0.30	0.10
Seg. - motion unfilled figures	5	0.059 ± 0.24	0.091 ± 0.30	0.74
Masking/Distractors	7	0.38 ± 0.74	0.45 ± 0.69	0.60
Figure Ground/Depth	3	0.18 ± 0.39	0.091 ± 0.30	0.51
Total Binding	6	0.44 ± 0.75	0.45 ± 0.93	0.91
Binding - 3D shapes	3	0.38 ± 0.65	0.091 ± 0.30	0.17
Binding - line binding	3	0.059 ± 0.24	0.36 ± 0.92	0.21
Name Real Object/Recognition	15	0.32 ± 0.73	0.45 ± 1.2	0.94
Visual Memory	10	0.68 ± 0.68	0.82 ± 0.98	0.86
Face Perception	8	0.62 ± 0.74	0.45 ± 0.69	0.52

*Shows significance of $p<0.05$ based on the Wilcoxon rank sum test.
None of the comparisons are statistically significant.

Table 3c: Average Time taken on Wenzhou protocol by basal ganglia subjects

Wenzhou Protocol Categories	Controls Time (seconds) (Mean ± SD)	Basal Ganglia Time (seconds) (Mean ± SD)	P-value
Total Average time for Wenzhou Protocol categories	36.1 ± 13.3	37.7 ± 18.2	0.83
Shape Matching	5.4 ± 2.0	6.0 ± 3.8	1.0
Total Segmentation	6.5 ± 2.6	7.1 ± 4.0	0.76
Specific Segmentation	8.4 ± 3.7	8.0 ± 4.4	0.77
Seg. - static unfilled figures	5.3 ± 2.6	6.8 ± 4.8	0.34
Seg. - motion unfilled figures	4.7 ± 1.7	5.5 ± 3.1	0.92
Masking/Distractors	6.4 ± 3.1	6.6 ± 3.6	0.86
Figure Ground/Depth	3.8 ± 2.9	3.3 ± 1.2	0.77
Total Binding	4.8 ± 2.3	5.3 ± 2.9	0.80
Binding - 3D shapes	4.7 ± 2.9	5.9 ± 4.6	0.48
Binding - line binding	5.0 ± 3.0	4.7 ± 2.8	0.88
Name Real Object/Recognition	4.6 ± 2.4	4.6 ± 3.9	0.43
Visual Memory	2.6 ± 1.3	2.8 ± 1.4	0.69
Face Perception	3.6 ± 1.8	3.1 ± 0.71	0.96

*Shows significance of $p<0.05$. None of the comparisons are statistically significant.

Basal ganglia subjects do not show any deficits on the Wenzhou Protocol testing, and spend a similar amount of time as control patients for each of the categories (Refer to Table 3c). This indicates that this anatomical location is not playing a direct role in binding, parsing, or any other of the higher order functions.

We now look at some lesion areas that show significant functional deficits.

Occipital Subjects

There were 6 patients with lesions isolated to the occipital lobe. Table 4a shows the mean and standard deviation age of occipital subjects. Occipital patients are similar in age to control patients, with only a 3-year average difference.

Table 4a: Number and age of occipital patients included in the study

Variable	**OCCIPITAL**
Number of Subjects	7
Age (Mean ± SD)	59.0 ± 16.4

Table 4b: Mean errors for occipital subjects vs. controls for the total Wenzhou Protocol

Wenzhou Protocol Results	**Number of Questions**	**CONTROLS (Mean ± SD)**	**OCCIPITAL (Mean ± SD)**	**P-value**
Total # of Incorrect on the protocol	75	4.1 ± 4.2	12.6 ± 9.1	0.0064*
Shape Matching	11	0.38 ± 0.85	1.6 ± 2.4	0.20
Total Segmentation	17	1.4 ± 1.7	3.4 ± 3.5	0.15
Specific Segmentation	5	0.56 ± 0.86	1.6 ± 1.7	0.12
Seg. - static unfilled figures	5	0.44 ± 0.66	0.86 ± 0.90	0.21
Seg. - motion unfilled figures	5	0.059 ± 0.24	0.71 ± 1.1	0.0066*
Masking/Distractors	7	0.38 ± 0.74	1.0 ± 1.3	0.23
Figure Ground/Depth	3	0.18 ± 0.39	0.14 ± 0.38	0.85
Total Binding	6	0.44 ± 0.75	1.29 ± 1.6	0.12
Binding - 3D shapes	3	0.38 ± 0.65	0.43 ± 0.53	0.64
Binding - line binding	3	0.059 ± 0.24	0.86 ± 1.5	0.055
Name Real Object/Recognition	15	0.32 ± 0.73	1.3 ± 1.6	0.038*
Visual Memory	10	0.68 ± 0.68	2.7 ± 2.7	0.013*
Face Perception	8	0.62 ± 0.74	1.4 ± 0.79	0.019*

*Shows significance of $p<0.05$ based on the Wilcoxon rank sum test.
Five categories showed significance: total # of incorrect, unfilled figures segmentation with motion, name a real object, visual memory and face perception.

Table 4c: Average Time taken on Wenzhou protocol by occipital subjects

Wenzhou Protocol Categories	Controls Time (seconds) (Mean ± SD)	Occipital Lobe Time (seconds) (Mean ± SD)	P-value
Total Average time for Wenzhou Protocol categories	36.1 ± 13.3	55.5 ± 25.5	0.03*
Shape Matching	5.4 ± 2.0	8.3 ± 5.5	0.35
Total Segmentation	6.5 ± 2.6	10.0 ± 4.5	0.031*
Specific Segmentation	8.4 ± 3.7	9.4 ± 5.3	0.82
Seg. - static unfilled figures	5.3 ± 2.6	10.1 ± 5.6	0.0064*
Seg. - motion unfilled figures	4.7 ± 1.7	7.9 ± 4.1	0.052
Masking/Distractors	6.4 ± 3.1	10.4 ± 5.8	0.044*
Figure Ground/Depth	3.8 ± 2.9	6.3 ± 5.0	0.2
Total Binding	4.8 ± 2.3	8.6 ± 5.7	0.029*
Binding - 3D shapes	4.7 ± 2.9	10.3 ± 6.7	0.0065*
Binding - line binding	5.0 ± 3.0	7.2 ± 5.5	0.35
Name Real Object/Recognition	4.6 ± 2.4	6.5 ± 2.7	0.11
Visual Memory	2.6 ± 1.3	3.6 ± 1.4	0.0092*
Face Perception	3.6 ± 1.8	4.1 ± 1.8	0.25

*Shows significance of $p<0.05$ based on the Wilcoxon rank sum test.
Seven categories showed significance: total # of incorrect, specific total segmentation, static unfilled figure segmentation, masking/distractors, total binding, 3D shape binding, and visual memory.

The results of the Wenzhou Protocol for occipital patients are shown in table 4b. A significant difference between controls and occipital patients was found for total number of errors on the Wenzhou Protocol, with P=0.0064. The poor performance by occipital subjects over controls was also reflected in how long they took to complete the Wenzhou Protocol, P=0.03 (Refer to Table 4c). We now analyze which categories on the Wenzhou Protocol account for this overall result.

Occipital subjects do not show a significant deficit in segmentation. Although performance on total segmentation and specific segmentation was worse in occipital patients than controls, this difference approached, but did not reach significance. Occipital subjects also take longer to perform many of the segmentation questions. Segmentation of unfilled figures

with motion does reveal a significant difference between occipital patients and controls (P=0.0066), but this difference is not shown for the unfilled figures without motion (P=0.21). This result is due to the fact that the controls showed a strong improvement (nearly 7 times fewer errors) when the figures moved, while the occipital patients showed relatively little improvement with motion.

Occipital patients perform worse on binding than controls, but this difference does not reach significance, with P=0.12 on total binding and P=0.64 on 3-D shape binding. However, these subjects spend significantly longer performing both tasks (P=0.029 for total binding and P=0.0065 for 3-D shape binding). While line binding approaches significance, it does not reach it, with P=0.055. Occipital patients do not spend longer than controls on the line-binding task (P=0.35). Perhaps there is a binding deficit in this patient population. We will investigate this further when looking at lesion size.

The categories of the Wenzhou Protocol in which occipital patients performed significantly worse than controls were: visual memory (P=0.013), face perception (p=0.019) and naming a real object (P=0.038). On average, occipital patients made 20 times as many errors as the controls when naming real objects, more than 6 times as many errors for face perception, and 5 times as many errors for visual memory. Only the visual memory category showed occipital patients spending more time than controls (P=0.0092).

These findings for the occipital lobe lesions suggest that there are different pathways for face perception, visual memory, and object naming compared to binding and segmentation, or there is an element common to these categories different than for other tasks. Note that faces and real objects are things we recognize through memory. The findings from the lesion group in the next section emphasize this point.

Temporal-Parietal+ Subjects

This group is made up of 25 subjects that have lesions that are at least 1 cm (in height, width and length) in the temporal and or parietal lobe, and these lesions may infringe on the adjacent occipital or frontal lobes. Table 5a shows the mean and standard deviation age of occipital subjects. Temporal-parietal+ patients are nearly the same age as control patients, with only a 1-year average difference.

The results of the Wenzhou Protocol for temporal-parietal+ patients are shown in table 5b. These patients make significantly more errors than control patients on the whole Wenzhou protocol (P=0.0033). They also take longer to complete the protocol than controls, P=0.0015 (Refer to table 5c). This difference in performance is due to poor performance in categories that differ from the deficits in other patient populations: shape matching (P=0.013), masking/distractors (P=0.0031), and figure ground/depth (P=0.026).

Table 5a: Number and age of Temporal-Parietal+ patients included in the study

Variable	**Temporal-Parietal+ Patients**
Number of Subjects	25
Age (Mean ± SD)	62.9 ± 13.7

Table 5b: Mean errors for temporal-parietal+ subjects vs. controls for total Wenzhou Protocol

Wenzhou Protocol Results	**Number of Questions**	CONTROLS (Mean ± SD)	TEMPORAL-PARIETAL (Mean ± SD)	P-value
Total # of Incorrect on the protocol	75	4.1 ± 4.2	9.0 ± 8.4	0.0033*
Shape Matching	11	0.38 ± 0.85	1.3 ± 1.6	0.013*
Total Segmentation	17	1.4 ± 1.7	3.0 ± 3.0	0.0095*
Specific Segmentation	5	0.56 ± 0.86	1.0 ± 0.22	0.084
Seg. - static unfilled figures	5	0.44 ± 0.66	0.68 ± 1.1	0.75
Seg. - motion unfilled figures	5	0.059 ± 0.24	0.40 ± 0.87	0.083
Masking/Distractors	7	0.38 ± 0.74	1.3 ± 1.6	0.0031*
Figure Ground/Depth	3	0.18 ± 0.39	0.52 ± 0.71	0.026*
Total Binding	6	0.44 ± 0.75	0.76 ± 1.2	0.29
Binding - 3D shapes	3	0.38 ± 0.65	0.44 ± 0.58	0.520
Binding - line binding	3	0.059 ± 0.24	0.32 ± 0.90	0.37
Name Real Object/Recognition	15	0.32 ± 0.73	0.92 ± 2.8	0.50
Visual Memory	10	0.68 ± 0.68	1.1 ± 1.1	0.22
Face Perception	8	0.62 ± 0.74	1.0 ± 1.1	0.23

*Shows significance of $p<0.05$ based on the Wilcoxon rank sum test.
Five categories showed significance: total # of incorrect, shape matching, total segmentation, masking/distractors, and figure ground/depth.

Table 5c: Average Time taken on Wenzhou protocol by temporal-parietal+ subjects

Wenzhou Protocol Categories	**Controls Time (seconds) (Mean ± SD)**	**Temporal-Parietal+ Time (seconds) (Mean ± SD)**	**P-value**
Total Average time for Wenzhou Protocol categories	36.1 ± 13.3	50.2 ± 25.8	0.0013*
Shape Matching	5.4 ± 2.0	7.3 ± 4.2	0.13
Total Segmentation	6.5 ± 2.6	10.8 ± 5.7	0.0015*
Specific Segmentation	8.4 ± 3.7	10.7 ± 5.8	0.082
Seg. - static unfilled figures	5.3 ± 2.6	9.7 ± 6.5	0.022*
Seg. - motion unfilled figures	4.7 ± 1.7	7.0 ± 4.6	0.17
Masking/Distractors	6.4 ± 3.1	11.1 ± 6.7	0.0011*
Figure Ground/Depth	3.8 ± 2.9	5.5 ± 3.2	0.0014*
Total Binding	4.8 ± 2.3	7.8 ± 4.7	0.0078*
Binding - 3D shapes	4.7 ± 2.9	7.8 ± 5.7	0.015*
Binding - line binding	5.0 ± 3.0	7.2 ± 4.0	0.014*
Name Real Object/Recognition	4.6 ± 2.4	5.9 ± 4.0	0.45
Visual Memory	2.6 ± 1.3	3.0 ± 1.7	0.35
Face Perception	3.6 ± 1.8	4.3 ± 2.2	0.07

*Shows significance of $p<0.05$ based on the Wilcoxon rank sum test.
Eight categories showed significance: total # of incorrect, specific total segmentation, static unfilled figure segmentation, masking/distractors, figure ground/depth, total binding, 3D shape binding, and line binding.

These subjects perform poorly on masking/distractors (P=0.0031) and figure ground/depth (P=0.026). These patients also spend a longer time completing these tasks than controls (P=0.0011 for masking/distractors, P=0.0014 for figure ground/depth).

Temporal-parietal+ patients show decreased performance on shape matching compared to controls (P=0.013), even though shape matching is a relatively simple task. These subjects also spend longer than controls on shape matching slides, but it does not reach statistical significance (P=0.13). The poor performance on shape matching may be explained by crowding or simple masking, due to having multiple shapes on each slide. In some slides, there are up to 9 shapes present.

Specific segmentation for the temporal-parietal+ group approaches but does not reach significance for performance (P=0.084) and time (P=0.082). Furthermore, static unfilled figure segmentation is far from statistical significance (P=0.75); therefore, poor performance on specific segmentation is likely attributed to masking due to the complex nature of these slides rather than a deficit in segmentation/parsing itself.

In addition, performance for total binding (P=0.29), 3D shape binding (P=0.52) and line binding (P=0.37) do not approach statistical significance.

These findings show that temporal-parietal+ subjects have a deficit in masking as they have trouble deciphering figures of interest that are masked or distracted by other shapes/stimuli.

Lesion Size Analysis

We now turn our attention to the effect of the size of the lesion on Wenzhou Protocol performance. Only two neurological lesion location groups revealed interesting deficits on the

Wenzhou Protocol. These were occipital and temporal-parietal+ subjects. As a result, lesion size analysis was only conducted in these two groups, to better understand the impact of lesion size.

One would hypothesize larger lesions cause greater loss of function; therefore, we look at which functions are most impacted by larger lesions in our two groups of interest.

Occipital Subjects

Table 6 shows the results of the lesion size analysis by comparing occipital patients with an average lesion dimension (take the average of the length, width and height of the lesion) less than 4cm to those greater than 4cm. There are 4 patients in the small lesion group and 3 in the large lesion group.

Table 6: Performance on the Wenzhou Protocol for occipital subjects with small vs. large lesions

Wenzhou Protocol Results	**Number of Questions**	**SMALL LESIONS (Mean ± SD)**	**LARGE LESIONS (Mean ± SD)**	**P-value**
Number of Patients		4	3	
Seg. - motion unfilled figures	5	0.0 ± 0.0	1.7 ± 1.2	0.030*
Masking/Distractors	7	0.0 ± 0.0	2.3 ± 0.58	0.030*
Shape Matching	11	0.0 ± 0.0	3.7 ± 2.5	0.032*
Specific Segmentation	5	0.25 ± 0.50	3.3 ± 0.58	0.042*
Total # of Incorrect on the protocol	75	5.8 ± 4.3	21.7 ± 1.5	0.050*
Total Segmentation	17	0.75 ± 0.96	7.0 ± 1.0	0.050*
Total Binding	6	0.25 ± 0.50	2.7 ± 1.5	0.064
Name Real Object/Recognition	15	0.25 ± 0.50	2.7 ± 1.5	0.064
Binding - line binding	3	0.0 ± 0.0	2.0 ± 1.7	0.12
Seg. - static unfilled figures	5	0.50 ± 0.58	1.33 ± 1.2	0.35
Figure Ground/Depth	3	0.0 ± 0.0	0.33 ± 0.58	0.39
Binding - 3D shapes	3	0.25 ± 0.50	0.67 ± 0.58	0.41
Visual Memory	10	3.0 ± 3.6	2.3 ± 1.5	1.0
Face Perception	8	1.5 ± 0.58	1.3 ± 1.2	1.0

*Shows significance of $p<0.05$ based on the Wilcoxon rank sum test.
Five categories showed significance: motion of unfilled figures, masking/distractors, shape matching, specific segmentation and total # of incorrect.

There is a significant difference between small and large lesion groups for total number of errors made on the Wenzhou Protocol. As expected, larger lesions cause significantly more errors than smaller lesions (P=0.050), this difference is nearly a factor of four.

In addition, the large lesion group performed much worse in all categories, except for visual memory (P=1.0), face perception (P=1.0), 3-D shape binding (P=0.41) and figure ground/depth (P=0.39). Recall that the earlier lesion location analysis of occipital patients revealed a significant deficit in visual memory and face perception. This finding suggests that occipital patients' deficit in face perception and visual memory is not dependent on lesion size.

Lesion location analysis of occipital patients revealed a deficit in naming real objects/object recognition and in questions with motion of unfilled figures. These deficits appear to be dependent largely on lesion size. For object recognition, larger lesions cause more than 10 times more errors than smaller lesions, this difference approaches but does not reach significance (P=0.064). While unfilled figures with motion reached significance as small lesions show no errors, and large lesions get nearly 2 questions wrong (P=0.03).

Many other categories are also greatly impacted by lesion size. Shape matching (P=0.032) and masking/distractor (P=0.030) show a significant difference between lesion groups, with large lesion patients showing multiple errors, and small lesion patients having no errors. For specific segmentation, large lesions show significantly more errors than small lesions (more than 13 times), with P=0.042. Unfilled static figures do not show a significant difference due to lesion size; however, patients with larger lesions show more than two times the number of errors as small lesions. These findings indicate that although segmentation may not occur primarily in the occipital lobe, this cortical region can play a role in segmentation if the lesion is large enough.

Total binding shows a similar finding. Patients with large lesions show more than 10 times as many errors as those with smaller lesions on total binding. This difference approaches, but does not reach significance (P=0.064). This difference in performance is not explained by 3-D shape binding (P=0.41), but by line binding. In line binding, the large lesion group had an average of 2 errors out of 3 questions, while the small lesion group had no errors. This comparison approached but did not reach statistical significance (P=0.12). Recall that lesion location analysis in the occipital lobe showed borderline yet non-significant performance on line binding (P=0.055). Poor performance on line binding by occipital patients is driven mainly by large lesions. This suggests the occipital lobe plays a secondary role in line binding, rather than a primary role. Furthermore, line binding and 3-D shape binding both appear to be occurring through different pathways.

Temporal-Parietal+ Subjects

The temporal-parietal+ patients were divided into two groups, with 6 subjects in the small lesion group (lesion size is less than 4cm for the average lesion dimension) and 19 in the large lesion group (lesion size is greater than 4cm for the average lesion dimension). Refer to Table 7 for the performance of these groups on the categories of the Wenzhou Protocol.

Table 7 is arranged from smallest to largest p-value, which shows the categories most affected by lesion size at the top of the table. As expected, the larger the lesion, the greater the total number of errors on the Wenzhou Protocol (P=0.0044). This is true for the majority of categories. Categories that reached statistical significance for lesion size comparison include: face perception (P=0.026), 3D shape binding (P=0.029), and static unfilled objects (P=0.049). In addition, naming approached but did not reach statistical significance (P=0.099). None of these

categories were statistically significant for lesion location analysis. This suggests that the temporal and or parietal lobes play a role in shape/figure/face interpretation and processing, but not a primary role.

Table 7: Performance on the Wenzhou Protocol for temporal-parietal+ subjects with small vs. large lesions

Wenzhou Protocol Results	**Number of Questions**	**SMALL LESIONS (Mean ± SD)**	**LARGE LESIONS (Mean ± SD)**	**P-value**
Number of Patients		6	19	
Face Perception	8	0.17 ± 0.41	1.3 ± 1.1	0.026*
Binding - 3D shapes	3	0.0 ± 0.0	0.58 ± 0.61	0.029*
Total # of Incorrect on the protocol	75	4.2 ± 2.6	10.5 ± 9.0	0.044*
Seg. - static unfilled figures	5	0.0 ± 0.0	0.89 ± 1.2	0.049*
Name Real Object/Recognition	15	0.0 ± 0.0	1.2 ± 3.2	0.099
Total Segmentation	17	1.3 ± 0.82	3.5 ± 3.2	0.15
Masking/Distractors	7	0.50 ± 0.55	1.6 ± 1.7	0.17
Seg. - motion unfilled figures	5	0.0 ± 0.0	0.53 ± 0.96	0.19
Total Binding	6	0.33 ± 0.82	0.89 ± 1.2	0.21
Shape Matching	11	0.67 ± 1.2	1.5 ± 1.7	0.28
Specific Segmentation	5	0.83 ± 0.98	1.05 ± 1.2	0.79
Binding - line binding	3	0.33 ± 0.82	0.32 ± 0.95	0.82
Figure Ground/Depth	3	0.67 ± 1.2	0.47 ± 0.51	0.83
Visual Memory	10	1.0 ± 1.1	1.1 ± 1.1	0.89

*Shows significance of $p<0.05$ based on the Wilcoxon rank sum test.
Four categories showed significance: face perception, binding of 3D shapes, total # of incorrect, and static segmentation of unfilled figures.

Earlier lesion location analysis for temporal-parietal+ patients showed deficits in distractors/masking, figure ground/depth, shape matching, with specific segmentation approaching but not reaching significance. Lesion size analysis confirms that deficits in figure ground/depth (P=0.83), line binding (P=0.82) and specific segmentation (P=0.79) are not dependent on lesion size. While masking/distractors (P=0.17) and shape matching (P=0.28) are not heavily influenced by lesion size. Therefore, these deficits appear to be present in this

population regardless of the lesion size, consistent with temporal-parietal+ patients having a deficit in masking.

The contrasting findings of different lesion sizes for line and 3-D shape binding (shown in Table 7) supports the idea that these two types of binding use unique shape/figure processing pathways.

Motion Information

In order to understand the impact of motion on the perception of objects or shapes, we look at the categories of static unfilled figures (5 questions) and unfilled figures with motion (5 questions) (refer to table 8 and figure 16). We find that motion information is helpful in reducing errors on unfilled figure slides for subjects in almost all of the patient groups regardless of lesion size. The only group that did not benefit from motion was the occipital patients with large lesions. This may be due to chance, as there are only 3 subjects in this group. But this small group had by far the worst performance in both the stable and motion conditions so they may differ from other patients in some real way.

Control patients benefit greatly from motion information (P=0.0026), with a 7-fold improvement on the task. Brain atrophy patients also show a large improvement, while basal ganglia patients perform well in both the static and motion scenarios. Occipital and temporal-parietal+ patients benefit the least from motion. While, patients with the smaller lesions in this group performed well in both scenarios or improved with motion, those with larger lesions showed minimal or no improvement, likely due to the complex nature of these lesions that likely disrupt object/shape interpretation, as discussed above in the lesion size analysis section.

Table 8: Comparison of means for static unfilled figures and unfilled figures with motion within each patient group

Subject Group (# of subjects)	Static Unfilled Figures (Mean ± SD)	Unfilled Figures with Motion (Mean ± SD)	P-value
Control Patients (34)	0.44 ± 0.66	0.059 ± 0.24	0.0026*
Brain Atrophy/Small Infarcts (11)	0.33 ± 1.00	0.00 ± 0.00	0.37
Basal Ganglia (9)	0.091 ± 0.30	0.091 ± 0.31	1.00
Occipital (7)	0.86 ± 0.90	0.71 ± 1.11	0.68
Occipital Small Lesions (4)	0.50 ± 0.58	0.0 ± 0.0	0.18
Occipital Large Lesions (3)	1.3 ± 1.15	1.7 ± 1.15	1.00
Temporal-Parietal+ (25)	0.68 ± 1.14	0.40 ± 0.87	0.26
Temporal-Parietal+ Small Lesions (6)	0.0 ± 0.0	0.0 ± 0.0	NA
Temporal-Parietal+ Large Lesions (19)	0.89 ± 1.24	0.53 ± 0.96	0.25

*Shows significance of $p<0.05$ based on the Wilcoxon rank sum test.
One subject group showed significance: control patients.

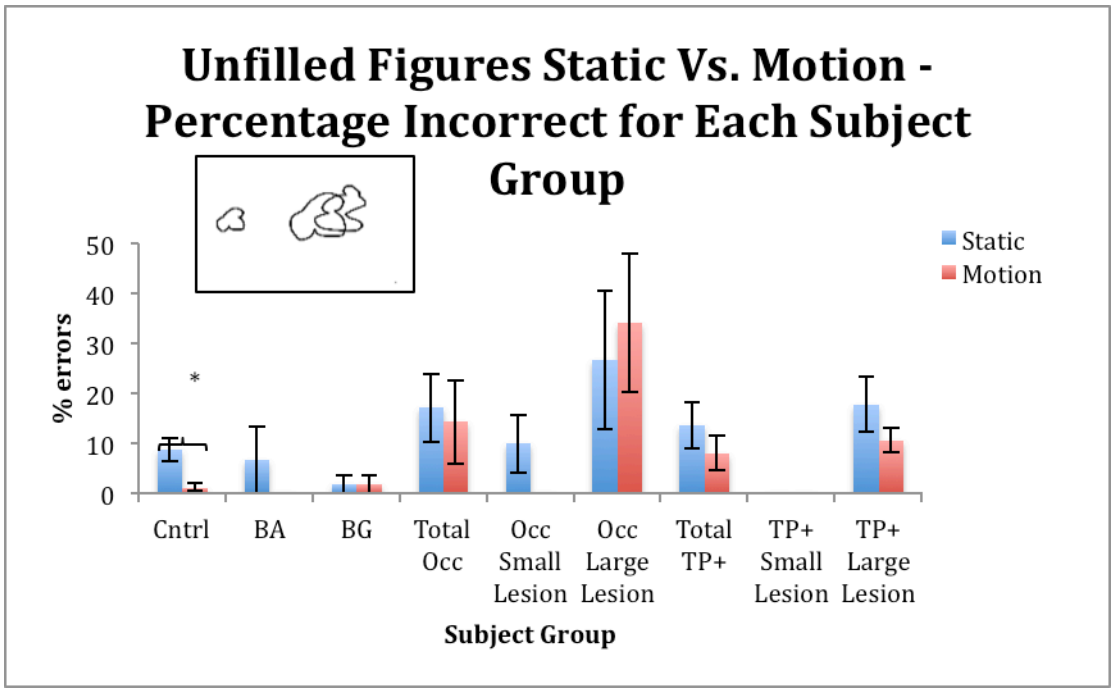

Figure 16: Graph of Unfilled Figures - Performance for Static Vs. Motion

The graph shows performance of all subject groups for unfilled figures. Motion helps increase performance by decreasing errors. Notice that this finding is significant in controls, and is present but non-significant in brain atrophy, occipital and TP+ patients. Basal Ganglia patients do not show improvement. Occipital patients with large lesions show the opposite trend, as motion does not improve performance (7% increase in errors). However, this may be due to chance, as there are only 3 subjects in this group.

Visual Acuity Analysis

Next, we look at visual acuity, to understand the impact of visual acuity on performance of the Wenzhou protocol for different lesion groups. Recall, that this study measured visual acuity using three different Landolt C tests. One test contained a single 'isolated" Landolt C; the other two tests had multiple Landolt Cs on the chart, with different spacing between the optotypes, either 1 stroke separation or 5 stroke separation. See figure 17a, b and c for scatterplots showing Wenzhou protocol performance, compared to the three types of visual acuity in control, occipital and temporal-parietal+ subjects. As expected, Wenzhou protocol performance improved for all groups with better visual acuity, while this correlation was only statistically significant in control subjects, not in neurological subjects. The strength of the correlation ranged from weak to moderate across the subject groups. Therefore, worsening visual acuity does not heavily influence performance of the neurological subjects.

Figures 17A, B & C: Scatter plot for the three types of visual acuity vs. performance on the Wenzhou Protocol for control, occipital and temporal-parietal+ subjects

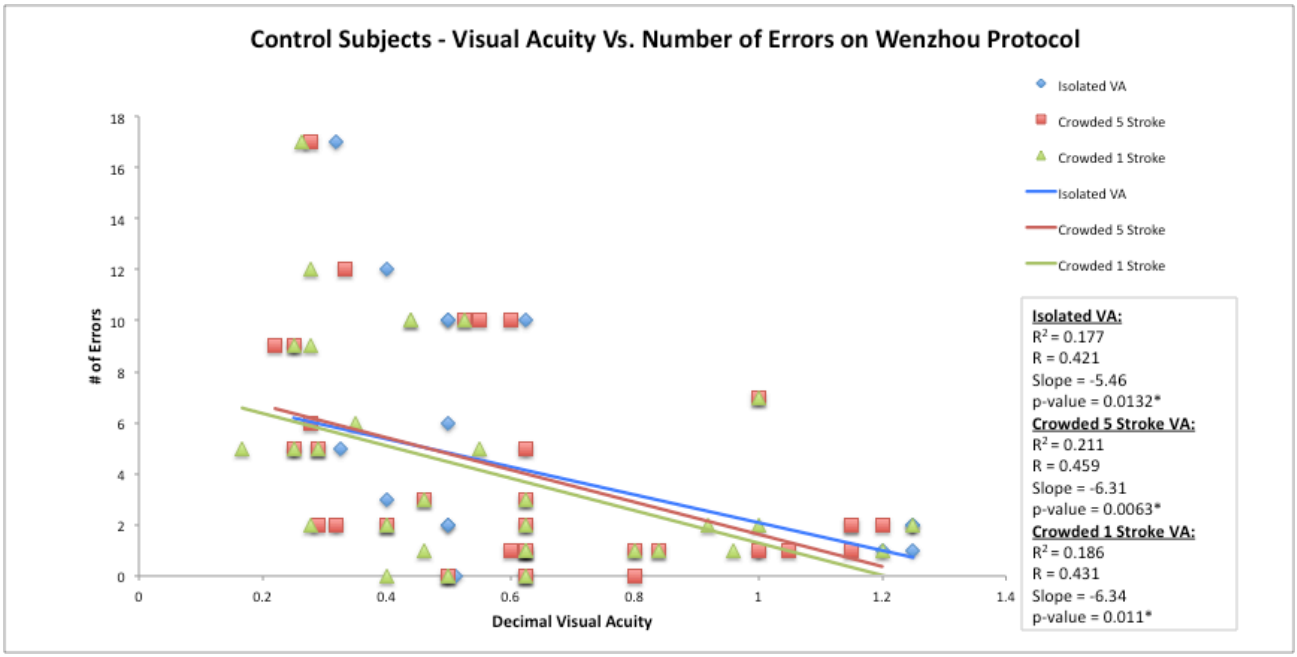

Figure17A Shows the scatter plot for control subjects, comparing the three types of visual acuity to performance on the Wenzhou Protocol. Notice that performance improves (fewer errors) with better visual acuity. This is a significant finding, based on the p-values less than 0.05. This trend has moderate strength, as seen by the Pearson correlation coefficients in the table (Isolated VA R=0.421, Crowded 5 Stroke R=0.459, Crowded 1 Stroke R=0.431). In addition, the slopes of the three visual acuity regression lines are nearly identical to each other. Note, that visual acuity explains only 18-21% of the variance in performance.

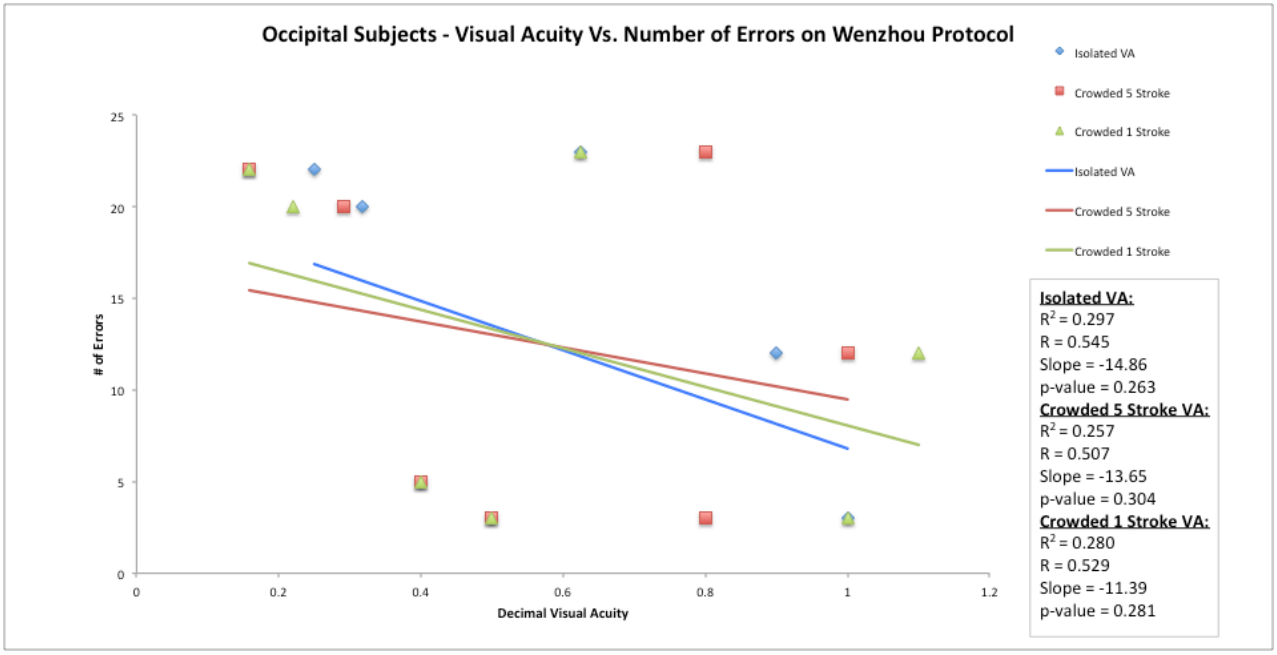

Figure 17B shows the scatter plot for occipital subjects, comparing the three types of visual acuity to performance on the Wenzhou Protocol. Notice that performance improves (fewer errors) with better visual acuity. This is a non-significant finding, based on the p-values greater than 0.05. This trend has moderate strength, as seen by the Pearson correlation coefficients in the table (Isolated VA R=0.545, Crowded 5 Stroke R=0.507, Crowded 1 Stroke R=0.529). In addition, the slopes of the three visual acuity regression lines are similar to each other. Note, that visual acuity explains only 26-30% of the variance in performance.

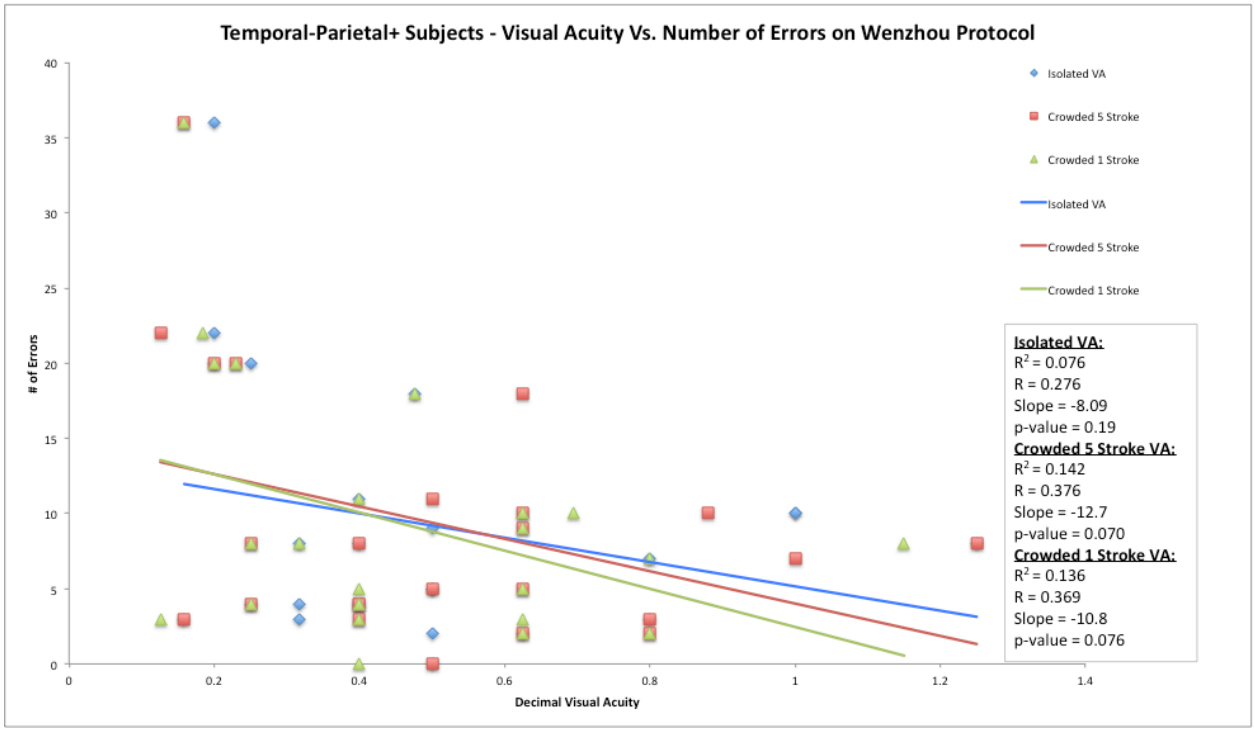

Figure 17C shows the scatter plot for temporal-parietal+ subjects, comparing the three types of visual acuity to performance on the Wenzhou Protocol. Notice that performance improves (fewer errors) with better visual acuity. This is a non-significant finding, based on the p-values greater than 0.05. This strength of the correlation is mild, as seen by the Pearson correlation coefficients in the table (Isolated VA R=0.276, Crowded 5 Stroke R=0.376, Crowded 1 Stroke R=0.369). In addition, the slopes of the three visual acuity regression lines are similar to each other. Note, that visual acuity explains only 8-14% of the variance in performance.

It was hypothesized that certain patient populations would have trouble with visual acuity tests that had multiple optotypes in close proximity, due to a segmentation deficit. However, difference of means for the acuity tests within each lesion and control group, were not statistically significance. Therefore, results of the three visual acuity tests were combined for the control group and each lesion population. Refer to Appendix C for more information about why the visual acuity test results were combined.

The mean decimal visual acuity was compared across groups (Refer to Table 9). A significant difference was found between “relatives” and “cataracts”, $P<0.0001$, with “cataracts” having Snellen acuity less than 0.5 (20/50), while “relatives” had an average visual acuity of approximately 0.8 (20/25). The combination of these two populations into one control group

provided a broader spectrum of visual acuities that was comparable to that of the neurological subject groups.

The visual acuities of control patients (better than 0.6 (>20/33) Snellen visual acuity) compared to all of the neurological groups together (better than 0.55 (20/36) Snellen visual acuity) yielded no significant difference, P=0.15. When comparing each neurological group's visual acuities to that of the controls, only the temporal-parietal+ group (mean almost 0.5 (>20/40) Snellen visual acuity) showed a statistically significant difference, with poorer visual acuity than controls. Although this difference is statistically significant, it is only one Snellen visual acuity line different than the controls. All other groups did not differ from the controls. Furthermore, temporal-parietal+ patients have almost the same visual acuity as brain atrophy patients (slightly better than 0.4 (20/50) Snellen acuity), and the brain atrophy group does not show a significant difference from controls, P=0.27. Therefore, we must conclude that visual acuity does not account for performance differences on the Wenzhou protocol.

Table 9: Comparison of means for visual acuity within control group, between all neurological groups and controls, and between lesion groups and controls

COMPARISON GROUPS (Group#1 VS. Group#2)	**DECIMAL VA GROUP#1 (Mean ± SD)**	**DECIMAL VA GROUP#2 (Mean ± SD)**	**P-value**
Relatives vs. Cataracts	0.81 ± 0.35	0.48 ± 0.17	P<0.0001*
All Neurological vs. Controls	0.56 ± 0.30	0.61 ± 0.30	P=0.15
Basal Ganglia vs. Controls	0.73 ± 0.36	0.61 ± 0.30	P=0.083
Brain Atrophy vs. Controls	0.51 ± 0.23	0.61 ± 0.30	P=0.27
Occipital vs. Controls	0.57 ± 0.31	0.61 ± 0.30	P=0.52
Temporal-Parietal+ vs. Controls	0.49 ± 0.27	0.61 ± 0.30	P=0.033*

*Shows significance of p<0.05 based on the Wilcoxon rank sum test.
2 comparisons showed significance: relatives vs. cataracts and temporal-parietal+ vs. controls.

Subject Age Analysis

Next, we look at whether older age impacts performance of the Wenzhou protocol. Wenzhou protocol performance decreased slightly with older age for control and neurological subjects, with both groups having similar slopes of 0.148 and 0.135, respectively (refer to Figure 18a and 18b). The correlation had moderate strength in the controls R=0.461, with 21% of the variance in performance explained by age. The correlation was weak in neurological subjects R=0.228, and only 5% of the variance in performance was explained by age. Based on these findings, age does not appear to contribute heavily to poor performance on the Wenzhou Protocol in both groups. Poor performance in the neurological subjects is therefore largely explained by location and size of brain lesions in this group.

Figures 18A & B: Scatter plot for age vs. performance on the Wenzhou Protocol for controls, and neurological subjects

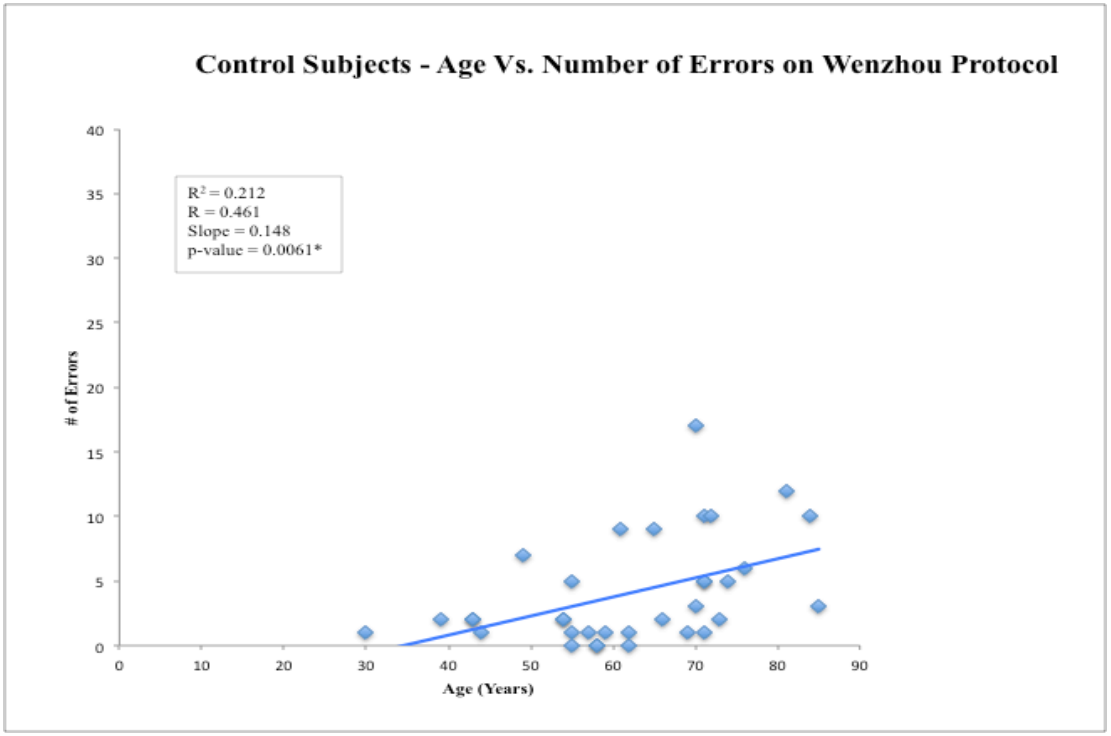

Figure 18A shows the scatter plot for all control subjects, comparing the performance on the Wenzhou Protocol to age. Performance on the Wenzhou Protocol decreases slightly (more errors) with older age, with slope of 0.148. As seen by the R=0.461, this correlation has only moderate strength. Based on R^2= 0.212, only 21% of the variance in performance is explained by age.

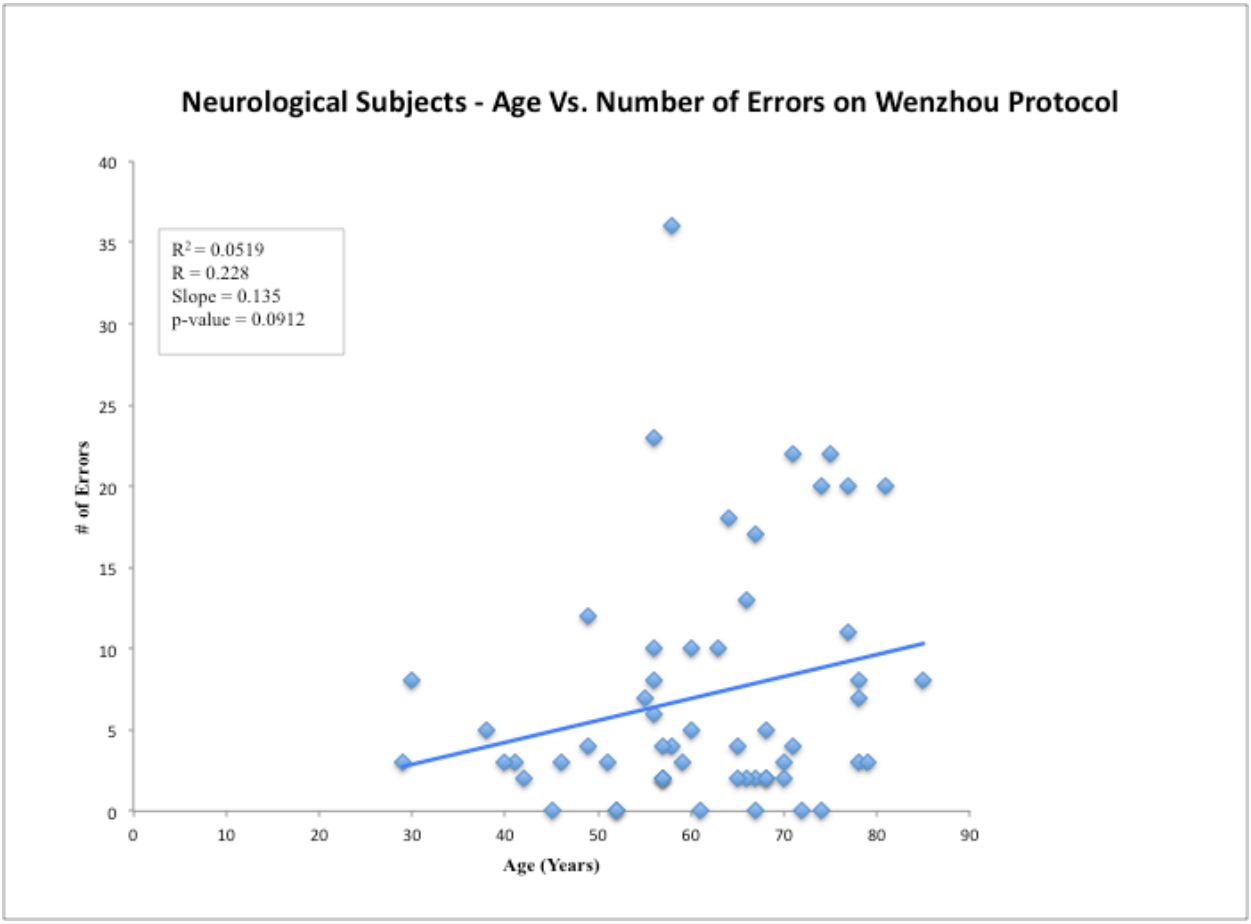

Figure 18B shows the scatter plot for all neurological subjects included in the study, comparing the performance on the Wenzhou Protocol to age. Performance on the Wenzhou Protocol decreases slightly (more errors) with older age, with slope of 0.135. As seen by the R=0.228, this correlation has is weak. Based on R^2= 0.0519, only 5% of the variance in performance is explained by age.

DISCUSSION

In this study, we compared the performance on various sections of a high-level visual perception test for different groups of patients, each with a localized brain lesion. In doing so, we hoped to determine whether high-level visual perception deficits occur in the stroke and/or brain injury population and to understand the neural loci of binding and parsing. The results of this study show that visual perception deficits in parsing, binding, face perception and more do occur in this population. However, there are limitations in the methodology and tools utilized in the study that limit our ability to make firm conclusions.

The Wenzhou Protocol is a modified high-level vision perception test adapted from the Pawan Sinha lab at MIT. It has been shown to be sensitive to segmentation and binding deficits in patients who undergo surgery for bilateral congenital cataracts (Ostrovsky et al., 2009). In this study, a shortened version of the protocol was used which takes only 15-20 minutes to administer. While this appears to be a short period of time, it could still be a challenge for some neurological patients, as fatigue and loss of concentration could occur. Breaks were allowed during the protocol at particular points, but the impact of fatigue on the results is not known, especially due to the subjective differences in trauma and their symptoms.

Results of the Wenzhou Protocol testing showed that the higher visual perceptual phenomena in the study are not impaired in patients with extensive brain atrophy and multiple punctate white matter lesions, even though their brains appear to be functionally endangered. Only larger volume brain lesions caused deficits in the higher visual perception functions.

The visual perceptual deficits of two brain lesion groups (occipitals and temporal-parietal+) stood out. Their performance was compared to controls and analyzed for small vs.

large lesion sizes. In the results, performance data for the various categories within the Wenzhou protocol were presented for individual lesion groups. The results indicated that there are different pathways or primary cortical areas for face perception and visual memory compared to binding and segmentation. We will outline the results above through a graphical representation of performance for patient groups for each perception test category and discuss the impact of this study as it relates to the literature.

Total Performance on the Wenzhou Protocol

First, results of the study showed that higher level visual perceptual deficits can be demonstrated in patient's with brain lesions, as evident from the deficits shown by occipital and temporal-parietal+ subject groups (Refer to Figure 19). Occipital patients had 3.1 times more errors than controls, while temporal-parietal+ patients had 2.2 times more errors. Furthermore, larger brain lesions cause poorer performance on the Wenzhou Protocol. This is illustrated in Figure 15 for occipital and temporal-parietal+. Patients with larger lesion have reduced performance with 3.7 and 2.5 times more errors when compared to their smaller lesion counterparts.

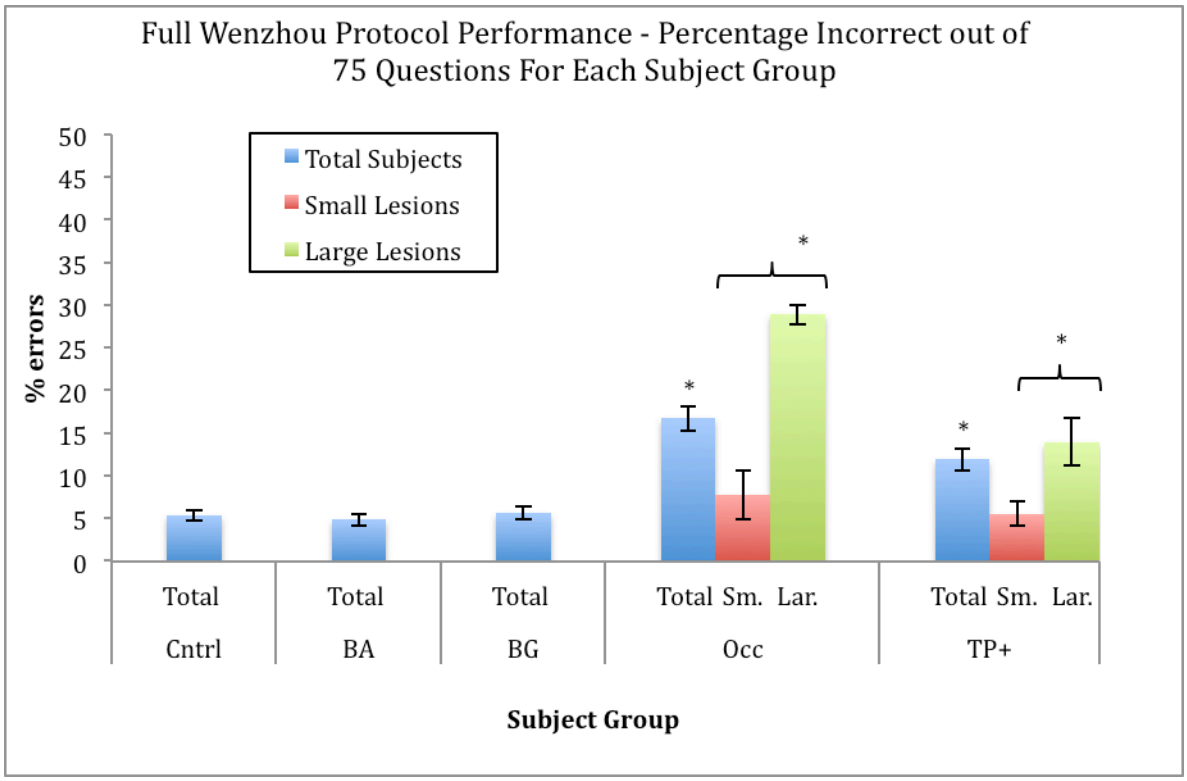

Figure 19: Graph of total performance for each subject group on the Wenzhou Protocol

Error percentages for the full Wenzhou Protocol (75 questions). Each group is compared to control subjects, while lesion size is compared within the group between small and large lesions (*$p<0.05$; Wilcoxon rank sum test). Occipital and temporal parietal patients perform significantly worse than control patients, while brain atrophy and basal ganglia patients perform similar to controls. Large lesions in the temporal-parietal+ region and in the occipital lobes cause significantly more errors than smaller lesions. 'Cntrl'=control patients, 'BA'=brain atrophy patients, 'BG'=basal ganglia patients, 'Occ'=occipital patients, 'TP+'=temporal-parietal+ patients.

Face Perception

One important and well-known area of study in visual perception, for which it is claimed that there are specific brain sites, is face perception. Faces are complex images that are made up of many smaller component features. In isolation, the small shapes/features of the face (ear, nose, eye) are meaningless and a face is virtually unrecognizable; however, together these features may be 'bound' into a whole. The resulting global image that results is perceived as a 'face' and may even be recognized as the face of a famous individual. Several studies have found that face perception may be isolated to certain brain regions. One such area is the fusiform face area

(FFA) found in the mid-fusiform gyrus at the boundary between the ventral temporal and occipital lobes (McCarthy, Puce, Gore, & Allison, 1997). A lesion to this area results in a deficit in face recognition known as prosopagnosia. Two other areas involved in face recognition: occipital face area (OFA) in the inferior lateral occipital gyrus and (fSTS) in the posterior aspect of the superior temporal sulcus (Haxby, Hoffman, & Gobbini, 2000). OFA and fSTS are only sensitive to the components of a face such as nose and eyes, while FFA ultimately responds to the global face image by recruiting other face-selective areas to analyze different aspects of faces. Evidence shows that normal face perception requires both the FFA and OFA, not just FFA alone (J. Liu, Harris, & Kanwisher, 2010; Rossion et al., 2003).

The results of face perception in our study, is shown in figure 20. As discussed in the results section, occipital lobe lesions cause a deficit in face perception (approximately 18% errors), which is more than 2 times as many errors as for the controls. In addition, the large temporal-parietal lesions (16.3% errors) show similar performance to occipital patients, suggesting that these larger lesions extend far enough posteriorly to affect the specific brain areas responsible for determining if the image is a face or not. An fMRI study by Meng et al. showing that face/non-face judgments involve the right fusiform gyrus in particular, and the OFA bilaterally to a lesser degree (Meng, Cherian T Fau - Singal, Singal G Fau - Sinha, & Sinha) supports these findings.

While the specificity of the imaging methods used in this study makes it difficult to point to specific localized neural areas, the results shown for face perception in the Wenzhou Protocol are consistent with previous studies on face perception.

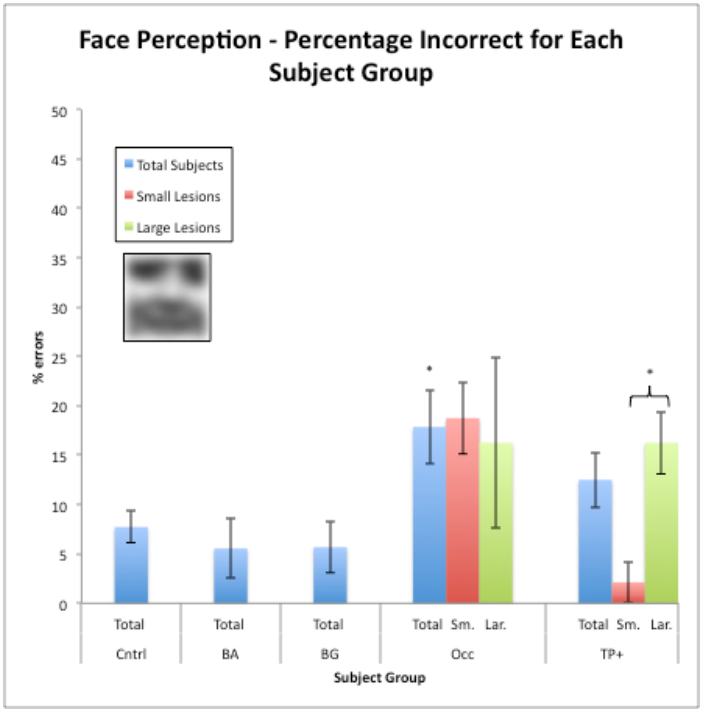

Figure 20: Graph of face perception performance on the Wenzhou Protocol

Percentage of errors on face perception (8 questions). All subjects within a group are compared to control subjects, while lesion size is compared within the group between small and large lesions. (*$p<0.05$; Wilcoxon rank sum test) Occipital patients perform significantly worse than control patients, regardless of lesion size. While brain atrophy and basal ganglia patients perform similarly to controls. Large lesions in the temporal-parietal+ group cause significantly more errors than smaller lesions.

Visual Memory

In this study, the short-term visual memory task for shapes reveals that only occipital patients have a deficit, independent of lesion size. Although the Pawan Sinha lab thinks of this task as a short-term or working memory task for shapes, it may also be considered to be a task demonstrating the ability to differentiate complex shapes from each other. In essence this is a pattern identification or shape-matching task presented with a temporally separated group of choices rather than the spatially separated choices in the early part of the Wenzhou protocol. Our results show that lesions in the occipital cortex cause deficits in visual memory/complex shape identification (figure 21).

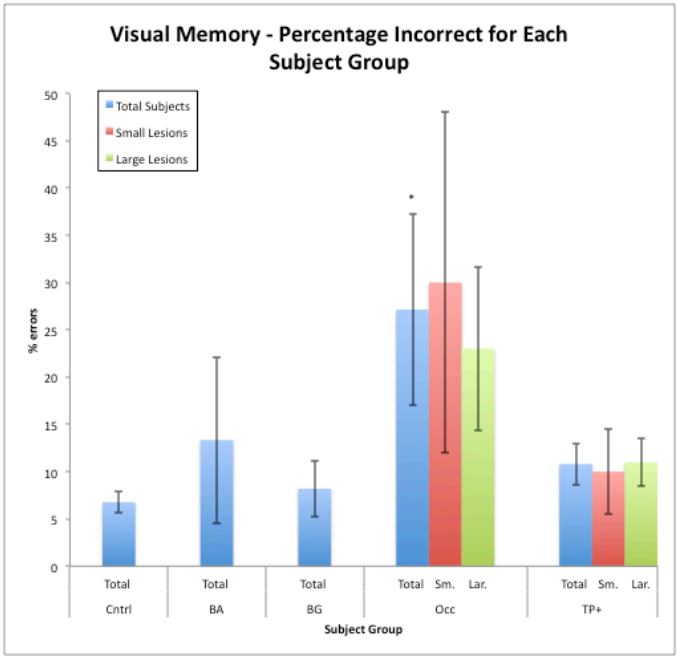

Figure 21: Graph of visual memory performance on the Wenzhou Protocol

The percentage of visual memory errors (10 questions). Each group is compared to control subjects, while lesion size is compared within the group between small and large lesions. (*$p<0.05$; Wilcoxon rank sum test) Occipital patients perform significantly worse than control patients, regardless of lesion size. While brain atrophy, basal ganglia and temporal-parietal+ patients perform similar to controls.

It is thought that multiple cortical areas are responsible for short-term visual memory. The prefrontal and frontal cortices are involved in attention and retention of information, the posterior parietal/superior occipital cortices (intraparietal sulcus and intraoccipital sulcus) are involved in retaining the information from multiple object features, including color, orientation and type of shapes (Todd & Marois, 2005; Xu, 2007; Xu & Chun, 2006). Parra et al. found that areas within the ventral stream (fusiform gyrus/occipito-temporal gyrus, inferior temporal gyrus, and lateral occipital cortex) were involved in short-term visual memory of objects through shape encoding and processing, and suggests that parietal region involvement maintains feature representations from the ventral stream (Parra, Della Sala, Logie, & Morcom, 2014). Therefore,

it is not unexpected that the occipital lobe lesions (which in some cases may extend a little bit into the parietal or temporal lobes) effect complex pattern identification in this study, and the occipital lobe contains the beginning of the object identification pathway.

Shape Matching/Masking Distractors

Shape matching is a relatively simple task that does not contain overlapping shapes, and therefore does not require segmentation. In the study of bilateral congenital cataract by Ostrovsky et al., patients showing a segmentation deficit, performed well on shape matching, indicating the independence of the two tasks (Ostrovsky et al., 2009).

Temporal-parietal+ patients perform significantly poorer on shape matching (11.6% errors; 3.4 times that of the controls) (Figure 22). Only the large lesion size group is associated with reduced performance. Reduced performance in occipital patients is also solely due to large lesions (33.6% errors on shape matching, 9.7 times more errors than controls). The larger lesions in these two populations (occipital and temporal-parietal+) are likely affecting important cortical areas for object or shape processing. These results are in line with previous evidence of the importance of the occipital-temporal cortex being involved in processing higher order object representation. The lateral occipital cortex (LOC) has been implicated in higher level object structure or shape information, and the downstream areas, mid-fusiform gyrus and inferior temporal cortex are important in making distinctions between objects or shapes that are similar. In particular, the bilateral mid-fusiform gyrus is important for performing correct matches of objects and shapes (Joseph & Gathers, 2003; Kourtzi & Kanwisher, 2001; X. Liu, Steinmetz, Farley, Smith, & Joseph, 2008).

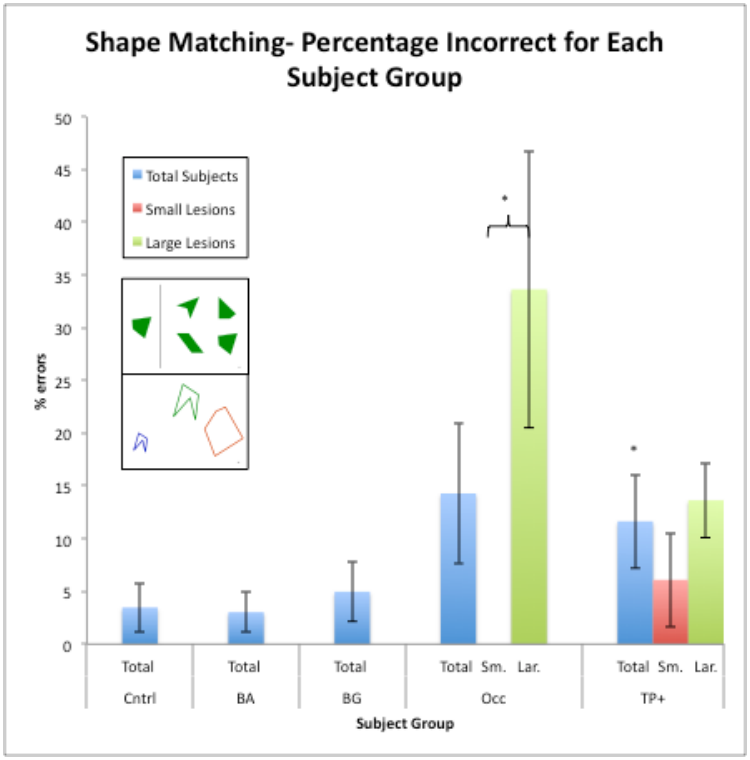

Figure 22: Graph of shape matching performance on the Wenzhou Protocol

Percentage of errors for shape matching (11 questions). All groups are compared to control subjects, while lesion size is compared within the group between small and large lesions (*$p<0.05$; Wilcoxon rank sum test). Temporal-parietal+ patients perform significantly worse than control patients. Larger temporal-parietal+ lesions have a higher percentage of errors compared to smaller lesions, which approach but do not reach significance. Although occipital patients have more errors than controls (and temporal-parietal+) patients, this difference does not reach significance. However larger occipital lesions have significantly more errors than small occipital lesions.

Masking/distractors is a task that contains simple figures or shapes (e.g. triangle, circle) that are overlapped by line distractors or masking scribbled lines. Like shape matching, it too does not resemble the frank parsing/segmentation questions outlined by specific segmentation and unfilled figures segmentation. In this task, the subjects stated how many shapes or objects are on the slide and named the objects. Note, that this is a different type of task compared to shape matching. However, the significantly poorer performance on shape matching shown by temporal-parietal+ patients (11.6% errors; 3.4 times that of the controls) (Figure 22), is similar to the poor performance shown by this group on masking/distractors (18.9%; 3.4 times that of the

controls) (figure 23). In both categories, large lesion size is associated with reduced performance. In addition, reduced performance for masking/distractors in occipitals is only due to large lesions (32.9% on masking/distractors, 6.1 times more errors than controls), similar to shape matching. The larger lesions, like in shape matching, are likely affecting specific important cortical areas for object and shape processing. This lesion evidence is in line with studies in macaque monkeys that have shown that area V4 plays a role in discriminating shapes that are partially occluded (Kosai, El-Shamayleh, Fyall, & Pasupathy, 2014). While there is debate in the literature as to the associated region in humans along the ventral visual processing pathway, it is likely anterior occipital, and/or posterior temporal in humans. There is also evidence in humans that the lateral occipital cortex (LOC) responds to objects or shapes even when partially occluded by line grids (a form of masking) (Kourtzi & Kanwisher, 2001).

Lateral occipital cortex (LOC) appears to be one area that is important for both shape matching and masking/distractors tasks. This could explain the similarity of results across subject groups, especially in the occipital patients.

A more theoretical explanation of the similarity of results on shape matching and masking/distractors could be that both categories have elements of masking in the form of crowding or visual confusion on the slides. The shape matching slides could be seen as having a 'passive' form of masking, with multiple shapes on each slide (in some slides, there are up to 9 possible shapes for matching). While the masking/distractor slides, may be seen as having 'active' form of masking, with overlapping lines on the shapes. In both cases, the 'masking' makes object/shape matching and recognition difficult for occipital and temporal-parietal+ patients.

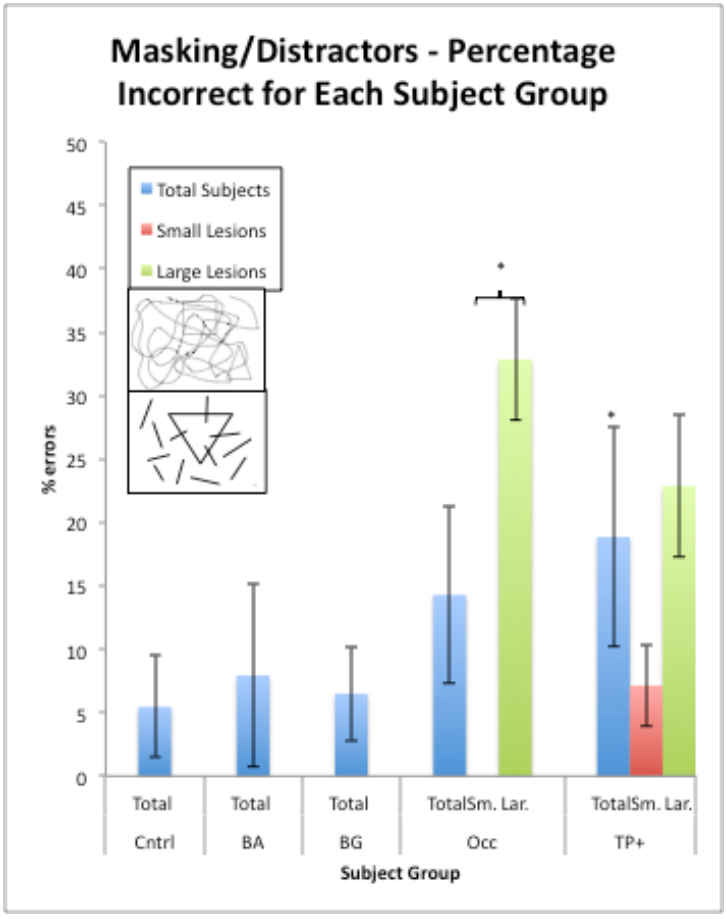

Figure 23: Graph of masking/distractors performance on the Wenzhou Protocol

Percentage of errors for masking/distractors (7 questions). All groups are compared to control subjects, while lesion size is compared within the group between small and large lesions. (*$p<0.05$; Wilcoxon rank sum test) Temporal-parietal+ patients perform significantly worse than control patients. Larger temporal-parietal+ lesions have a higher percentage of errors compared to smaller lesions, but do not reach significance. Occipital patients have more errors than controls patients; does not reach significance. Larger occipital lesions have significantly more errors than small occipital lesions.

Binding

In this study, two types of binding were tested: line binding, as well as binding of 3-D shaded shapes. In both cases, individuals must pull together features or parts of figures in order to perceive them as a 'whole.' In the study by Ostrovsky et al. (2009), subjects with a 'true' binding deficit had trouble with both types of binding, not just one type.

Line binding slides have an element of masking. While there may be some masking present due to multiple straight and curved lines, the main goal of the slide is to perceptually put the longest continuous line together. The results for line binding showed that temporal-parietal+ patients perform adequately, with 10.6% errors (Figure 24 B) while for masking/distractors they did not, which showed that this group has significantly poorer performance than controls. It can be inferred that poor performance in the occipital group (28.6% errors), especially by large occipital lesions (66.7%% errors) is not caused by masking, but is due to a binding deficit that implicates the occipital lobe. This is supported by fMRI studies showing that the lateral occipital cortex (LOC) is involved in perceptually completing outlined images or shapes that are incomplete due to a grid of multiple lines blocking the images (Lerner, Hendler, & Malach, 2002). Another fMRI study in monkeys and humans looked at the integration of local image features, in particular collinear contours (similar to the current study, except that the current study did not use closed shapes, rather it uses curved lines), into global shapes. The study found that contour integration for processing global shapes required involvement of: early visual areas, which depended on receptive field size, V1 (for linking similarly oriented lines together) and V2 (separating the figure/shape from the background); and higher visual areas, LOC (implicated in the shape processing), to encode the global shape (Kourtzi & Kanwisher, 2001).

A)

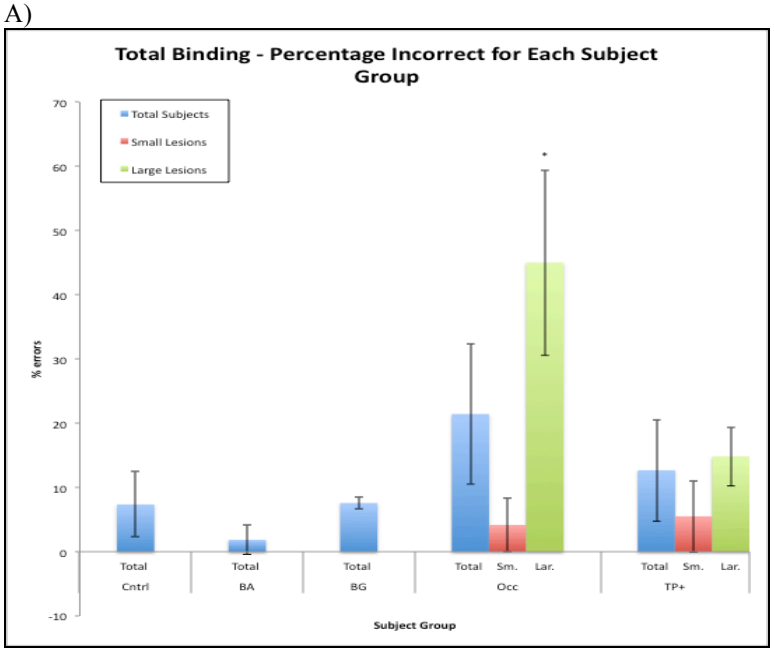

B)

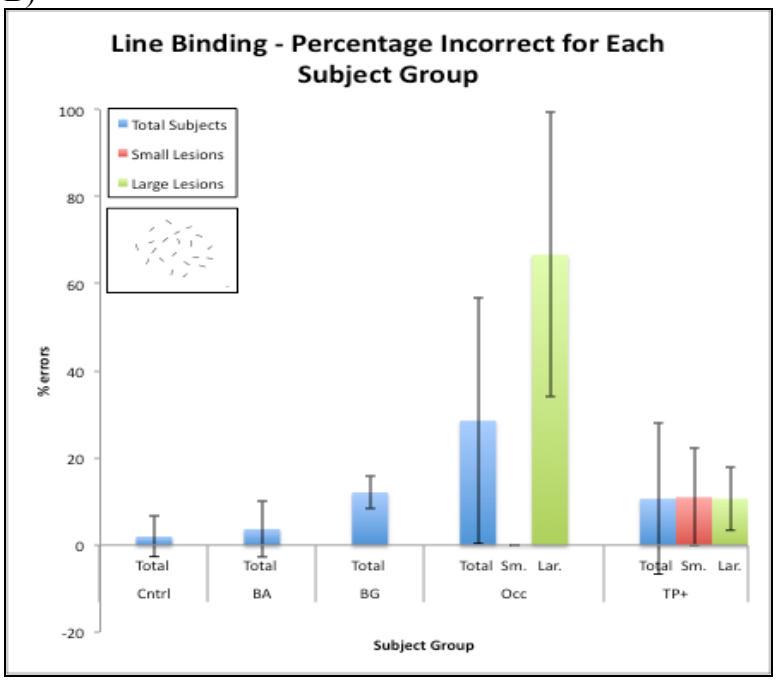

Figures 24A & B: Graph of performance on total binding and line binding on the Wenzhou Protocol.

Percentage of errors for A) total binding (6 questions, made up of line binding and 3-D shape binding) and B) line binding (3 questions). All groups are compared to control subjects, while lesion size is compared within the group between small and large lesions. (*$p<0.05$; Wilcoxon rank sum test) A) Occipital patients perform nearly 3 times worse than control patients (approaches but does not reach significance, P=0.12). Occipital lesions have a significantly higher percentage of errors compared to smaller lesions. B) Occipital patients have many more errors than controls (approaches but does not reach significance, P=0.055). Larger occipital lesions drive this finding, compared to smaller lesions (approaches but does not reach significance, P=0.12). Brain atrophy, basal ganglia and temporal-parietal+ patients perform similarly to controls for total and line binding.

A) B)

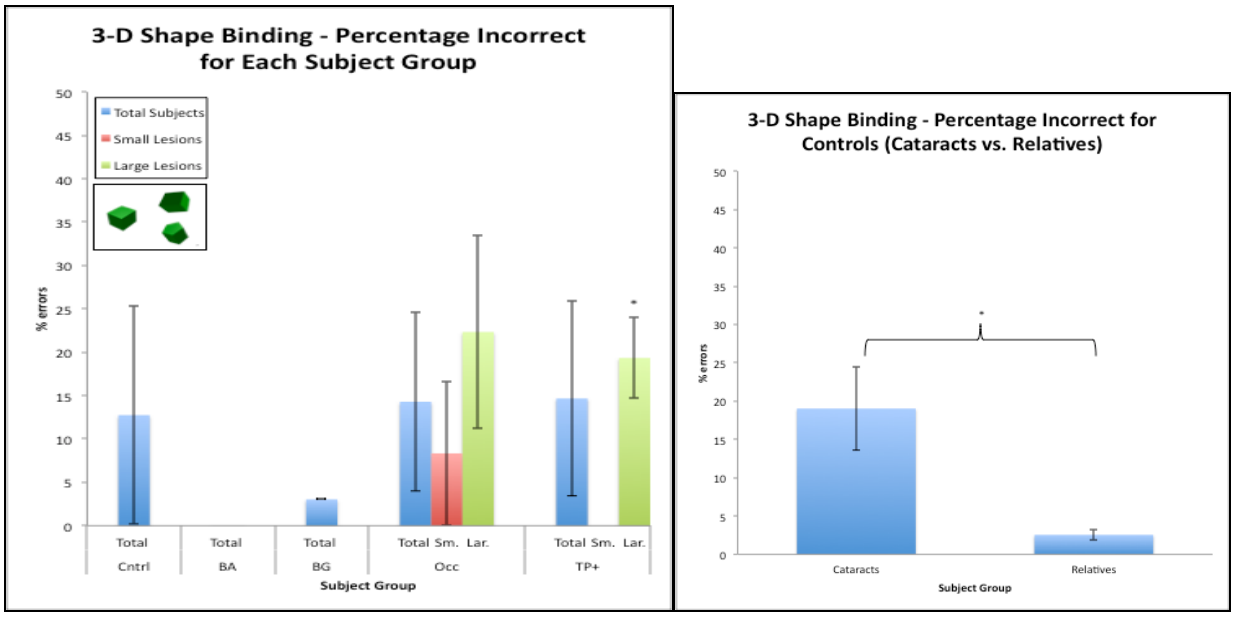

Figures 25A & B: Graph of 3-D shape binding performance for each subject group on the Wenzhou Protocol, and for cataracts vs. relatives

Percentage of errors for A) 3-D shape binding for each subject group studied (3 questions) and B) 3-D shape binding for cataracts vs. relatives (3 questions). All groups are compared to control subjects, while lesion size is compared within the group between small and large lesions. (*$p<0.05$; Wilcoxon rank sum test) A) Shows occipital and temporal-parietal+ patients perform similarly to control patients. Larger temporal-parietal and occipital lesions have a higher percentage of errors compared to smaller lesions (significant for temporal-parietal+ group). Brain atrophy and basal ganglia patients perform better than controls. B) Cataract controls performed significantly worse than relative controls.

Both occipital (14.3% errors) and temporal-parietal+ (14.7%) patients perform similar to controls (12.7% errors) on 3-D shapes (refer Figure 25A). However, control patients show a large difference in performance within the group (Figure 25B), with cataract controls performing nearly 7 times worse than relatives, suggesting that cataract patients have a unique deficit on 3-D shape binding (cataracts show 19% errors, and relatives show 2.6% errors).

Occipital patients, with poorer performance on both line and 3-D shape binding, appear to have a ‘true’ binding deficit similar to the subjects in the study by Ostrovsky et al. Although it

is not known whether the occipital lobe is the only region responsible for binding (as seen by large lesions driving the deficit compared to small lesions), it certainly plays an important role. In addition, temporal-parietal+ patients only show a deficit on 3-D shape binding. An explanation for the differences in subject group performance could lie on the two types of binding tasks used, strongly suggesting that line and 3-D shape binding occur through two different pathways. While both binding tasks require the occipital lobe, 3-D shape binding appears to recruit more anterior cortical regions. The idea of response dependent differences is supported by the meta-analysis by Joseph (Joseph, 2001), showing that the spatial distribution and localization of cortical responses is influenced by the response demands of an object-recognition task. In this case, there is a difference in response demand: requiring binding of 3-D shapes as shown by a matching response; and binding of lines using tracing of the longest line for the line binding task. This difference in response demand is likely causing differences in findings between the two groups. While, bilateral inferior temporal and mid-fusiform regions are involved in shape matching, it is the right mid-fusiform gyrus that is responsible for 3-D shape recognition and interpretation of these 3-D shapes through different viewpoints (rotational manipulation of 3-D objects) (X. Liu et al., 2008). Due to this specific cortical localization (right hemisphere only), it is likely that only right hemispheric or large temporal lesions would cause a direct deficit in 3-D shapes, while occipital lesions along the ventral visual processing stream would likely also contribute to this deficit.

Ostrovsky et al., provide further support for these two types of binding tasks occurring through different pathways when looking at visual binding performance and recovery in the post-cataract surgery patients. When tested shortly after surgery, the subjects performed at or below chance for line binding, while having no correct responses on 3-D shape binding. Nearly a year

later, performance on line binding improved greatly past chance, while 3-D shape binding remained at or below chance (Ostrovsky et al., 2009).

Cataract patients poor results on just 3-D shape binding (19% errors for cataracts, compared to 2.6% errors for relatives), does not indicate a 'true' binding deficit. This result in our acquired/age-related cataract population could be attributed to their increasing reliance on visual cues such as lighting/shading over the years as cataracts worsened, and visual detail faded. Recall that 3D shape binding slides require a subject to match the 3-D shapes (with each face of the shape having different lightness/brightness based on their orientation) with orientation manipulation. The cataract patients were tested only 1-2 days after undergoing cataract surgery and although they had adequate visual acuity for the task, they could still be relying on orientation-based brightness cues of the shape faces, instead of relying on detailed shape information. For example, figure 5a shows a 3D-shape binding slide. A normal subject would match the cube on the left to its counter part on the top right. However, due to the change in the orientation of the top right cube, its shading/lighting are different from the cube on the left. Due to this shading difference, cataract patients may be inclined to choose the bottom right object (even though it is a 3D pentagon), as it has an identical orientation and shading appearance to the cube on the left. It would be advantageous to study this finding over time to learn more about the nature of this deficit in cataract patients, especially to determine if there is improvement on 3-D shape binding, and how long it would take for improvement to occur.

Segmentation

A) B)

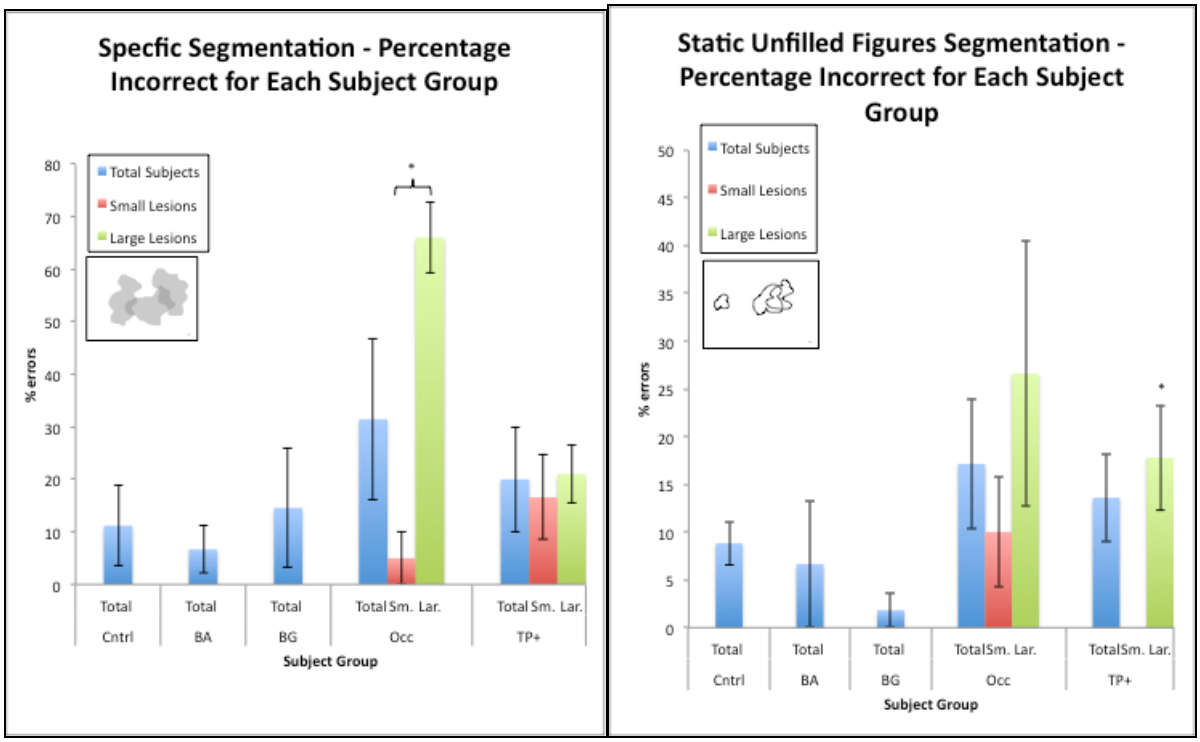

Figures 26A & B: Graph of performance on specific segmentation and static unfilled figures on the Wenzhou Protocol

Percentage of errors for A) specific segmentation (5 questions) and B) static unfilled figures segmentation (5 questions). All groups are compared to control subjects, while lesion size is compared within the group between small and large lesions. (*$p<0.05$; Wilcoxon rank sum test) A) Shows occipital patients perform nearly 3 times worse than control patients (approaches but does not reach significance, $P=0.12$); larger occipital lesions have significantly more errors compared to smaller lesions. Temporal-parietal+ patients perform much better than occipitals, with no difference in lesion size. B) Occipital patients have nearly 2 times more errors than controls (not significant). Larger occipital lesions drive this finding, compared to smaller lesions (not significant). Large temporal-parietal+ lesions cause poor performance on unfilled figures, while brain atrophy, basal ganglia and temporal-parietal+ patients perform similar or better than controls.

Segmentation was studied through two tasks: specific segmentation (Figure 26A) and static unfilled figures segmentation (Figure 26B). In both cases, subjects must visually separate overlapping shapes or figures and recognize them as being unique independent figures. One of the main differences between specific segmentation and static unfilled segmentation was the

complexity of stimuli or shapes, with specific segmentation containing a higher level of complexity including, changes in luminance, shadow, greater number of shapes on the slide.

Occipital patients' poor performance (3 times more errors than controls on specific segmentation, and 2 times more errors than controls on static unfilled figures) mainly due to large lesions, especially for specific segmentation (66% errors for large occipital lesions on specific segmentation, 27% for large occipital lesions on static unfilled figures), suggests that the occipital cortex is important for segmentation tasks. Temporal-parietal+ patients do not perform much worse than controls on specific segmentation, while decreased performance on unfilled figures, is mainly influenced by large lesions.

The difference in performance observed between the two segmentation tasks could be due to the difference in stimuli. Unfilled figures only have slides with overlapping black outlines. On the other hand specific segmentation questions consist of varying stimuli: 2 slides with multiple white shapes and black outlines; 2 slides containing translucent grey shapes; and one slide containing multiple opaque wooden blocks with shadows. This suggests that there are different types of segmentation, based on different stimulus features, governed by different types of pathways/cortical areas. Furthermore, it outlines the complicated nature of the visual functions being studied, and shows that increased complexity of stimuli/objects reduces subject performance.

There is limited evidence in the literature regarding the neural correlates of figure segmentation. Primate studies have shown neurons in V4 (anterior occipital lobe) are tuned to curves found at boundaries between two overlapping objects/shapes, suggesting that V4 is involved in contour based image segmentation. Primate lesion studies have also shown that lesions of V4 cause large deficits in segmenting an object from the background (Pasupathy,

2014). It is difficult to draw conclusions based on our study regarding the cortical regions involved. Nonetheless, our results point to the occipital lobe.

Furthermore, the results of this study do suggest a link between binding and parsing. Performance by occipital patients for specific segmentation (Figure 26A) resembles that of line binding (Figure 24B), suggesting a link between these two higher visual perceptions. It is important to note that these perceptual tasks have different degrees of stimulus complexity (collinear contours vs. outlined shapes/translucent shapes and opaque objects). However, the link between these two processes arises in task demand. While line binding appears to only require perceptual connection of collinear lines, it also requires that the subject parse out the figure from the surrounding environment. Thus, this binding task has an element of segmentation. Similarly, specific segmentation requires parsing of figures, as well as binding of the shapes to ensure object recognition. These tasks more closely resemble natural scenes that require both segmentation and binding for interpretation. As a result, specific segmentation likely utilizes a similar pathway to line binding that includes specific areas of the occipital lobe, starting in V1, and progressing through V2 to the lateral occipital area (LOC), implicated in object processing (Kourtzi & Kanwisher, 2001). It is possible that a segmentation deficit is accompanied by a binding deficit, as seen in our patients.

The study of patient MM exemplifies the potential link between binding and parsing. MM had lost vision for 40 years since 3.5 years of age, and then regained vision in one eye with surgery. When tested, he was found to have significant deficits in line contour integration, and complex form processing (shape/feature segmentation and 3-D shape integration/binding), with no trouble on simple form, color, depth and motion processing (Fine et al., 2003).

Motion

Motion processing develops early in infancy compared to form processing and is thought to aid in acquiring and developing form or shape perception as early as a few months (Johnson, Bremner Jg Fau - Slater, Slater Am Fau - Mason, Mason Uc Fau - Foster, & Foster). Studies have shown that motion processing after prolonged visual deprivation is important for acquiring form or shape information and for figure ground distinction (Fine et al., 2003; Ostrovsky et al., 2009).

Motion information is processed as early as V1 and V2 in the occipital cortex, and as far as V5/MT in the anterior occipital/posterior temporal area. Motion processing in V5 has been found to be independent of V1 and V2 input, and is likely responsible for global motion processing for shapes/objects (McKeefry, Watson Jd Fau - Frackowiak, Frackowiak Rs Fau - Fong, Fong K Fau - Zeki, & Zeki, 1997).

The current study found that normal subjects, brain atrophy patients, basal ganglia patients all benefited from motion, while occipital lobe lesion patients benefited least from motion and temporal-parietal+ lesion patients benefited minimally from motion in a specific segmentation task (unfilled figure segmentation). Lesions along the ventral visual processing stream (occipito-temporal) as well as in areas of global motion processing in the occipital lobe appear to disrupt motion processing, making it unusable in this context. Despite these findings, we have not studied motion in other types of segmentation tasks (specific segmentation); therefore, it is not known whether motion would be helpful in different stimulus situations for these stroke patients.

Lesions that minimize motion's ability to improve performance in the segmentation task in the study also cause deficits in object segmentation, binding, and figure from ground

separation. As motion is important for acquiring and developing form information, we hypothesized that it would serve as an important cue for performing object discriminations. This raises questions whether form information processing can be re-acquired or improved in such patients. If so, what mechanism can help to achieve this improvement?

Figure Ground/Depth

The figure ground/depth task used in this study requires an individual to not only determine that there are two separate but overlapping shapes, but also indicate which one is in front of the other. In the study by Ostrovsky et al. (2009), the subjects with a segmentation deficit performed figure ground/depth questions better than the segmentation questions. The figure ground/depth task has opaque stimuli, making it a fundamentally different task compared to specific and unfilled figures segmentation.

In this study, only temporal-parietal+ patients showed reduced performance on the figure/ground task (3 times worst than controls), while occipital patients performed adequately (Figure 27). This is consistent with evidence from Fischmeister et al. (2006) showing that visual processing of monocular depth cues in natural scenes activated temporal lobes bilaterally, which extended along the right fusiform gyrus into the occipital region. This study suggests that occipito-temporal regions, (along the ventral visual pathway/object processing pathway) are important for the processing of depth based on edges and shapes independent of binocular disparity (Fischmeister & Bauer, 2006). Due to the use of natural scenes in the study by Fischmeister et al., there were multiple monocular depth cues present in their images. This is in contrast to the present study, which only makes use of the monocular cue of occlusion or interposition (where the object or shape that blocks part of another shape is seen as being in

front). The current study also suggests that the shape processing, basic parsing and monocular depth interpretation task used in this study involves the temporal lobe.

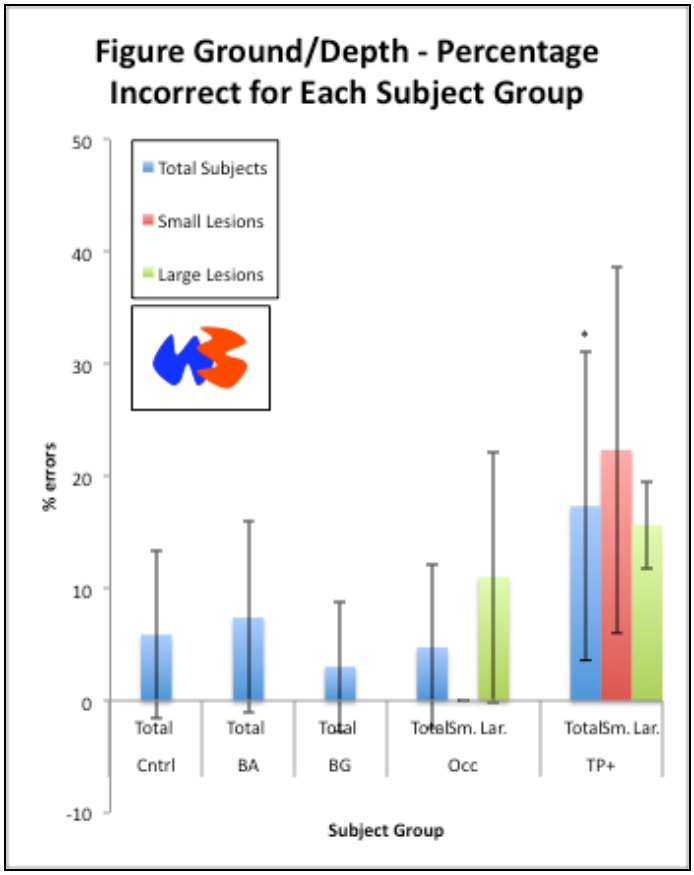

Figure 27: Graph of performance on figure ground/depth on the Wenzhou Protocol

Percentage of figure ground/depth errors (3 questions). All group are compared to control subjects, while lesion size is compared within the group between small and large lesions. (*p<0.05; Wilcoxon rank sum test) Temporal-parietal+ patients perform significantly worst than controls, regardless of lesion size. All other groups perform similar to controls.

Naming Real Objects

The everyday task of recognizing objects in the environment requires binding of various elements or components of an image, as well as segmentation to determine the difference between a single entity and its surroundings or the difference between two overlapping objects.

Figure 6b is an image that requires segmentation to differentiate the snake from the fish, while using binding through continuity of the snake's figure to determine that there is only one snake, not multiple. This was a particularly challenging slide. Not all naming slides had this level of difficulty, as some simple slides contained an object on a plain white background such as a chair and a soda bottle; while more challenging slides contained an object in its natural environment, such as a fruit on a tree, etc. This range of stimuli allowed us to test object recognition in a general sense.

Occipital lesion patients show a mild deficit in naming real objects (8.6% errors) (Figure 28). Large lesions heavily influenced this finding (18% errors). While temporal-parietal+ patients show a relatively small deficit in naming real objects (6.1%), larger lesions in this group make up the entirety of errors on this task (8% errors) and have a similar proportion of errors as occipital lesions. Although the proportion of errors was low in both groups, the similarity of results suggests the involvement of particular areas in the temporal and/or parietal lobes, and in the occipital lobe for relaying the information needed to recognize everyday objects.

A study of neurological patients by Damasio et al. showed that focal lesions could cause deficits in naming of animals and tools, while a parallel PET study in healthy subjects showed the brain activation patterns for the naming of animals and tools. Animal naming was associated with the left anterior inferior temporal area, while tool naming was associated with the occipito-temporal region. Thus, different cortical regions were involved in naming different object categories (Damasio, Grabowski Tj Fau - Tranel, Tranel D Fau - Hichwa, Hichwa Rd Fau - Damasio, & Damasio). On the other hand, a study by Moore and Price showed that there might be additional visual processing in response to complex objects vs. simple ones. They defined complex objects as those having a greater number of structural components (including animals

and complicated manufacture objects such as an airplane), while simple objects included fruit. The right medial occipital cortex had greater activation in response to complex objects compared to simple ones (Moore & Price). Taken together, these studies point to the importance of the occipito-temporal areas for naming objects.

The results of our study indicated that the occipital cortex and temporal/parietal cortices are important for various types of binding and parsing/segmentation. We posit that feature/shape information from these pathways is integrated with segmentation and binding information in order to name/recognize real objects, especially in the case of complex images as in Figure 6b.

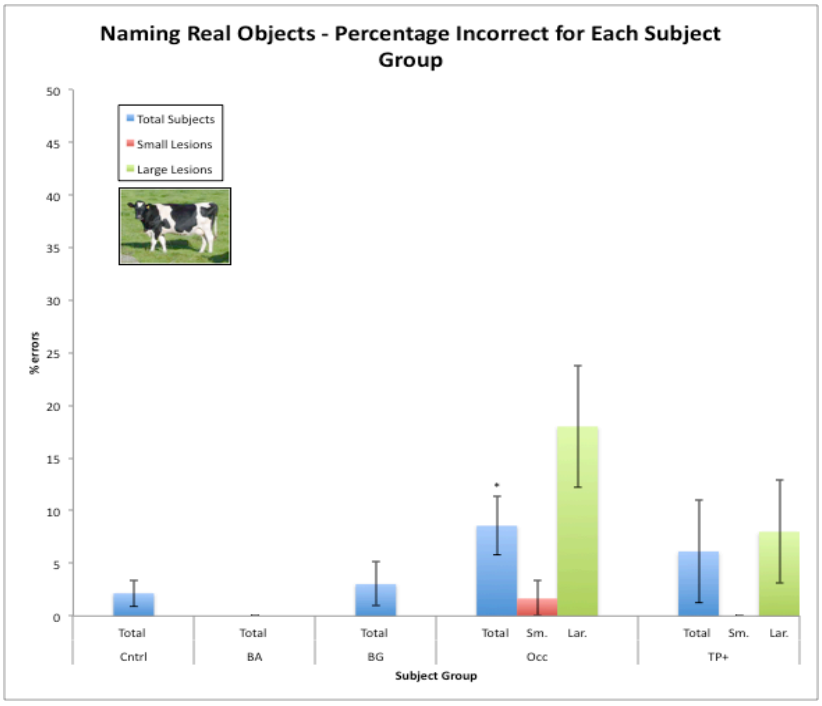

Figure 28: Graph of real objects performance on the Wenzhou Protocol

Percentage of errors for naming real objects (15 questions). All groups are compared to control subjects, while lesion size is compared within the group between small and large lesions. (*p<0.05; Wilcoxon rank sum test) Occipital patients perform significantly worse than control patients. Larger lesions in the occipital group show a higher percentage of errors compared to smaller lesions, which is not significant. Although temporal-parietal+ patients do not have more errors than controls, larger lesions in this group have more errors than smaller lesions (not significant). Brain atrophy and basal ganglia patients perform similar to controls.

Methodology Limitations

A meta-analysis performed by Joseph in 2001, showed evidence that spatial distribution and localization of cortical responses can be influenced by different procedural demands (e.g. viewing vs. matching vs. naming) and not just by the pictorial nature of the test objects (Joseph, 2001). The testing protocol is organized into different question types (matching, naming, counting) and contains an array of different stimulus types (grey vs. colored shapes, pictures, lines, faces). This allows for binding and segmentation to be analyzed in different contexts, in addition to visual memory and face perception, but it also requires adaptive thinking from patients, as they encounter different types of stimuli and question types. The questions are seen as 'easy' for a normal observer, and clear instructions were given to patients for each section of the test. However we are not sure how well each patient can adapt to the different tasks called upon by the protocol.

The testing protocol contains a reasonable number of questions for most test categories, allowing for good statistical power; however, it has limited questions for some other categories, especially line binding and 3-D shape binding, which have 3 questions each. These limited question profiles decrease statistical power for these types of visual perceptions.

A drawback of the study is small sample sizes for some subject groups and differences in subject numbers between groups. The control group is large and has a mixture of cataract patients (N=21) and relatives (N=13). A few lesion groups had sample sizes that were not large enough to be included in the study (eg. frontal lobe lesions). The largest group of patients (e.g. temporal-parietal+) had 25 subjects. The other key group (e.g. occipital lobe lesions) had only 7 subjects.

Neurological patients were tested for the purposes of this study within 2-3 weeks of onset of hospital admittance, with brain imaging occurring before the testing. Therefore, there were a variety of delays between brain imaging and testing, with little or no follow-up in this period. It is not clear how much this affects the results.

Strokes are naturally occurring processes that occur in different locations and in varying sizes. In some cases, brain lesions spanned across multiple lobes. This made grouping of subjects according to lesion location a challenge. Furthermore, brain lesions are rarely well defined, and accompanying edema that puts pressure on adjacent structures could also complicate the interpretation of images. Concerning the estimation of lesion size, a possible source of error was the variable number of images for each subject, and appropriate types of image were not always available (there were many axial images, fewer coronal and sagittal views). Lesion size was studied simply by dividing lesions into two groups (large and small). Due to the different shapes of lesions (long, wide, s-shaped, oval, etc.), division of lesion sizes was based on the average size of the each lesion's three dimensions (length, width and height/depth). This method is not as precise as many clinical algorithms, but is more than adequate to divide lesion size into two categories.

CONCLUSION

This study confirms that people with strokes or brain lesions can acquire visual perceptual deficits, including deficits in segmentation and binding. Furthermore, the results emphasize the complex nature of the visual functions being studied, and the challenges of drawing causal relationships when working with acquired brain injury. However, important findings did arise, prompting further questions and investigation.

The occipital cortex in particular appears to play an important role in segmentation tasks. Since unfilled figure segmentation shows the additional involvement of temporal and/or parietal lobes, it is likely that there are different types of segmentation based on different stimulus features, and unique cortical pathways may govern these. It is not known how 'unique' these specific pathways are, as well as the extent of the relationship between the involved cortical areas. Future studies can investigate the similarities and differences in cortical activation through fMRI in healthy subjects by varying the stimuli used in the segmentation task.

The occipital lobe also appears to play an important role in both line and 3-D shape binding. Similar to segmentation, line and 3-D shape binding appear to occur through different pathways. Specifically, the temporal lobes appear to be involved with 3-D shape binding. Future research studies in binding should examine the differences in line and 3-D shape binding in terms of specific areas of cortical involvement for both tasks in healthy subjects through fMRI, as well as looking at patterns of recovery for both types of binding in lesion patients.

A potential link between line binding and specific segmentation was discussed. These two perceptual processes likely use similar pathways in the occipital lobe. A comparative study using specific stimuli in order to independently analyze these two processes would be helpful in understanding their relationship.

Specific cortical areas in the temporal and/or parietal lobes, and especially the occipital lobe, are important for recognizing everyday objects. Previous studies have shown that the temporal and parietal lobes contain object recognition and spatial localization pathways, respectively. We believe that feature/shape information from these pathways is likely shared or integrated for the purposes of segmentation and binding. The LOC appears to play a role in visual information integration; future studies should investigate how segmentation and binding information is integrated.

Patients in Ostrovsky et al.,(Ostrovsky et al., 2009) continued to show binding and segmentation deficits for months after surgery. It was only after this time, that these patients began to exhibit increased binding abilities presumably due to acquired visual information through motion. Motion was not as helpful in our brain lesion patients for a particular type of segmentation task (unfilled figures). But it should be studied with different segmentation or binding tasks in this population to determine if it can assist this population with recovery as well. In the future, longitudinal studies can be performed to look at the pattern of recovery in this population and whether recovery to 'normal' levels is possible. These studies could suggest the mechanism of recovery, through which treatment tools could be developed for this population.

APPENDIX A

A) B)

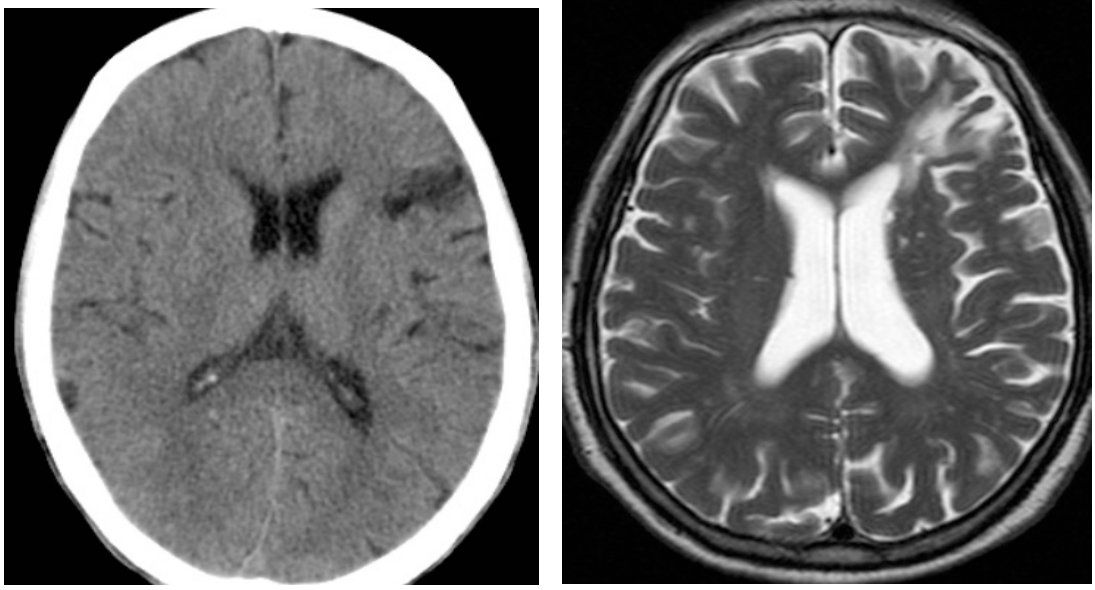

Appendix A Figures 1A & B: Frontal Lobe Lesions. A) Axial CT scan image of a 56-year old with left frontal lobe infarction, anterior to the lateral sulcus. The infarction appears hypo fluorescent in this image. B) Axial MRI image of a 66-year old with left frontal lobe infraction. The infarction is hyper fluorescent in the image.

A) B)

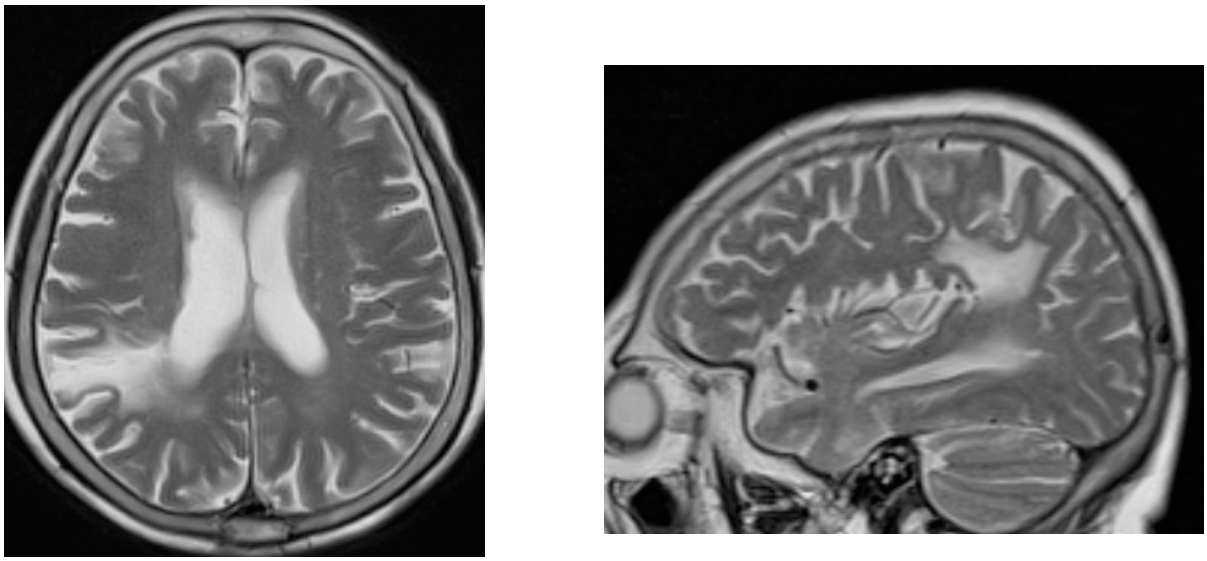

Appendix A Figures 2A & B: Parietal Lobe Lesion. A) Axial view of 78-year old with right parietal lobe infarction. Infarction is hyper fluorescent in the image. B) Sagittal view of the same patient's parietal lobe lesion.

A) B)

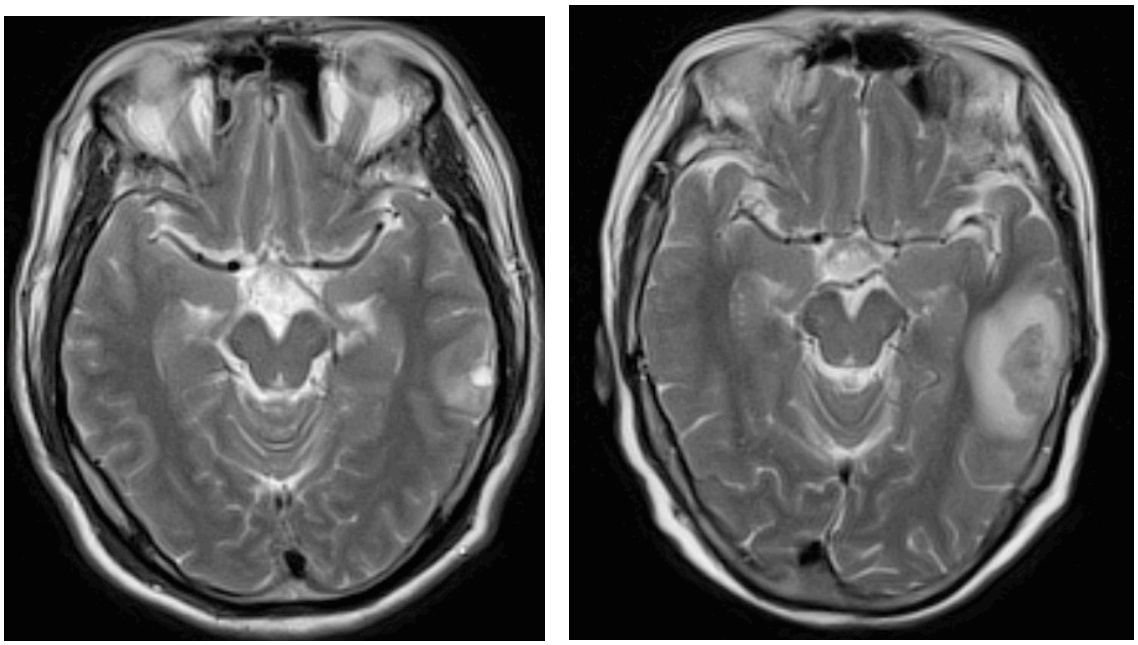

Appendix A Figures 3A & B: Temporal Lobe lesions. A) Axial MRI image of a 51-year old with a small left lateral temporal lobe hemorrhage, with surrounding edema. The hemorrhage appears hyper fluorescent in the image. B) Axial MRI image of a 70 year old with a large left temporal lobe hematoma, with extensive surrounding edema. A region of hyper fluorescent edema surrounds the hemorrhage.

A) B) C)

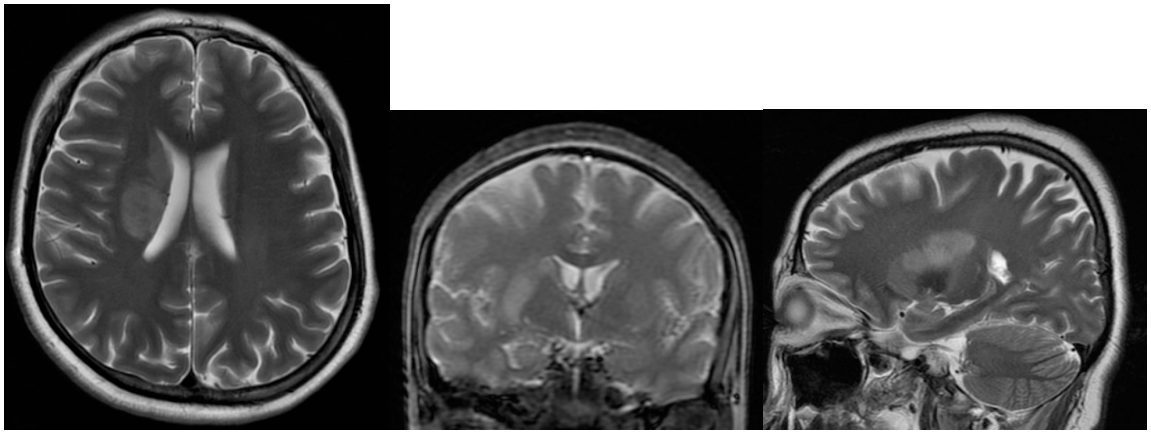

Appendix A Figures 4A, B & C: Basal Ganglia lesion. A) Axial MRI image of a 42-year old with a space-occupying lesion in the right basal ganglia. The hyper fluorescent lesion is compressing the adjacent right lateral ventricle. B) Coronal MRI image of the same patient. C) Sagittal MRI image of the same patient.

Appendix A Figure 5: Basal Ganglia Lesion. Axial CT Scan of a 67-year old with a left lacunar infarct, probably hemorrhagic. The lesion appears hyper fluorescent.

A) B)

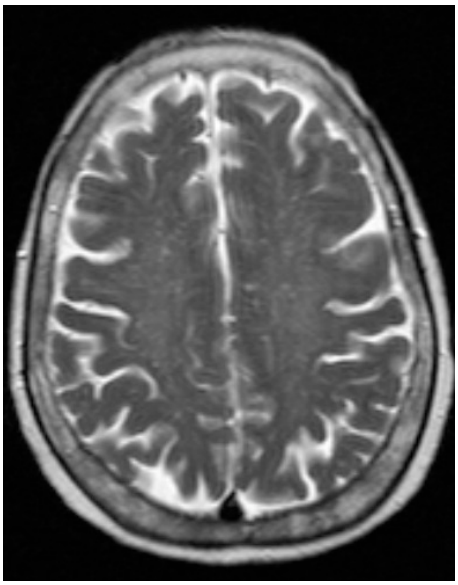

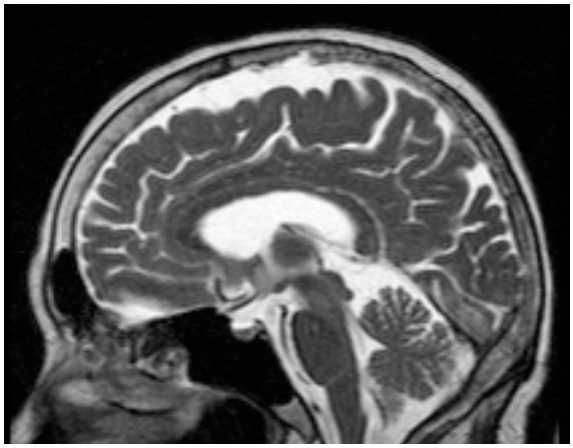

Appendix A Figures 6A & B: Small White Matter Infarctions. A) Axial MRI image of a 66-year-old patient with multiple small-scattered white matter infarctions. The small infarctions appear as tiny hyper fluorescent spots. B) Sagittal MRI image of the same patient with multiple white matter infarctions.

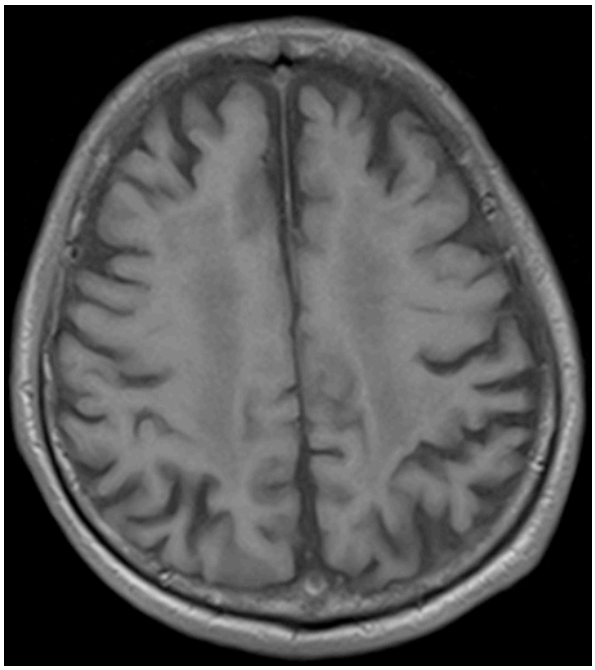

Appendix A Figure 7: General brain atrophy. Axial MRI image of an 85-year old patient with generalized brain atrophy. The shrinkage of the brain is seen by the large spaces between the gyri.

A) B)

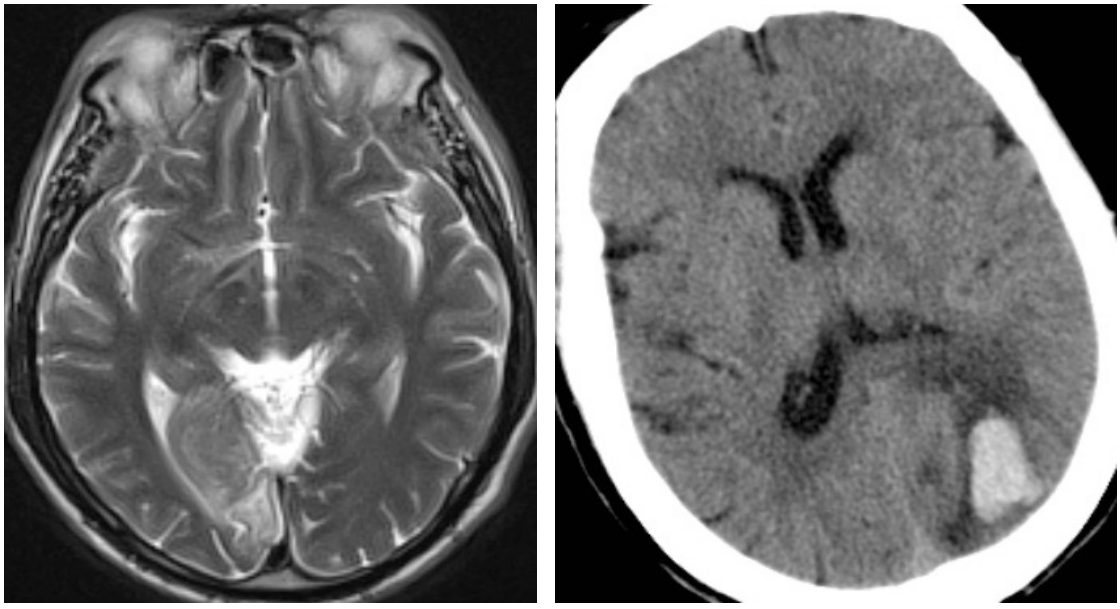

Appendix A Figures 8A & B: Occipital Lobe Lesions. A) Axial MRI image of a 60-year old patient with a left occipital lobe infarction (hyper fluorescent area) that extends to V1. B) Axial CT Scan of a 74-year old with a left occipital lobe hemorrhage (hyper fluorescent area) with surrounding edema.

A) B)

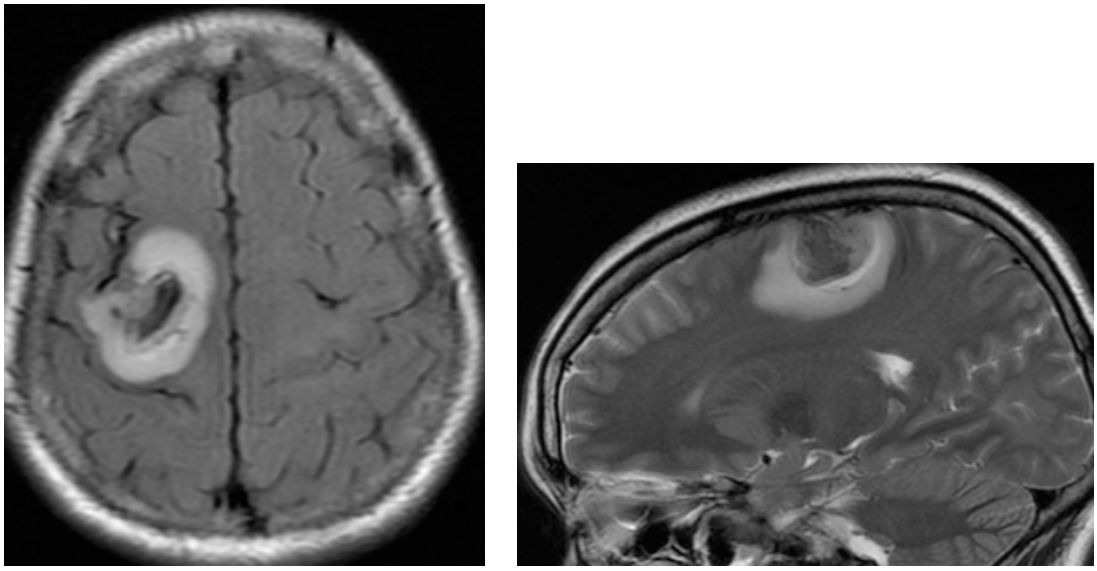

Appendix A Figures 9A & B: Small temporal-parietal+ lesion, probably neoplastic despite clinical history. Calcification and location suggest meningioma. A) Axial MRI image of a 41-year old patient with a right frontal-parietal lesion with surrounding edema (hyper fluorescent edema surrounds hypo fluorescent hematoma) that is para-sagittal and mainly posterior to the central sulcus (mostly parietal lobe). In the study, this lesion was classified as a 'small' lesion. The lesion is placed in the temporal-parietal + category as it spans two brain lobes. B) Sagittal MRI image of the same patient.

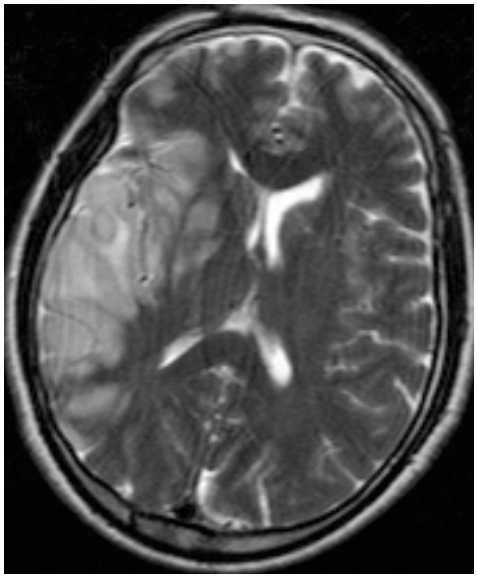

Appendix A Figure 10: Large temporal-parietal+ lesion in the distribution of the right middle cerebral artery. Axial MRI image of a 49-year old patient with a right frontal-parietal-temporal-anterior occipital lesion (large hyper fluorescent area) that compresses the right lateral ventricle. In the study, this lesion was classified as a 'large' lesion. This lesion is placed in the temporal-parietal+ group, as it spans across multiple brain lobes, including the temporal and parietal lobes.

APPENDIX B

Control Group Variance and Normality Testing

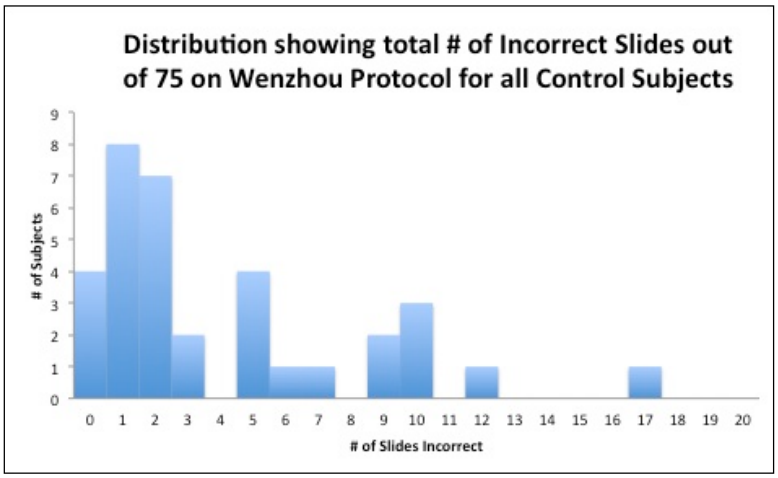

Appendix B Figure 1: The distribution of Wenzhou Protocol results (total # of incorrect answers out of 75) for both cataract patients and relatives. The graph is not normally distributed and is skewed to the right.

Two-sided F-test (testing for equal variance)
F-test: F-ratio = 2.34, **p=0.133**, equal variance for the two groups
Shapiro-Wilk Test
W=0.831, **p=0.0001*,** not normally distributed.

APPENDIX C

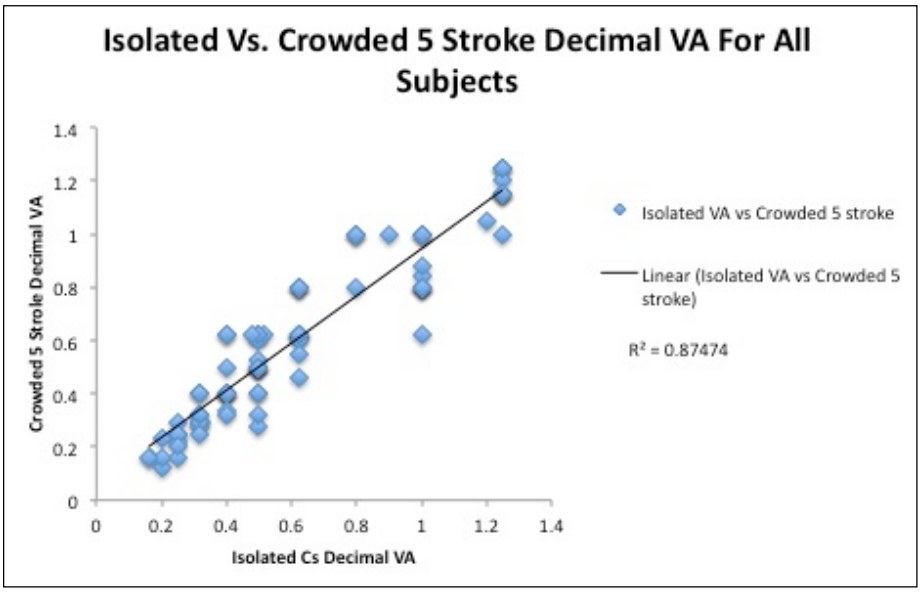

Appendix C Figure 1: The correlation between isolated decimal visual acuity and 5-stroke crowded visual acuity. As seen by the $R^2 = 0.87$, with $R = 0.94$, there is a very strong linear relationship between the two visual acuity tests.

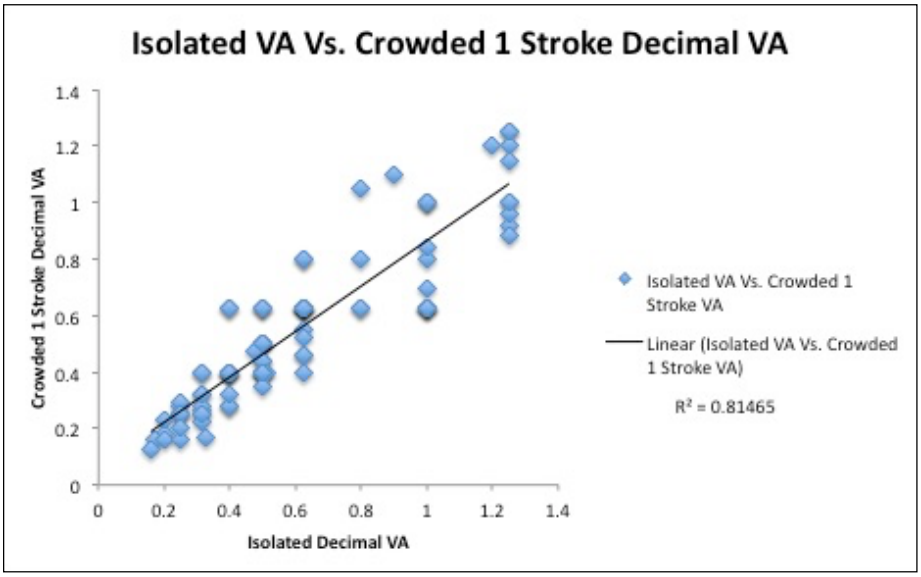

Appendix C Figure 2: The correlation of isolated decimal visual acuity to 1-stroke crowded visual acuity. As seen by the $R^2 = 0.81$, with $R = 0.90$, there is a very strong linear relationship between the two visual acuity tests.

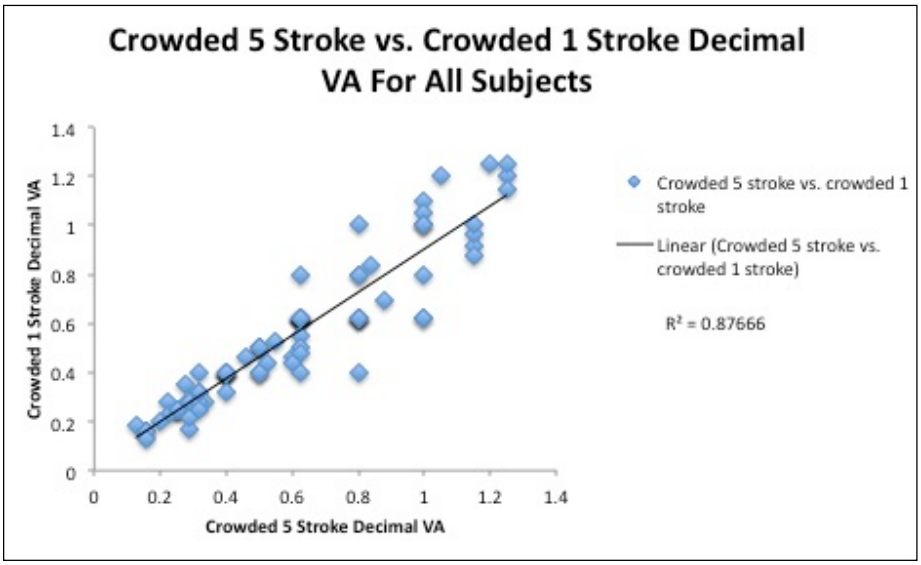

Appendix C Figure 3: The correlation of 5-stroke crowded visual acuity to1-stroke crowded visual acuity. As seen by the $R^2 = 0.88$, with $R = 0.94$, there is a very strong linear relationship between the two visual acuity tests.

The three graphs shown above show strong correlations between the three types of visual acuity tests used in this study. As a result, we have good reason to combine the three visual acuity measures for each patient group.

BIBLIOGRAPHY

Antranik. (2011). Blood Vessels [Online image]. Retrieved January 3, 2015 from http://antranik.org/blood-vessels/

Bach, M. (1995). The Freiburg Vision Test. Automated determination of visual acuity]. *Der Ophthalmologe: Zeitschrift der Deutschen Ophthalmologischen Gesellschaft, 92*(2).

Constantine-Paton, M. (2008). Pioneers of cortical plasticity: six classic papers by Wiesel and Hubel. (0022-3077 (Print)).

Damasio, H., Grabowski Tj Fau - Tranel, D., Tranel D Fau - Hichwa, R. D., Hichwa Rd Fau - Damasio, A. R., & Damasio, A. R. A neural basis for lexical retrieval. (0028-0836 (Print)).

Dubuc, B. The Brain From Top To Bottom. 2014, from http://thebrain.mcgill.ca/

Fine, I., Wade, A. R., Brewer, A. A., May, M. G., Goodman, D. F., Boynton, G. M., . . . MacLeod, D. I. (2003). Long-term deprivation affects visual perception and cortex. *Nature Neuroscience, 6*(9), 915-916.

Fischmeister, F. P. S., & Bauer, H. (2006). Neural correlates of monocular and binocular depth cues based on natural images: A LORETA analysis. *Vision Research, 46*(20), 3373-3380. doi: http://dx.doi.org/10.1016/j.visres.2006.04.026

Furl, N., & Averbeck, B. B. Parietal cortex and insula relate to evidence seeking relevant to reward-related decisions. (1529-2401 (Electronic)). doi: D - NLM: NIHMS413399

D - NLM: PMC3474936 EDAT- 2011/12/02 06:00 MHDA- 2012/02/10 06:00 CRDT- 2011/12/02 06:00 AID - 31/48/17572 [pii] AID - 10.1523/JNEUROSCI.4236-11.2011 [doi] PST - ppublish

Gilman, S. (1998). Imaging the Brain. *New England Journal of Medicine, 338*(12), 812-820. doi: doi:10.1056/NEJM199803193381207

Haxby, J. V., Hoffman, E. A., & Gobbini, M. I. (2000). The distributed human neural system for face perception. *Trends in cognitive sciences, 4*(6), 223-233. doi: 10.1016/s1364-6613(00)01482-0

Jeannerod, M., Arbib Ma Fau - Rizzolatti, G., Rizzolatti G Fau - Sakata, H., & Sakata, H. (1995). Grasping objects: the cortical mechanisms of visuomotor transformation. (0166-2236 (Print)).

Johnson, S. P., Bremner Jg Fau - Slater, A. M., Slater Am Fau - Mason, U. C., Mason Uc Fau - Foster, K., & Foster, K. Young infants' perception of unity and form in occlusion displays. (0022-0965 (Print)).

Joseph, J. (2001). Functional neuroimaging studies of category specificity in object recognition: A critical review and meta-analysis. *Cognitive, Affective, & Behavioral Neuroscience, 1*(2), 119-136. doi: 10.3758/CABN.1.2.119

Joseph, J., & Gathers, A. (2003). Effects of structural similarity on neural substrates for object recognition. *Cognitive, Affective, & Behavioral Neuroscience, 3*(1), 1-16. doi: 10.3758/CABN.3.1.1

Koffka, K. (1935). *Principles of Gestalt Psychology*: Harcourt, Brace.

Kosai, Y., El-Shamayleh, Y., Fyall, A. M., & Pasupathy, A. (2014). The Role of Visual Area V4 in the Discrimination of Partially Occluded Shapes. *The Journal of Neuroscience, 34*(25), 8570-8584. doi: 10.1523/jneurosci.1375-14.2014

Kourtzi, Z., & Kanwisher, N. (2001). Representation of Perceived Object Shape by the Human Lateral Occipital Complex. *Science, 293*(5534), 1506-1509. doi: 10.1126/science.1061133

Lerner, Y., Hendler, T., & Malach, R. (2002). Object-completion Effects in the Human Lateral Occipital Complex. *Cerebral Cortex, 12*(2), 163-177. doi: 10.1093/cercor/12.2.163

Liu, J., Harris, A., & Kanwisher, N. (2010). Perception of face parts and face configurations: an FMRI study. *J Cogn Neurosci, 22*(1), 203-211. doi: 10.1162/jocn.2009.21203

Liu, X., Steinmetz, N. A., Farley, A. B., Smith, C. D., & Joseph, J. E. (2008). Mid-fusiform Activation during Object Discrimination Reflects the Process of Differentiating Structural Descriptions. *Journal of Cognitive Neuroscience, 20*(9), 1711-1726. doi: 10.1162/jocn.2008.20116

Mandavilli, A. (2006). Visual neuroscience: look and learn. *Nature, 441*(7091), 271-272. doi: 10.1038/441271a

McCarthy, G., Puce, A., Gore, J. C., & Allison, T. (1997). Face-specific processing in the human fusiform gyrus. *J Cogn Neurosci, 9*(5), 605-610. doi: 10.1162/jocn.1997.9.5.605

McKeefry, D. J., Watson Jd Fau - Frackowiak, R. S., Frackowiak Rs Fau - Fong, K., Fong K Fau - Zeki, S., & Zeki, S. (1997). The activity in human areas V1/V2, V3, and V5 during the perception of coherent and incoherent motion. (1053-8119 (Print)).

Meng, M., Cherian T Fau - Singal, G., Singal G Fau - Sinha, P., & Sinha, P. Lateralization of face processing in the human brain. (1471-2954 (Electronic)). doi: D - NLM: PMC3311882 EDAT- 2012/01/06 06:00 MHDA- 2012/10/04 06:00 CRDT- 2012/01/06 06:00 PHST- 2012/01/04 [aheadofprint] AID - rspb.2011.1784 [pii] AID - 10.1098/rspb.2011.1784 [doi] PST - ppublish

Mishkin, M., Ungerleider, L. G., & Macko, K. A. (1983). Object vision and spatial vision: two cortical pathways. *Trends in Neurosciences, 6*, 414-417. doi: 10.1016/0166-2236(83)90190-X

Moore, C. J., & Price, C. J. Three distinct ventral occipitotemporal regions for reading and object naming. (1053-8119 (Print)).

Ostrovsky, Y., Andalman, A., & Sinha, P. (2006). Vision following extended congenital blindness. *Psychological science, 17*(12), 1009-1014. doi: 10.1111/j.1467-9280.2006.01827.x

Ostrovsky, Y., Meyers, E., Ganesh, S., Mathur, U., & Sinha, P. (2009). Visual parsing after recovery from blindness. *Psychological science, 20*(12), 1484-1491. doi: 10.1111/j.1467-9280.2009.02471.x

Parra, M. A., Della Sala, S., Logie, R. H., & Morcom, A. M. (2014). Neural correlates of shape–color binding in visual working memory. *Neuropsychologia, 52*(0), 27-36. doi: http://dx.doi.org/10.1016/j.neuropsychologia.2013.09.036

Pasupathy, A. (2014). The neural basis of image segmentation in the primate brain. LID - S0306-4522(14)00802-1 [pii] LID - 10.1016/j.neuroscience.2014.09.051 [doi]. (1873-7544 (Electronic)).

Pasupathy, A., & Connor, C. E. (1999). Responses to contour features in macaque area V4. *J Neurophysiol, 82*(5), 2490-2502.

Pasupathy, A., & Connor, C. E. (2002). Population coding of shape in area V4. (1097-6256 (Print)).

Rizzolatti, G., & Matelli, M. (2003). Two different streams form the dorsal visual system: anatomy and functions. *Exp Brain Res, 153*(2), 146-157. doi: 10.1007/s00221-003-1588-0

Robertson, L., Treisman, A., Friedman-Hill, S., & Grabowecky, M. (1997). The interaction of spatial and object pathways: Evidence from Balint's syndrome. *Journal of Cognitive Neuroscience, 9*(3), 295-317.

Robertson, L. C., & others. (2003). Binding, spatial attention and perceptual awareness. *Nature Reviews Neuroscience, 4*(2), 93-102.

Rossion, B., Caldara, R., Seghier, M., Schuller, A. M., Lazeyras, F., & Mayer, E. (2003). A network of occipito-temporal face-sensitive areas besides the right middle fusiform gyrus is necessary for normal face processing. *Brain, 126*(Pt 11), 2381-2395. doi: 10.1093/brain/awg241

Sacks, O. (1985). *The Man Who Mistook His Wife for a Hat and Other Clinical Tales*: Summit Books.

Silver B, W. S. R. (2014). Stroke: Diagnosis and Management of Acute Ischemic Stroke. *FP Essent.*(420), 16-22.

Todd, J. J., & Marois, R. (2005). Posterior parietal cortex activity predicts individual differences in visual short-term memory capacity. *Cognitive, Affective, & Behavioral Neuroscience, 5*(2), 144-155. doi: 10.3758/CABN.5.2.144

Xu, Y. (2007). The Role of the Superior Intraparietal Sulcus in Supporting Visual Short-Term Memory for Multifeature Objects. *The Journal of Neuroscience, 27*(43), 11676-11686. doi: 10.1523/jneurosci.3545-07.2007

Xu, Y., & Chun, M. M. (2006). Dissociable neural mechanisms supporting visual short-term memory for objects. *Nature, 440*(7080), 91-95. doi: http://www.nature.com/nature/journal/v440/n7080/suppinfo/nature04262_S1.html

Zeki, S. (1993) A Vision of the Brain: Blackwell, Oxford